Article:
Aad, G. orcid.org/0000-0002-6665-4934, Abbott, B. orcid.org/0000-0002-5888-2734, Abeling, K. orcid.org/0000-0002-1002-1652 et al. (2928 more authors) (2023) Search for heavy Majorana or Dirac neutrinos and right-handed W gauge bosons in final states with charged leptons and jets in pp collisions at √s = 13 TeV with the ATLAS detector. The European Physical Journal C, 83. 1164. ISSN 1434-6044

https://doi.org/10.1140/epjc/s10052-023-12021-9

Eur. Phys. J. C (2023) 83:1164
https://doi.org/10.1140/epjc/s10052-023-12021-9

THE EUROPEAN PHYSICAL JOURNAL C

Regular Article - Experimental Physics

Search for heavy Majorana or Dirac neutrinos and right-handed W gauge bosons in final states with charged leptons and jets in pp collisions at $\sqrt{s} = 13$ TeV with the ATLAS detector

ATLAS Collaboration[⋆]

CERN, 1211 Geneva 23, Switzerland

Received: 20 April 2023 / Accepted: 10 September 2023

Abstract A search for heavy right-handed Majorana or Dirac neutrinos N_{R} and heavy right-handed gauge bosons W_{R} is performed in events with energetic electrons or muons, with the same or opposite electric charge, and energetic jets. The search is carried out separately for topologies of clearly separated final-state products ("resolved" channel) and topologies with boosted final states with hadronic and/or leptonic products partially overlapping and reconstructed as a large-radius jet ("boosted" channel). The events are selected from pp collision data at the LHC with an integrated luminosity of 139 fb^{-1} collected by the ATLAS detector at $\sqrt{s} = 13$ TeV. No significant deviations from the Standard Model predictions are observed. The results are interpreted within the theoretical framework of a left-right symmetric model, and lower limits are set on masses in the heavy right-handed W_{R} boson and N_{R} plane. The excluded region extends to about $m(W_{\mathrm{R}}) = 6.4$ TeV for both Majorana and Dirac N_{R} neutrinos at $m(N_{\mathrm{R}}) < 1$ TeV. N_{R} with masses of less than 3.5 (3.6) TeV are excluded in the electron (muon) channel at $m(W_{\mathrm{R}}) = 4.8$ TeV for the Majorana neutrinos, and limits of $m(N_{\mathrm{R}})$ up to 3.6 TeV for $m(W_{\mathrm{R}}) = 5.2$ (5.0) TeV in the electron (muon) channel are set for the Dirac neutrinos. These constitute the most stringent exclusion limits to date for the model considered.

1 Introduction

The very small mass of neutrinos is one of the biggest puzzles in the Standard Model (SM) of particle physics. The seesaw mechanism [1–3] is a proposed solution, in which the light neutrinos acquire their Majorana masses through heavy right-handed neutrinos. From the effective field theory point of view, this is equivalent to dimension-5 operators [4] through electroweak symmetry breaking. Several types of the seesaw mechanism are proposed; for example, Type-I with right-handed neutrinos [1–3], Type-II with a scalar triplet [5–7] and Type-III with at least two fermion triplets [5,8] scenarios. Type-I and Type-II models can further be embedded into the Left-Right Symmetric Model (LRSM) [9–11]. The LRSM attempts to explain the broken parity symmetry of the weak interaction in the SM and can introduce, depending on the form of the model, right-handed counterparts to the W and Z bosons (W_{R} and Z_R), and right-handed heavy neutrinos N_{R} as the parity gauge partners of the corresponding left-handed neutrino fields.

In this analysis, a search for W_{R} bosons decaying to N_{R} and a charged lepton $\ell^{\pm}$ in proton–proton (pp) collisions at a centre-of-mass energy $\sqrt{s} = 13$ TeV with the ATLAS detector is presented, where $\ell^{\pm}$ denotes an electron/positron ($e^{\pm}$) or a muon ($\mu^{\pm}$). The exact process of interest is the Keung–Senjanović (KS) process [11]. In the case where the mass of W_{R} is larger than the N_{R} mass, $m(W_{\mathrm{R}}) > m(N_{\mathrm{R}})$, N_{R} decays into a charged lepton and an off-shell $W_{\mathrm{R}}(W_{\mathrm{R}}^{*})$. In the case of $m(W_{\mathrm{R}}) < m(N_{\mathrm{R}})$, a W_{R} produced off-shell decays into a pair of N_{R} and ℓ, and the N_{R} subsequently decays via the W_{R} resonant state. The charge of the final state leptons is a key feature of the analysis, as it determines the Dirac or Majorana nature of N_{R}. The focus of the search is on hadronic decays of the final-state $W_{\mathrm{R}}^{(*)}$ because of their high branching fractions. The leading-order Feynman diagrams for the KS process targeted by this analysis are shown in Fig. 1. Depending on the target mass range, two types of analyses are performed; one requiring that the two quarks in the final state are clearly separated geometrically and are reconstructed as two separate jets (hereafter labelled as the "resolved" channel), with the second one targeting the $m(W_{\mathrm{R}}) \gg m(N_{\mathrm{R}})$ region where particles from the N_{R} decay are merged due to the Lorentz boost, and are reconstructed as a single large-radius (large-R) jet (the "boosted" channel) [12,13].

Multiple experimental results can give constraints on the target signal of this analysis [14,15]. The LRSM can enhance some low-energy processes, such as K-$\overline{K}$ and $B_{d,s}$-$\overline{B_{d,s}}$ oscillations, via W_{R} contributions in the box diagram. The lower limit on $m(W_{\mathrm{R}})$ from the latest mixing results is about

⋆ e-mail: atlas.publications@cern.ch

Published online: 20 December 2023

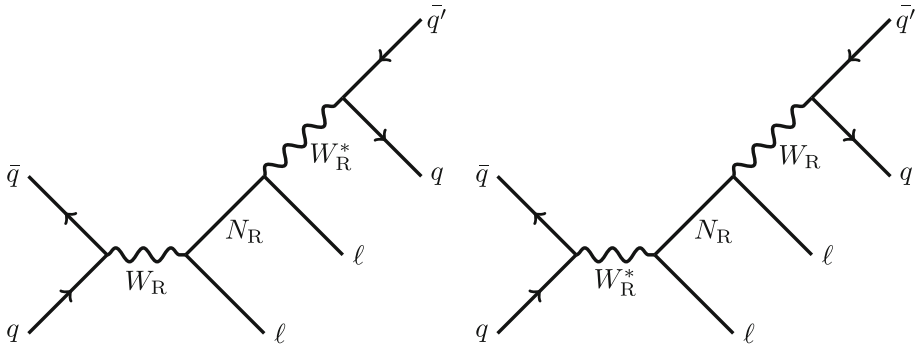

Fig. 1 The Keung–Senjanović process for the $\mathrm{m}(W_{\mathrm{R}}) > \mathrm{m}(N_{\mathrm{R}})$ (left) and the $\mathrm{m}(N_{\mathrm{R}}) > \mathrm{m}(W_{\mathrm{R}})$ (right) cases. The asterisk (*) on the W_{R} denotes an off-shell particle. In the case of Majorana N_{R}, the final state appears with two same-sign charged leptons 50% of the time, violating the lepton number conservation

3 TeV [16,17], assuming equal mixing matrices for left- and right-handed quarks. A Majorana right-handed electron neutrino and W_{R} boson can contribute to the neutrinoless double beta decay ($0\nu\beta\beta$) diagram. Assuming purely right-handed contributions to the $0\nu\beta\beta$ decay, the non-observation of this lepton number violating process can be used to set limits on the W_{R} and N_{R} masses in the LRSM. As an example, at $m(W_{\mathrm{R}}) = 3$ TeV (5 TeV), the upper limit on the N_{R} mass is about 180 GeV (20 GeV) [18,19].

The pp collisions at the Large Hadron Collider (LHC) offer a window into a unique phase space for this search, allowing the exploration of $m(N_{\mathrm{R}})$ in a range from $O(100)$ GeV to a few TeV. Searches by the ATLAS [20–22] and CMS [23–27] collaborations have excluded signals in the LRSM with $m(W_{\mathrm{R}})$ up to about 4.7 TeV and 5 TeV in the electron and muon final states, respectively, for a $m(N_{\mathrm{R}})$ range from 100 GeV to 3 TeV.

2 Signal model

The theoretical framework of LRSM offers the prediction of a right-handed charged current and a mass-generating mechanism for light and heavy neutrinos. The small left-handed neutrino masses are naturally explained via right-handed neutrinos in the Type-I seesaw mechanism, or via SU(2)-triplet scalars in the Type-II seesaw model. Both Type-I and Type-II contributions can coexist in the LRSM.

In the minimal LRSM, the left-handed (i.e. SM-like) neutrinos as well as the right-handed neutrinos are predicted to be Majorana particles. The model thus features the violation of the global lepton number symmetry. In the target KS process, same- and opposite-sign lepton pairs would be equally observed in a 50–50% admixture of signal events. In the LRSM variants that include the inverse seesaw mechanism [28–31], the N_{R} neutrinos are pseudo-Dirac particles formed by two Majorana particles with identical masses [32]. For simple versions of LRSMs incorporating the inverse seesaw mechanism, lepton-number-violating processes are not expected [33]. In this paper we explore both "Dirac" and "Majorana" interpretations of the LRSM.

3 ATLAS detector

The ATLAS experiment [34] at the LHC is a multipurpose particle detector with a forward–backward symmetric cylindrical geometry and a near 4π coverage in solid angle.[1] It consists of an inner tracking detector surrounded by a thin superconducting solenoid providing a 2T axial magnetic field, electromagnetic and hadron calorimeters, and a muon spectrometer (MS). The inner tracking detector covers the pseudorapidity range $|\eta| < 2.5$. It consists of silicon pixel, silicon microstrip, and transition radiation tracking detectors. Lead/liquid-argon (LAr) sampling calorimeters provide electromagnetic (EM) energy measurements with high granularity. A steel/scintillator-tile hadron calorimeter covers the central pseudorapidity range ($|\eta| < 1.7$). The endcap and forward regions are instrumented with LAr calorimeters for both the EM and hadronic energy measurements up to $|\eta| = 4.9$. The MS surrounds the calorimeters and is based on three large superconducting air-core toroidal magnets with eight coils each. The field integral of the toroids ranges between 2.0 and 6.0 T m across most of the detector. The MS includes a system of precision tracking chambers and fast detectors for triggering. A two-level trigger system is used to select events. The first-level trigger (L1) is implemented in hardware and uses a subset of the detector information to accept events at a rate below 100 kHz. This is followed by a software-based high-level trigger (HLT) that reduces the accepted event rate to 1 kHz on average depending on the data-taking conditions. An extensive software suite [35] is used in the reconstruction and analysis of real and simulated data, in detector operations, and in the trigger and data acquisition systems of the experiment.

[1] ATLAS uses a right-handed coordinate system with its origin at the nominal interaction point (IP) in the centre of the detector and the z-axis along the beam pipe. The x-axis points from the IP to the centre of the LHC ring, and the y-axis points upwards. Cylindrical coordinates (r, ϕ) are used in the transverse plane, ϕ being the azimuthal angle around the z-axis. The pseudorapidity is defined in terms of the polar angle θ as $\eta = -\ln\tan(\theta/2)$. Angular distance is measured in units of $\Delta R \equiv \sqrt{(\Delta\eta)^2 + (\Delta\phi)^2}$.

Table 1 Summary of the simulated background events used in this analysis, including name of the event generator, accuracy in QCD when the matrix element is calculated, parton shower algorithm, underlying event (UE) tune, and accuracy in QCD when the cross section is calculated. NLO, NNLO and NNLL denote the next-to-leading order, next-to-next-to-leading order, and next-to-next-to-leading logarithm, respectively, and n_{parton} is the number of partons in the matrix-element calculation. V denotes a W or Z boson

Sample	Generator	Matrix element	Parton shower	UE tune	Cross section
$Z \to \ell\ell$ + jets and	Sherpa 2.2.11 [56]	NLO@$n_{\text{parton}} \leq 2$	Sherpa default [57]	Sherpa default	NNLO [58]
$W \to \ell\nu$ + jets		LO@$n_{\text{parton}} = 3, 4, 5$			
$t\bar{t}$ and single-t	Powheg-Box v2 [59–62]	NLO	Pythia 8.230	A14 tune [54]	NNLO+NNLL [63–69]
VV and VVV	Sherpa 2.2.1 or 2.2.2 [56]	NLO@$n_{\text{parton}} \leq 1$	Sherpa default	Sherpa default	NLO (VV) [70]/
		LO@$n_{\text{parton}} = 2, 3$			NNLO (VVV) [71]
γ + jets	Sherpa 2.1 [56]	LO@$n_{\text{parton}} \leq 3$	Sherpa default	Sherpa default	LO
Multijet	Pythia 8.230 [44]	LO for dijet events	Pythia 8.230	A14 tune [54]	LO

4 Dataset and simulated event samples

The data used in this analysis were collected with the ATLAS detector between 2015 and 2018, and correspond to an integrated luminosity of 139 fb^{-1}. The average number of pp interactions per bunch crossing ("pile-up") in the dataset is 33.7. Only high-quality data, collected when the LHC has declared the beams to be stable and all of the ATLAS subdetectors are reported to be operating well, are analysed [36,37]. All events are required to have a vertex with at least two associated ID tracks with $p_{\text{T}} > 500$ MeV [38,39]. The one with the highest $\sum p_{\text{T}}^2$ of the associated tracks is selected as the primary vertex.

The dataset was collected by single or dilepton triggers with a variety of transverse momentum (p_{T}) and isolation requirements, which depend on the data-taking period. In both resolved and boosted channels, only events in the region of trigger efficiency plateau [40,41] are used. Trigger thresholds are no higher than (24 GeV, 24 GeV) for dielectrons and (22 GeV, 8 GeV) for dimuons in the resolved channel, and 140 GeV for electrons and 50 GeV for muons in the boosted channel. The trigger efficiency for most signal points for both resolved and boosted channels ranges from 90 to 95%, dropping to 85% in the $m(W_{\text{R}}) \sim m(N_{\text{R}})$ region where the compressed phase space affects the charged lepton kinematics. For the resolved analysis, the $e\mu$ trigger is used for the $t\bar{t}$ background estimation. In addition, for the study of mis-identified leptons in the resolved analysis (Sect. 6) some non-isolated, heavily-prescaled single lepton triggers were also used.

Monte-Carlo (MC) simulated events are used to optimise the event selections, and to estimate the background contribution and the systematic uncertainties. For all MC events, the response of the ATLAS detector is simulated using the GEANT4 toolkit [42]. The same reconstruction and trigger algorithms are applied for data and simulated events, using the default ATLAS software [43]. Multiple overlaid pp collisions are simulated with the soft QCD processes of Pythia 8.230 [44] using the A3 set of tuned parameters [45] and the NNPDF2.3LO parton distribution function (PDF) set [46]. MC events are reweighted so that the distribution of the average number of interactions per bunch crossing agrees with the data ("pile-up reweighting").

Table 1 summarises the simulation packages used for the SM background processes. More details are found in other recent ATLAS publications, for example Refs. [47–50]. The multijet and γ + jets samples are used only in the boosted channel.

The signal events for $pp \to W_{\text{R}}^{(*)} \to \ell\ell qq'$ in the LRSM are generated at leading-order (LO) using FeynRules [51] implemented in MadGraph5_aMC@NLO [52] and further modified as described in Ref. [53], where ℓ includes the tau lepton. The generated events are interfaced with

Pythia 8.230 [44] for parton showering and hadronisation. The A14 parameter set is used for tuning the shower [54]. The NNPDF3.1NLO [55] PDF set enters in the matrix element calculation and the NNPDF2.3LO is used in the parton shower.

Lepton flavour mixing, albeit possible in principle in the LRSM, is not considered in this analysis. The branching fractions for the electron, muon and tau channels for W_R decays to N_R of equal masses are assumed to be exactly one-third for each flavour due to lepton universality. For sufficiently heavy W_R masses, $m(W_R) > m_t$, the hadronic final state also includes the $W_R \to tb$ channel. However, b-jets are vetoed in this search to reduce the top background contamination, effectively limiting the phase space to hadronic W_R decays excluding b-quarks. At very low N_R masses of less than 50 GeV, the decay length of N_R is greater than 1 mm [53]. This mass range can be explored by dedicated ATLAS and CMS analyses requiring a displaced vertex, and is beyond the scope of this paper. The $m(W_R)$ and $m(N_R)$ are sampled from 1 TeV to 7 TeV and from 50 GeV to 4 TeV, respectively, at intervals of about 500 GeV. In the $m(W_R) > 10 \times m(N_R)$ region, which is the focus of the boosted channel, the N_R mass is further sampled in steps of 100 GeV. The simulation assumes a Majorana N_R, giving a 50% mixture of same-sign and opposite-sign lepton pairs. For the Dirac neutrino case, only the opposite-sign events are used in the analysis as no other differences are expected, and the production cross section is adjusted appropriately.

5 Object reconstruction

The definitions of the physics objects used in this analysis are summarised in Table 2. Physics objects in the events (electrons, muons, jets, and missing transverse momentum) are separately defined for the resolved and boosted analyses. The orthogonality between the two channels is not enforced: the same event can be used in both analyses, which are not statistically combined.

Electrons are reconstructed as ID tracks, matched to energy clusters in the EM calorimeter within $|\eta| < 2.47$ [72]. The electron candidates in the crack region of the EM calorimeter ($1.37 < |\eta| < 1.52$) are discarded. The electron identification utilises a multivariate likelihood-based discriminant that exploits the shower shapes in the EM calorimeter and the associated track properties. There are 'Loose', 'Medium' and 'Tight' identification working points described in Ref. [72]. To further suppress the mis-identified electrons, an isolation criterion can be applied to the electron candidates. Several isolation working points are defined in Ref. [72] e.g. 'Loose' and 'HighPtCaloOnly'. Slightly different p_T thresholds are used across the resolved and boosted channels to ensure the operation at a region of constant trigger efficiency. For the resolved analysis, electrons are required to have $p_T > 25$ GeV and to satisfy Tight identification and Loose isolation criteria. For the boosted analysis, electrons must have $p_T > 25$ GeV, and satisfy Medium identification and Loose isolation criteria. Additional cuts are applied for the highest-p_T electron candidate in the boosted channel (Sect. 7.1), to ensure that $p_T > 200$ GeV, and to satisfy the Tight identification and HighPtCaloOnly isolation criteria. Tighter isolation criteria are required in the boosted channel because the multijet process with a mis-identified electron is a major source of background.

Muons are reconstructed from MS tracks matching ID tracks in the $|\eta| < 2.5$ region. There are several muon identification working points described in Ref. [73], namely 'Loose', 'Medium', 'Tight' and 'High-p_T'. The resolved channel uses muons with $p_T > 25$ GeV satisfying the Medium identification working point. For muons with $p_T > 300$ GeV, the High-p_T working point requirements must be met. For the boosted channel, muons with $p_T > 28$ GeV satisfying the Medium working point are used. As with electrons, several muon isolation working points are defined in Ref. [73], e.g. 'FixedCutTightTrackOnly' and 'Tight'. The resolved channel requires muons to satisfy the FixedCutTightTrackOnly working point. In the boosted channel, no isolation criterion is required on the muon from the $N_R \to \mu qq'$ decay, as it is not expected to be clearly isolated from the hadrons. Further selection cuts are applied for the highest-p_T muon candidate in the event, namely to have $p_T > 200$ GeV and satisfy the Tight identification and Tight isolation criteria (Sect. 7.1).

For both electrons and muons, track-to-vertex association requirements are employed by using the impact parameter observables. The longitudinal impact parameter of the lepton track, z_0, is required to satisfy $|z_0 \sin\theta| < 0.5$ mm, where θ is the polar angle of the track. In addition, the transverse impact parameter divided by its uncertainty, $|d_0|/\sigma(d_0)$, is required to be less than 5 (3) for electrons (muons). The leptons' reconstruction, identification, isolation and trigger efficiencies differ slightly between simulation and data. The simulation is corrected with scale factors to match the data efficiencies [72,73].

Apart from the baseline leptons described above, leptons with modified requirements are employed for control samples for the estimation of jets misidentified as leptons or non-prompt leptons from decays of hadrons. In the resolved channel, the isolation requirement is inverted and the Loose identification is employed. In the boosted channel, the fraction of events containing fake muons surviving the $p_T > 200$ GeV requirement for the leading lepton is negligibly small. To estimate the hadrons mis-identified as electrons, electron candidates satisfying the Loose but failing the HighPtCaloOnly isolation criterion are used.

Table 2 Definitions of the electrons, muons, small-R and large-R jets, used in this analysis. Optimisations of the object selections are performed separately for the resolved and boosted analyses. See text about the definitions of 'Baseline' and 'Leading' leptons as well as leptons for 'Fake estimation'

		Resolved		Boosted		
		Baseline	**Fake estimation**	**Baseline**	**Leading**	**Fake estimation**
Electrons	$\|\eta\|$	$(0, 1.37]$ or $[1.52, 2.47]$				
	p_{T} (GeV)	> 25		> 25	> 200	
	Quality	`Tight`	`Loose`	`Medium`	`Tight`	
	Isolation	Loose	Fail `Loose` or `Tight`	`Loose`	`HighPtCaloOnly`	`Loose` but fail `HighPtCaloOnly`
		Baseline	**Fake estimation**	**Baseline**	**Leading**	
Muons	p_{T} (GeV)	> 25		> 28	> 200	—
	$\|\eta\|$	< 2.5			< 2.5	—
	Quality	`High-`p_{T} if pT > 300 GeV else `Medium`		`Medium`	`Tight`	—
	Isolation	`FixedCutTightTrackOnly`	fail `FixedCutTightTrackOnly`	—	`Tight`	—
Small-R jet	p_{T} (GeV)	> 20				
	$\|\eta\|$	< 2.5				
Large-R jet	p_{T} (GeV)	—		> 200		
	$\|\eta\|$	—		< 2		

Jets are reconstructed from particle-flow objects [74] using the anti-k_t algorithm [75,76] with radius parameter $R = 0.4$. They are referred to as 'small-R jets' hereafter. A detailed description of the calibration of these jets is found in Ref. [77]. Only small-R jets with $p_{\mathrm{T}} > 20$ GeV and $|\eta| < 2.5$ are considered. Small-R jets with $p_{\mathrm{T}} < 60$ GeV and $|\eta| < 2.4$ from pile-up interactions are suppressed using a jet-vertex tagging (JVT) discriminant [78]. Small-R jets containing b-flavoured hadrons (b-jets) are identified with the `DL1r` multivariate b-tagging algorithms [79,80]. A working point to achieve 77% efficiency for b-jets is employed, which has a rejection factor of 5 for c-jets and 169 for light jets. It is only used to veto events containing jets identified as b-jets.

The missing transverse momentum, with magnitude $E_{\mathrm{T}}^{\mathrm{miss}}$, is calculated using the baseline electrons and the small-R jets in each event as described in Refs. [81,82] using the `Tight` working point. The particle-flow track-based soft term, built from tracks that are matched to the primary vertex but not associated with any other objects, is also used in the calculation. The $E_{\mathrm{T}}^{\mathrm{miss}}$ is used only in the electron channel, and muons are not considered in the calculation, since the muon momentum resolution is significantly degraded in the high-p_{T} region and affects the $E_{\mathrm{T}}^{\mathrm{miss}}$ calculation.

To avoid cases where the detector response to a single physical object is reconstructed as two different final-state objects, e.g. an electron reconstructed as both an electron and a jet, several steps are followed, as summarised in Table 3. To improve the efficiency for muons from N_{R} decays in the boosted analysis, the last step of muon-jet overlap removal is considered only for the highest-p_{T} muon in the event.

In the boosted analysis, the hadronic jets from the N_{R} decay are reconstructed as a single large-R jet. The large-R jet is reconstructed from the small-R jets described above, using the anti-k_t algorithm with $R = 1.0$. For such large-R jets, 're-clustered' from small-R jets, the small-R jet calibration can be propagated. Large-R jets with $p_{\mathrm{T}} > 200$ GeV and $|\eta| < 2.0$ are considered.

6 Resolved channel: event selection and background estimate

6.1 Event reconstruction and selection

The resolved channel targets signals with a mass splitting between W_{R} and N_{R}, i.e. $\Delta m \equiv m(W_{\mathrm{R}}) - m(N_{\mathrm{R}})$, up to 4 TeV. Events passing the following requirements are filtered into datasets comprising signal regions (`SRs`), namely regions where the presence of signal is hypothesised by the theoretical models and the analysis is expected to have high sensitivity. The definitions of the `SRs` are summarised in Table 4. Events are required to have exactly two baseline, same-flavour charged leptons, with $p_{\mathrm{T}} > 40$ GeV for the leading lepton, and at least two small-R jets with $p_{\mathrm{T}} > 100$ GeV. To suppress the Z + jets background, the dilepton invariant mass must satisfy $m_{\ell\ell} > 400$ GeV. Since the focus of this search is the high W_{R} mass region, the following requirements are imposed on the dijet invariant mass (m_{jj}), and the scalar sum of the transverse momentum of the leptons and the two leading small-R jets (h_{T}): $m_{jj} > 110$ GeV and $h_{\mathrm{T}} > 400$ GeV. Events are further separated into two categories based on the charge product of the two leptons: same- (`r`SRSS) or opposite-sign (`r`SROS) lepton pairs, where `r` denotes the resolved channel and `SR` the classification as signal region. The relatively small SM background in `r`SRSS increases the search sensitivity for Majorana N_{R} signals where half of the events are expected to appear with same-sign lepton pairs. The ΔR between the two leptons is required to be less than 3.9 in `r`SRSS to reduce some mismodelling of the simulated

Table 3 The order of overlap removal used in this analysis. ΔR is defined as $\Delta R = \sqrt{\Delta y^2 + \Delta\phi^2}$, where Δy and $\Delta\phi$ are the rapidity and azimuthal-angle differences between two objects. The variables $p_{\mathrm{T}}(e)$, $p_{\mathrm{T}}(\mu)$, $p_{\mathrm{T}}(j)$ and $p_{\mathrm{T}}(\mathrm{trk})$ are the transverse momenta of the corresponding electron, muon, small-R jets, and all tracks associated with the small-R jet. The baseline definitions of electrons and muons are used. In the boosted channel, the last step of muon-jet overlap removal is considered only for the highest-p_{T} muon in the event. Large-R jets are reclustered from small-R jets after the overlap removal

Order	Object discarded	Object kept	Matching condition
1.	Electron	Electron	If two electrons share a track, discard the softer electron
2.	Muon	Electron	If they share a track and the muon type is calorimeter-tagged [73]
3.	Electron	Muon	If they share a track with the remaining muon
4.	Small-R jet	Electron	$\Delta R < 0.2$, but step is skipped if jet is b-tagged and $p_{\mathrm{T}}(e) < 100$ GeV
5.	Electron	Small-R jet	$\Delta R < 0.4$
6.	Small-R jet	Muon	$\Delta R < 0.2$, number of tracks associated to the jet < 3, $p_{\mathrm{T}}(\mu)/p_{\mathrm{T}}(j) > 0.5$ and $p_{\mathrm{T}}(\mu)/\sum p_{\mathrm{T}}(\mathrm{trk}) > 0.7$
7.	Muon	Small-R jet	$\Delta R < 0.4$

diboson background without a signal efficiency loss. Finally, the SRs are separated into electron and muon channels. The four resulting SRs (rSROS2e, rSROS2mu, rSRSS2e and rSRSS2mu) are orthogonal to each other and combined for a statistical analysis in the Majorana N_{R} interpretation. For the Dirac N_{R} interpretation, only rSROS2e and rSROS2mu are considered.

In rSROS, the W_{R} mass is reconstructed by combining the two charged leptons and the two leading small-R jets ($m_{\ell\ell jj}$), and used as the final discriminant for signal points in the $m(W_{\mathrm{R}}) > m(N_{\mathrm{R}})$ region. The $0 < m_{\ell\ell jj} < 5$ TeV region is scanned with a step size of 500 GeV, with one additional overflow bin that includes all events with $m_{\ell\ell jj} > 5$ TeV. For signals with $m(W_{\mathrm{R}}) < m(N_{\mathrm{R}})$, the m_{jj} is used instead as a discriminant, with a similar 500 GeV binning in $0 < m_{jj} <$ 3 TeV, and one additional overflow bin for $m_{jj} > 3$ TeV. The significance of yields is checked in every bin for both discriminants ($m_{\ell\ell jj}$ and m_{jj}) and the appropriate one is used for each ($m(W_{\mathrm{R}})$, $m(N_{\mathrm{R}})$) hypothesis for the interpretation. In the smaller-background rSRSS subset, the variable h_{T} offers slightly better sensitivity and is used instead as the final discriminant. This variable is segmented into five bins: 400–600 GeV, 600–1000 GeV, 1–1.5 TeV, 1.5–2.2 TeV, and > 2.2 TeV, which take into consideration the signal resolution and MC statistical uncertainty in each bin.

6.2 Background estimation

The composition of the SM background is substantially different between rSROS and rSRSS, requiring different estimation techniques in the two categories. SM backgrounds containing two prompt leptons are estimated using simulations in both cases. An overall normalisation correction obtained from the observed data in control regions (CRs) is used for the main background sources: Z + jets, diboson, and $t\bar{t}$ processes. CRs are kinematically similar to SRs, and enriched in the process for which the normalisation correction is applied. Signal contamination is very low (typically 1–2%). A different normalisation correction factor is assigned to each process, and typically treated as a free parameter in the fit discussed in Sect. 9. The validity of the normalisation correction factor is confirmed in validation regions (VRs). The component containing non-prompt or mis-identified leptons is estimated separately by employing a data-driven method. The definitions of SRs, CRs and VRs for the resolved channel are visualised in Fig. 2.

6.2.1 Opposite-sign category

The main SM backgrounds contributing to rSROS are events with top quarks (mainly $t\bar{t}$) and Z + jets production, with contributions of 41% and 45% respectively in rSROS2e and

Table 4 Definition of signal regions in the resolved channel. The baseline definitions of electrons and muons are used

Variable	rSRSS2e	rSRSS2mu	rSROS2e	rSROS2mu
Number of electrons	2	0	2	0
Number of muons	0	2	0	2
Lepton charge	same sign		opposite sign	
Leading lepton p_{T} [GeV]	> 40			
Dilepton mass $m_{\ell\ell}$ [GeV]	> 400			
$\Delta R_{\ell\ell}$	< 3.9		—	
Number of small-R jets with $p_{\mathrm{T}} > 100$ GeV	≥ 2			
Number of b-tagged jets	0			
Dijet mass m_{jj} [GeV]	> 110			
$h_{\mathrm{T}} \equiv p_{\mathrm{T}}(\ell_1) + p_{\mathrm{T}}(\ell_2) + p_{\mathrm{T}}(j_1) + p_{\mathrm{T}}(j_2)$ [GeV]	> 400			

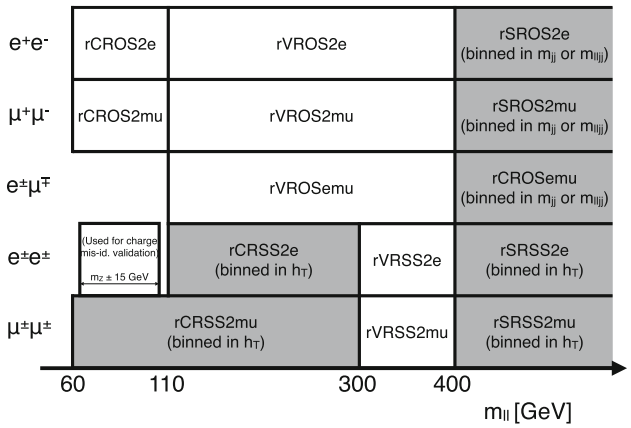

Fig. 2 Resolved channel: Schematic view of SR/CR/VRs definitions. The grey coloured regions are contributing simultaneously to the final fit in the electron or muons channels. The remaining regions are used to verify the background estimations (see text for details)

41% and 48% in rSROS2mu. Minor contributions arise from diboson processes (mainly $ZW \to \ell\ell jj$ and $ZZ \to \ell\ell jj$).

The normalisation factor for Z + jets is estimated in a control region defined by the same selection as rSROS with a modification in the dilepton mass selection: $60 < m_{\ell\ell} < 110$ GeV (rCROS). There is a known issue in the jet multiplicity description of the Z + jets MC sample observed in a previous analysis [21], leading to the mis-modelling of the dijet invariant mass m_{jj}. Following the prescription described therein, a data-driven method is employed to correct for this effect. Electron and muon channels are combined and used to derive the m_{jj}-dependent correction factor. The rCROS data is used after subtracting the top-quark (3%) and other minor prompt-lepton (2%) background contributions evaluated with MC simulation, leaving a distribution with a size of about 94% of the original dataset. The normalisation of the Z + jets MC sample is then scaled to match the resulting rCROS distribution. The data-to-Z + jets MC ratio, r, reaches a maximum value of about 1.05 at $m_{jj} = 300$ GeV, and decreases at the higher-mass region to reach a value of ~ 0.7 at $m_{jj} = 3$ TeV. The ratio r is parameterised by the Novosibirsk function, as discussed in Ref. [21]. The r is used to apply an event-by-event correction to the Z + jets simulated sample in the OS channel. The method corrects not only the m_{jj} shape but also the normalisation of Z + jets in the simulation. Therefore, rCROS is not used in the final distribution fit discussed in Sect. 9.

The $t\bar{t}$ background is estimated with the same selection as rSROS, but by requiring a different flavour for the two charged leptons i.e. $m_{e\mu} > 400$ GeV (rCROSemu). The normalisation factor is treated as a free parameter in the final fit, but determined mainly in rCROSemu due to its high purity in $t\bar{t}$($\sim 80\%$), with dibosons being the other main component ($\sim 19\%$).

The validity of the background estimations described above is checked in the validation region rVROS, defined in an intermediate $m_{\ell\ell}$ region between SR and CR, i.e. $110 < m_{\ell\ell} < 400$ GeV. An additional validation region is defined with the same selection as rSROS but with an $e\mu$ pair instead of two same-flavour charged leptons (rVROSemu). Validation results are presented in Sect. 9.1.

6.2.2 *Same-sign category*

Diboson processes (mainly $WZ \to \ell\ell$ and same-sign $W^{\pm}W^{\pm} \to \ell^{\pm}\nu\ell^{\pm}\nu$) are the main background source in rSRSS. In particular, about 83% of the background in rSRSS2mu can be attributed to dibosons. In addition, there are non-negligible contributions from $Z(\to ee)$ + jets and top-quark events with charge mis-identification in rSRSS2e. The background contributions from diboson and charge mis-identified processes in rSRSS2e are 29% and 39%.

The diboson background is estimated with the same selection as rSRSS, but by requiring $110 < m_{ee} < 300$ GeV or $60 < m_{\mu\mu} < 300$ GeV (rCRSS). To increase the CR dataset size, no selection is applied on h_{T} or m_{jj}. The validity of the background estimation technique is confirmed in

the $300 < m_{\ell\ell} < 400$ GeV validation region (rVRSS), with validation results shown in Sect. 9.1.

The charge-mis-identified background consists of events with two opposite-sign electrons, one of which has its charge sign mis-measured. The most frequent cause of electron charge flip is the bremsstrahlung effect. The probability of an electron undergoing charge mis-identification is measured in the data [83] and compared to the MC prediction. A correction factor is then derived for the charge flip probability and applied to simulated events featuring same-sign electron pairs. The method is validated in a same-sign dielectron region with $|m_{ee} - m_Z| < 15$ GeV, which does not overlap with the rCRSS region ($110 < m_{ee} < 300$ GeV). The data agrees well with the corrected prediction within uncertainties. This result confirms the validity of the correction factor for the charge-flip probability in a limited m_{ee} range, but does not cover a possible mis-modelling of the extended m_{ee} distribution. Unlike opposite-sign Z + jets, the normalisation of the same-sign Z + jet sample is therefore free to float and determined mainly in rCRSS2e.

Another smaller background contribution comes from mis-identified leptons originating from non-isolated, non-prompt electrons and muons produced by secondary decays of light- or heavy-flavour hadrons. Another significant component of fake electrons arises from photon conversions, as well as from jets that are misreconstructed as electrons. The contribution of events with mis-identified leptons is estimated by a data-driven technique, known as the "fake-factor" method. The fake factor F is defined as the ratio of mis-identified leptons satisfying the baseline lepton criteria (labelled as Tight in this section) to those satisfying the selection criteria for fake estimation (Loose). The factors are estimated separately for electrons and muons. The fake factors calculated in Ref. [84] are used in this analysis, as common object definitions are employed. Fake factors are measured in data as a function of lepton p_{T} and η in control samples that are orthogonal to the SR, VR, and CRs used in this analysis.

The contribution of mis-identified leptons in SR, VR, and CRs is estimated as follows. The calculated F is applied to events satisfying the same selection criteria as in SR, VR, and CRs but by lowering the lepton ID requirement from Tight to Loose for at least one lepton. The signal contamination in these regions is found to be small (typically 1–2%) and ignored here. Three categories are considered separately, depending on the identification criteria satisfied by the leading and sub-leading leptons: they are the LT (Loose–Tight), TL (Tight–Loose) and LL (Loose–Loose) categories. Data events are weighted with fake factors according to the loose-lepton multiplicity of the region:

$$N^{\text{fake}} = [F(N_{TL} + N_{LT}) - F^2 N_{LL}]_{\text{data}} - [F(N_{TL} + N_{LT}) - F^2 N_{LL}]_{\text{MC}}^{\text{prompt } \ell \text{ only}} \quad (1)$$

with N_{TL}, N_{LT}, N_{LL} denoting the number of events in the corresponding category. The prompt lepton contribution in the events with Loose leptons is subtracted using the MC simulation to account for the prompt-lepton contamination in the given category.

The composition of rCRSS is dibosons (32%), charge mis-identified background (45%) and fakes (20%) in the electron channel, and dibosons (65%), fakes (27%) and charge mis-identified background (8%) in the muon channel.

7 Boosted channel: event selection and background estimate

7.1 Event reconstruction and selection

The boosted analysis is designed for signals in the $\Delta m > 4$ TeV region by using the large-R jet to reconstruct the hadrons from the N_{R} decay. The signal events have a very energetic charged lepton and N_{R} from the W_{R} decay produced back-to-back in the x–y plane. In the highest Δm region, the large-R jet overlaps with the lepton from the N_{R} decay. In the muon channel, such a muon inside the jet can be identified, and a single SR (bSR2mu) with two baseline muons is used to cover the full Δm range. On the other hand, in the electron channel, calorimeter clusters from the electron from the N_{R} decay overlap with other hadron activities, making its identification challenging. Two signal regions, bSR1e and bSR2e, are thus defined requiring exactly one and two baseline electrons in the event, respectively, to cover the higher and lower Δm ranges. The W_{R} mass is reconstructed from the large-R jet and the electron (m_{eJ}) in bSR1e, and from the large-R jet and the two charged leptons (m_{eeJ} and $m_{\mu\mu J}$, or collectively $m_{\ell\ell J}$) in bSR2e and bSR2mu. Due to the relatively small background after the event selections, the sensitivity gain by separating SR into same- and opposite-sign events is marginal, hence the lepton charge is not considered in the boosted analysis.

For all three SRs, the requirement that only one large-R jet is reconstructed in the event is imposed, which is expected to cover about 90% of signal events. This selection cut is useful in suppressing the multijet background, and improving the fake-lepton, multijet and γ + jets modelling by the LO simulation with the exception of an overall normalisation factor. Assuming well-isolated and highly-boosted leptons from the prompt W_{R} decay, tighter identification and isolation criteria (as detailed in Sect. 5) are required for the lepton with the highest-p_{T} in the event. The azimuthal difference between the large-R jet and the highest-p_{T} lepton is required to be greater than 2. In addition, to suppress the top-quark backgrounds, the number of b-tagged small-R jets is required to be zero.

7.1.1 One-electron category (bSR1e)

Region bSR1e requires exactly one electron from the W_R decay, with the large-R jet encapsulating all decay products of the heavy neutrino $N_R \to eqq'$. A $E_T^{miss} < 200$ GeV selection is applied to suppress the main background process, $W(\to e\nu)$ + jets. The high-p_T electron and low E_T^{miss} requirements bias the W + jets events towards higher helicity angles, $|\cos\theta| \sim 1.0$, where θ is the polar angle of the electron from the W boson decay in the rest frame of the W.[2] The $|\cos\theta| > 0.7$ region is used for the signal search. The $|\cos\theta| < 0.7$ region is used for the normalisation of the W + jets contribution. To further reduce the γ + jets and dijet contributions, a selection on the η difference between the large-R jet and the electron candidate, $\Delta\eta = |\eta(J) - \eta(e)| < 2$ is applied. The bSR1e definition is summarised in Table 5.

7.1.2 Two-electrons category (bSR2e)

Region bSR2e covers the intermediate Δm region between bSR1e and the resolved analysis. The events are selected if they contain exactly two electrons and one large-R jet. The $E_T^{miss} < 200$ GeV selection is applied to further reduce the $t\bar{t}$ background. The dominant background source is $Z(\to ee)$ + jets. To remove contributions from the pole mass of the Z boson, a $m_{ee} > 200$ GeV selection is applied. The bSR2e definition is summarised in Table 5. bSR1e and bSR2e are orthogonal to each other and are statistically combined to obtain the final results.

7.1.3 Two-muons category (bSR2mu)

Events are selected in bSR2mu if they contain exactly two muons and one large-R jet. A $m_{\mu\mu} > 200$ GeV selection is applied. The upper cut on E_T^{miss} is not useful in this channel due to the deteriorated momentum resolution for very high-p_T muons. Instead, the dimuon system's p_T is required to be greater than 200 GeV to suppress the $t\bar{t}$ background. The bSR2mu definition is also summarised in Table 5.

7.1.4 Event categorisation for the background estimation

The normalisations of the main background sources, $W(\to e\nu)$ + jets and $Z(\to \ell\ell)$ + jets, as well as for the processes with less reliable yield predictions, γ + jets and multijet, are estimated from data in control regions and adjusted by using the SR-to-CR ratio in the simulation.

In each category, the reconstructed W_R mass distribution is segmented into four bins; 1–2 TeV, 2–3 TeV, 3–4 TeV, and > 4 TeV, having considered the search sensitivity for signals with various W_R masses and the stability of the background estimation. High-mass W_R signals are expected to be observed in the third and fourth bins, which are designated bins 1 and 2 of the SR for each channel (for example, bins 1 and 2 of bSR2mu for the two-muon case). The first bin of the W_R mass histogram is used for the SM background determination in a region where the presence of lower-mass W_R signals is negligibly small, given exclusion limits obtained in previous ATLAS analyses [22]. For the two-electron and two-muon categories, the first bin is used to estimate the Z + jets background normalisation in designated bCRZ2e and bCRZ2mu, respectively. In the one-electron case, the 1–2 TeV $m(W_R)$ bin is used to distinguish between γ + jets and W + jets events. If there is an additional ID track with opposite charge within $\Delta R < 0.3$ and $|\Delta z_0 \sin\theta| < 0.5$ from the electron candidate track, the electron is possibly coming from a photon conversion and the events are categorised into bCRγ1e. The remaining events are categorised into bCRLow1e. The fractions of W + jets, Z + jets, multijet and γ + jets are about 33%, 10%, 24% and 30%, respectively, in bCRγ1e, and approximately 73%, 17%, 3% and 1% in bCRLow1e.

The normalisation for $W(\to e\nu)$ + jets and multijet events is estimated in the dedicated control regions, bCRW1e and bCRFake1e, requiring $|\cos\theta| < 0.7$ and the inverted electron isolation cut, respectively, with the remaining selection identical to that of bCRLow1e. The purity of the W + jets and multijet events in bCRW1e and bCRFake1e is about 83% and 91%. One should note that the γ + jets contribution in bCRFake1e is not large since mis-identified electrons from photon conversions can satisfy the tight isolation requirement.

The estimated CR normalisation factors are extrapolated to higher-mass bins. The validity of the method is first checked in the second bin ($m(W_R) = [2, 3]$ TeV) in each channel: bVR2e, bVR2mu and bVR1e, for bSR2e, bSR2mu and bSR1e, before the third and fourth bins are tested. In addition, the regions with $|\cos\theta| < 0.7$ and the inverted electron isolation in the one-electron channel are used to check the extrapolation of W + jets and multijet normalisations from the lower to the higher W_R mass bins. The regions are segmented into 2–3 TeV and > 3 TeV and labelled as bVRW1e and bVRFake1e, respectively.

To check the extrapolation of the Z + jets normalisation from the lower to the higher W_R mass bins, additional validation regions are defined (bVRZ2e and bVRZ2mu), but which are not used in the final fit. They require $120 < m_{\ell\ell} < 200$ GeV instead of > 200 GeV.

[2] The W boson rest frame is calculated from the E_T^{miss} and the reconstructed electron by solving the kinematic equation for the neutrino momentum in the z-axis direction ($p_{z,\nu}$) and by assuming a W boson mass of 80.4 GeV.

Table 5 Definition of the signal regions in the boosted analysis. The baseline definitions of electrons and muons are used. Two regions in the electron channel cover higher- and lower-Δm regions, where Δm denotes the mass difference between W_R and N_R

Region	bSR1e (higher Δm)	bSR2e (lower Δm)	bSR2mu
Number of large-R jets	1		
Number of electrons	1	2	0
Number of muons	0	0	2
Leading lepton p_T [GeV]	> 200		
E_T^{miss} [GeV]	< 200		—
$\lvert\cos\theta\rvert$	> 0.7	—	—
$\Delta\phi_{J,\ell_1}$	> 2.0		
$\Delta\eta_{J,\ell_1}$	< 2.0	—	—
Dilepton p_T (GeV)	—	—	> 200
Dilepton mass $m_{\ell\ell}$[GeV]	—	> 200	
Number of b-tagged small-R jets	0		

The definitions of SRs, CRs and VRs for the boosted channel are visualised in Fig. 3. Validation results are presented in Sect. 9.2.

7.2 Background estimation

For the W + jets and Z + jets estimation in the boosted analysis, since the number of jets is forced to be one, the correction for jet multiplicity mis-modelling used in the resolved analysis is not required. The simulated W_R mass distributions for W + jets in bVRW1e (with $|\cos\theta| < 0.7$) and those for Z + jets bVRZ2e and bVRZ2mu agree well with the observed data. The W_R mass distributions in these regions are only used to confirm the normalisation methodology for each process and these are within the considered uncertainties.

The fake lepton contribution is negligibly small in bSR2e and bSR2mu after the requirement of a high-p_T selection on the leading lepton. It is, however, not negligible at the higher W_R mass tail in bSR1e. MC simulation is used to estimate the non-prompt electron contribution with a data-driven correction factor obtained in the CR. The simulated W_R mass in bVRFake1e agrees well with the multijet sample within the uncertainties considered. In the final fits the normalisation is mainly constrained by bCRFake1e and its validity in the SR relies on the good simulation of the isolation efficiency for fake electrons. To check the validity of this approach, two additional regions beyond those shown in Fig. 3 are defined, corresponding to bSR1e and bCRFake1e: the electron candidate is forced to satisfy the Medium identification but fail the Tight identification criterion in order to be orthogonal to the SR, CRs and VR. The remaining selection is the same as in bSR1e (bCRFake1e), with the requirement to satisfy (fail) the HighPtCaloOnly isolation criterion. In both regions, the purity of the multijet process is greater than 90%. By comparing data to MC in both regions, it is found that the simulated isolation efficiency for fake electrons agrees with the data within the considered uncertainties. A small data/MC disagreement on $m(W_R)$ distribution is considered as an additional uncertainty on the multijet estimation in bSR1e.

The γ + jets contribution with isolated electrons from photon conversions is also estimated by MC simulation with a normalisation factor determined in a data-driven way. Additional validation regions are defined requiring exactly one reconstructed photon instead of an electron, with the remaining selection the same as in bSR1e. The purity of γ + jets sample in this region is about 70%, and the fraction of multijet events is 30%. The reconstructed W_R mass with the photon (in the place of the electron) and the large-R jet agrees between data and MC within the considered uncertainties. The p_T- and η-dependent photon conversion rate may change the reconstructed W_R mass distribution for the γ + jets process, but this rate mainly depends on the detector geometry and it is well modelled in the simulation. The normalisation of the γ + jets contribution is estimated mainly from bCRγ1e, by requiring an additional ID track close to the electron. The modelling of the fraction of events with an ID track close to the electron in simulated W + jets and multijets can affect the γ + jets estimation, so a comparison is carried out with data in bCRW1e and bCRFake1e. For the γ + jets contribution, the same check is performed in the $\Delta\eta > 2.0$ region. The purity of γ + jets in this region is about 50%, and a conservative uncertainty on the other background subtraction is included in the study.

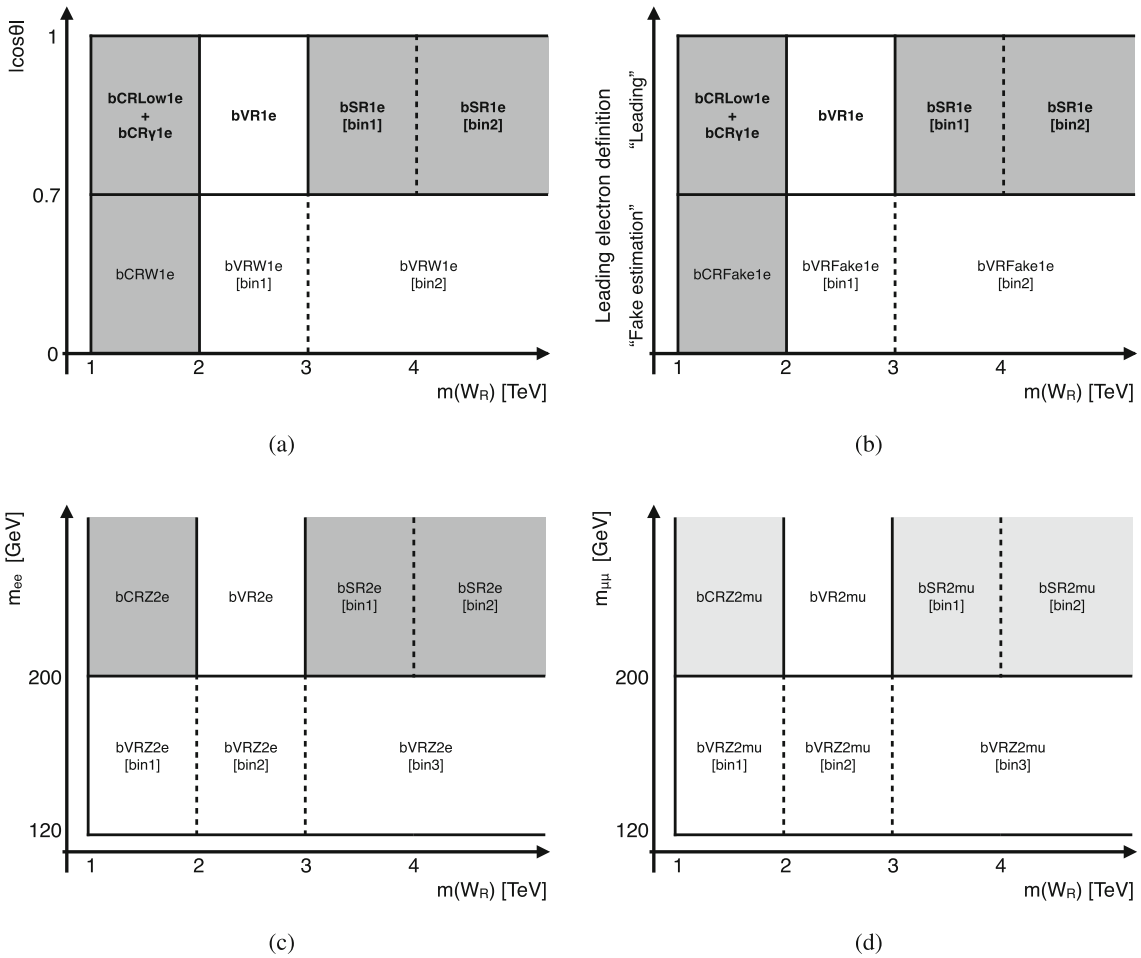

Fig. 3 Boosted channel: Schematic view of SR/CR/VRs definitions for bSR1e (**a**), (**b**), bSR2e (**c**) and bSR2mu (**d**). **a** and **b** show the regions for the estimation of W + jets and multijet backgrounds, respectively. The labels bSR1e, bVR1e, bCRLow1e and bCRγ1e shown in bold in the two figures correspond to the same regions. The dark-grey coloured regions in **a**, **b** and **c** are contributing simultaneously to the final fit in the electron channel, while the light-grey coloured regions in **d** are used for the muon channel, separately. The remaining regions are used to verify the background estimations (see text for details)

8 Systematic uncertainties

Several experimental and theoretical systematic uncertainties are considered, affecting both the background and signal predictions as well as the total event yield. In addition, the statistical uncertainty of the MC simulated events is also considered. These uncertainties also affect the shape of the variables used in the fit, with the exception of the luminosity and cross-section uncertainties.

The uncertainty on the integrated luminosity is 1.7% [85], It is obtained using the LUCID-2 detector [86] for the primary luminosity measurements. The uncertainty due to the pile-up reweighting procedure is estimated by varying the amount of pile-up in the simulation to cover the uncertainty in the ratio of the predicted and measured inelastic cross section [87].

A set of experimental systematic uncertainties arise from the energy and momentum calibrations of leptons and jets, the lepton reconstruction, isolation and trigger efficiencies, and the jet vertex tagger and flavour-tagging efficiencies. The largest uncertainty in the total SM yield arises from the energy calibration and smearing of jets, derived in Ref. [77], and is between 1 and 6% in the SS and about 4% in the OS in the resolved channel, and between 5 and 12% in the boosted channel, depending on the signal region. Uncertainties associated with lepton reconstruction, identification, isolation and trigger efficiencies, as well as energy or momentum calibration [41,72,88] and b-jet tagging [79,89], vary between 5% (OS) and 13% (SS) of the total SM yield in the resolved analysis, and between 2 and 5% in the boosted. These uncertainties are propagated to the $E_{\mathrm{T}}^{\mathrm{miss}}$ calculation. In addition, uncertainties on the scale and resolution of the 'soft term' of the $E_{\mathrm{T}}^{\mathrm{miss}}$ are taken into account [81]. In bSR2mu, the muon p_{T} is further smeared by taking into account the impact of MS outliers on the muon resolution not described by the simulation. This additional effect is considered as the high-p_{T} muon uncertainty.

There are three additional sources of systematic uncertainty associated with the background estimation techniques. In rSRSS, the uncertainty related to the charge misidentification probability of electrons arises from the statistical uncertainty of the data and simulated samples of Z + jets events used in this measurement. The uncertainty is around 6.8% with a mild dependence on the electron E_{T} and η [90]. The uncertainty on the fake estimation arises from the limited knowledge in the composition of fakes, as well as from the statistical uncertainty and prompt lepton subtraction used to derive F in the fake-enriched regions. The uncertainty due to the composition of fakes is estimated by varying the nominal criteria defining the selection sample used in the fake-factor measurement [84]. The effect on the SM yields is 3.8% (electrons) and 0.8% (muons). In rSROS, an additional uncertainty is associated with the m_{jj} reweighting of the Z + jets process. This is evaluated by comparing the shape difference between the reweighted simulated m_{jj} distribution and the one measured in data, using rVROS: the uncertainty in the reweighting factor is found to vary between 0.4 and 0.8%, as a function of the dijet invariant mass. This observed difference covers all possible mismodellings of the Z + jets shape, hence additional theoretical uncertainties for the Z + jets process are not considered in the resolved channel.

In the boosted channel, the theory uncertainties estimated for the W + jets, Z + jets, diboson, multijet and γ + jets background processes are considered, which include the choice of QCD renormalisation (μ_r) and factorisation (μ_f) scales, choice of the PDF set and α_S, as well as CKKW matching scale and the resummation scale. The QCD scale uncertainty is estimated by varying μ_r and μ_f to half and twice their nominal values. The PDF uncertainty is estimated using the envelope of the NNPDF3.0 PDF set, as recommended in Ref. [91]. In addition, the MMHT2014 [92] and CT14NNLO [93] PDF sets are used to estimate the uncertainty due to the PDF choice. Moreover, the uncertainty due to α_S is evaluated by varying its nominal value of 0.118 by ± 0.001. The CKKW matching scale is the parameter to remove the overlap between jets from the matrix element calculation and the parton shower algorithm. The nominal value is 20 GeV, and the uncertainty is estimated by varying it to 30 GeV and 15 GeV. The uncertainty on the resummation scale of soft gluon emission is estimated by varying the parameter to half and twice the nominal value. The largest theory uncertainties generally originate from the CKKW matching and Sherpa resummation scales ($\sim 20\%$), and QCD scales variations which range between 10% and 20%, depending on the simulated process and the mass of the target signal.

The theory uncertainties associated with $t\bar{t}$ processes are as follows. The uncertainty from hard scatter generation is evaluated by comparing the Powheg-Box and MG5_aMC@NLO generators, both interfaced to the Pythia 8.186 [94] parton shower model. The uncertainty due to the hadronisation and fragmentation model is determined by comparing the nominal Powheg-Box + Pythia 8.186 generated sample with the one generated by Powheg-Box interfaced to Herwig [95] (version 7.13). The uncertainty related to the amount of initial- and final-state radiation (ISR and FSR) is assessed by varying parton shower settings. The largest theory uncertainty generally originates from the amount of initial- and final-state radiation and is between 0.4–0.5% (ISR) and 0.6% (FSR) of the $t\bar{t}$ process yield.

In the boosted analysis, additional uncertainties are considered by comparing different MC samples on the possible variations of the reconstructed $m(W_{\mathrm{R}})$, $\cos\theta$ and the isolation efficiency for the fake electrons. For W/Z + jets, the nominal Sherpa 2.2.11 samples are compared with the samples generated with MadGraph5_aMC@NLO+Pythia 8.186. For γ + jets, the nominal Sherpa 2.1 sample is compared with the alternative sample generated with Pythia 8.235 [44]. The nominal Pythia 8.230 multijet MC sample is compared with the sample generated with Sherpa 2.2.5. For the multijet sample, an additional uncertainty on the $m(W_{\mathrm{R}})$ shape is considered by taking the residual non-closure in studies employing different electron identification discussed in Sect. 7.2. The possible mis-modelling of the bCRγ1e to bCRLow1e ratio is evaluated by considering the observed discrepancy in the CRs.

The theory uncertainty of the signal efficiency times acceptance amounts to 20%. It is evaluated by varying renormalisation and factorisation scales as described above and by using alternative PDF sets, CTEQ6 [96] and MSTW [97]. The α_S emission scale factor is also varied to half and twice the nominal value. The uncertainty is dominated by the variation in factorisation scale. The variations are performed using SysCalc [98].

The systematic uncertainties in each SR are summarised in Fig. 4. Individual uncertainties can be correlated with others, and do not necessarily add in quadrature towards the total background uncertainty.

9 Statistical analysis and results

The search for a W_{R} and N_{R} signal is carried out using the theoretical model described in Sect. 2. The statistical treatment is done separately for samples containing electrons and muons since there is no theoretical motivation that the N_{R} should have the same mass across different flavours. The resolved and boosted channels are analysed independently. The statistical interpretation is performed by carrying out binned maximum-likelihood fits using the HistFitter [99] framework. The likelihood is a product of Poisson probability density functions, describing the observed number of events in each bin of regions involved in the fit, and Gaussian distributions that describe the nuisance parameters asso-

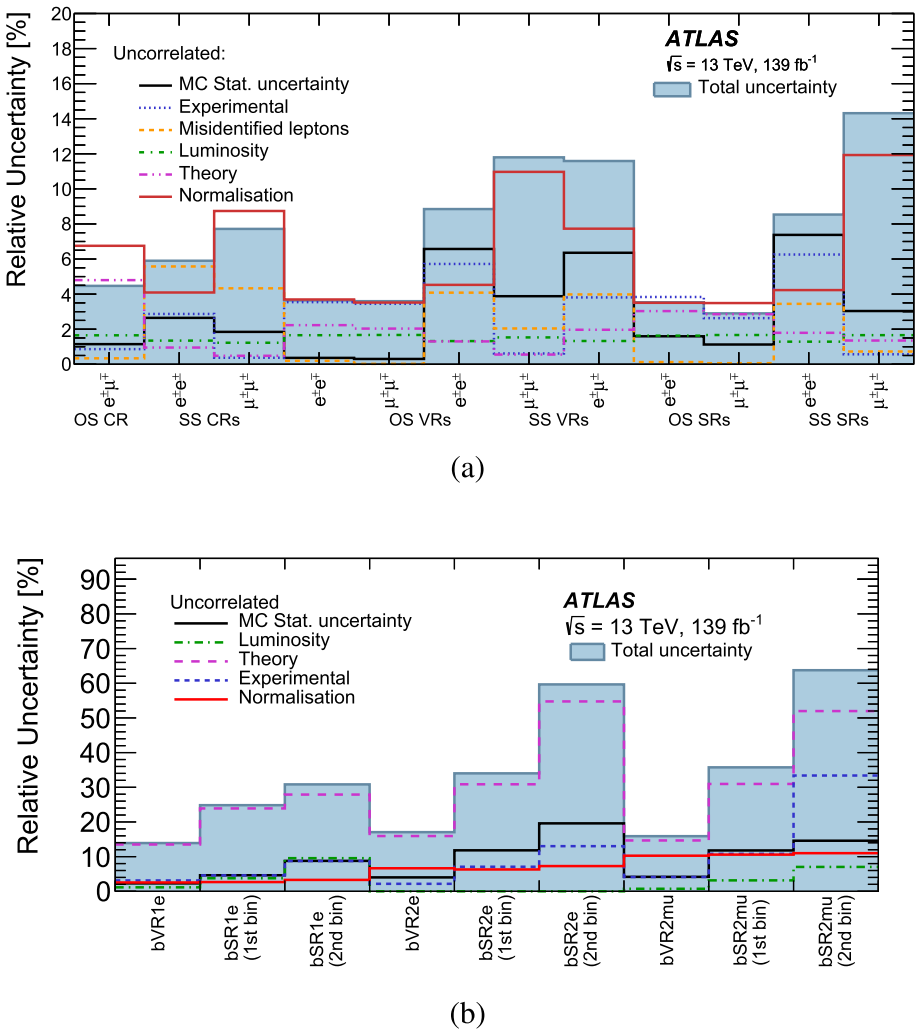

Fig. 4 Relative uncertainties in the total background yield post-fit estimates for the **a** resolved and **b** boosted channels. "Theory" indicates the theoretical uncertainty associated with the simulated physics processes (e.g. cross sections). "Normalisation" is the uncertainty associated with the yield variations of the dominant backgrounds in the fit. "Experimental" corresponds to the combined uncertainty on physics object efficiencies (such as trigger, identification or isolation) and uncertainties associated with $E_{\mathrm{T}}^{\mathrm{miss}}$ and pile-up. The total uncertainty takes into account any correlations among nuisance parameters

ciated with each of the systematic uncertainties. Systematic uncertainties that are correlated between different samples and different regions are accounted for via a common nuisance parameter.

A "background-only" fit is carried out first by using the observed event yield in CRs assuming that no signal contributes in these regions, and by applying the resulting normalisation factor to the number of background events predicted by simulation for the equivalent process in the validation regions. The normalisation factors of the background processes are allowed to vary freely. The VRs are only employed to confirm the validity of the background modelling in the background-only CR fits, and do not contribute to the search results presented here.

A non-zero signal contribution for each $m(W_{\mathrm{R}})$ and $m(N_{\mathrm{R}})$ mass point is then allowed involving both SR and CRs in the fit, as summarised in Figs. 2 and 3. The normalisation factors of the various (signal or background) processes are allowed to vary freely. Upper limits at 95% CL on the signal strength of the KS process are calculated using the $\mathrm{CL_s}$ method [100] and the profile likelihood-ratio as the test statistic. The asymptotic method [101] was used, but similar results were obtained with toy MC tests.

9.1 Resolved channel

In the resolved channel, the $m_{\ell\ell jj}$ distribution is used in the rSROS fit when $m(W_{\mathrm{R}}) > m(N_{\mathrm{R}})$. In the $m(W_{\mathrm{R}}) < m(N_{\mathrm{R}})$ case, the fit results are obtained by employing the m_{jj} distribution. The h_{T} distribution is used in the rSRSS fit. For the scenario in which the N_{R} neutrino is a Majorana particle, the OS and SS channels are fitted simultaneously, whereas for the Dirac neutrino scenario, only the OS channel is used in the fit.

A combined "background-only" fit is first carried out in the rCROSemu, rCRSS2e and rCRSS2mu regions. The free normalisation factors for the $t\bar{t}$ and diboson processes are estimated mainly from rCROSemu and rCRSS2mu. The validity of the evaluated normalisation factors for same-sign Z + jets, $t\bar{t}$ and diboson samples is confirmed by applying them in the rVROS2e, rVROS2mu, rVRSSemu, rVRSS2e, and rVRSS2mu regions. All systematic uncer-

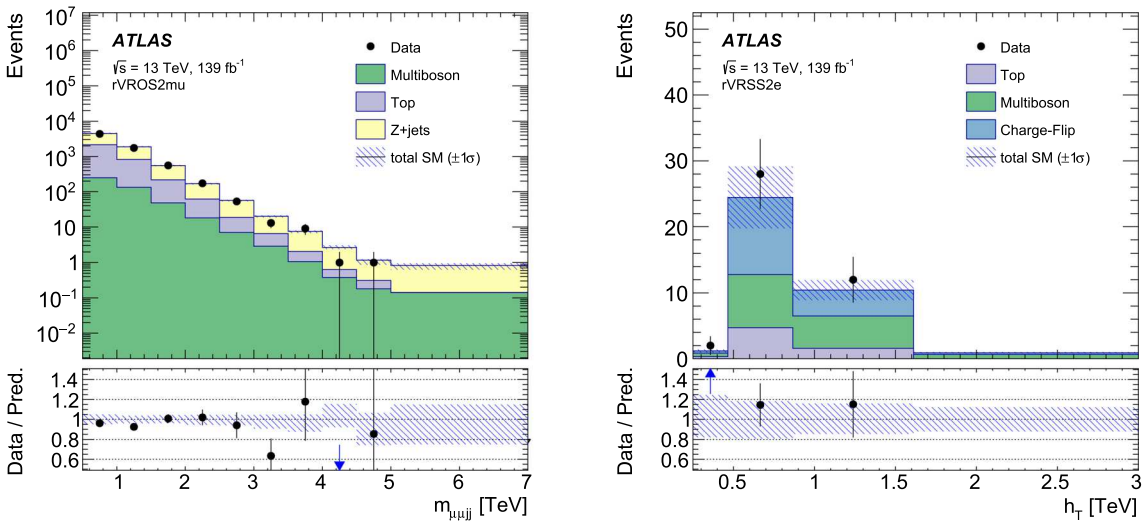

(a) (b)

Fig. 5 VR fits in the resolved channel: **a** $m_{\ell\ell jj}$ in rVROS2mu and **b** h_{T} distribution in rVRSS2e. 'Top' refers to all processes containing at least one top quark. 'Multiboson' refers to VV and VVV processes, where $V = W$ or Z. The expected background is determined via a fit on the CR data. The hatched band ('total SM') includes all post-fit systematic uncertainties, having taken into account all correlations among various sources. A blue arrow indicates an out-of-range data point for a given bin

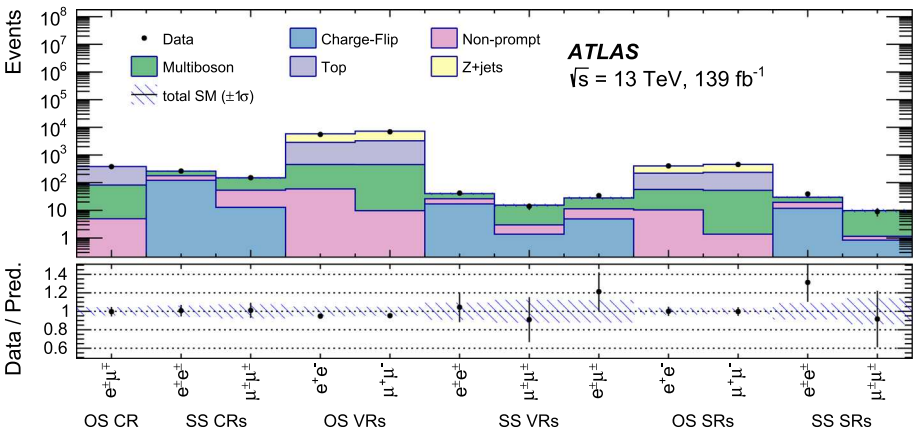

Fig. 6 CR/VR/SR fits in the resolved channel: Integrated number of events for observed data and expected background in $e\mu$ (OS), and ee and $\mu\mu$ (SS) CR, ee and $\mu\mu$ (OS), and ee, $\mu\mu$ and $e\mu$ VR and ee and $\mu\mu$ (both OS and SS) SRs. 'Top' refers to all processes containing at least one top quark. 'Multiboson' refers to VV and VVV processes, where $V = W$ or Z. The expected background is determined via a fit on the CR data. The hatched bands ('total SM') include all post-fit systematic uncertainties, having taken into account all correlations among various sources

tainties described in Sect. 8 are considered as nuisance parameters. Figure 5 shows an example of the post-fit $m_{\ell\ell jj}$ distribution in rVROS2mu and h_{T} distribution in rVRSS2e, showing a good agreement between the observed data and the expected background.

The integrated event counts for the observed data and the estimated background for the CR, VR and SR regions are shown in Fig. 6. The post-fit $m_{\ell\ell jj}$ and m_{jj} distributions in rSROS and h_{T} distributions in rSRSS are shown in Fig. 7. In all cases, no significant deviation above the expected background is observed in the data. The largest excess is observed in rSRSS2e around $h_T \sim 1.0$ TeV (Fig. 7e): 39 events are observed in a region where 24.0 ± 2.4 background events are expected. The observed deviation is in a background-rich region and is not consistent with the shape of the signal.

Exclusion limits at 95% CL on the signal strength of the KS process as a function of $m(W_{\mathrm{R}})$ and $m(N_{\mathrm{R}})$ are calculated. The results are shown in Fig. 9. For electron Majorana neutrinos, the excluded region extends to a W_{R} mass of 5.6 TeV and to a N_{R} mass of 3.5 TeV. For muon Majorana

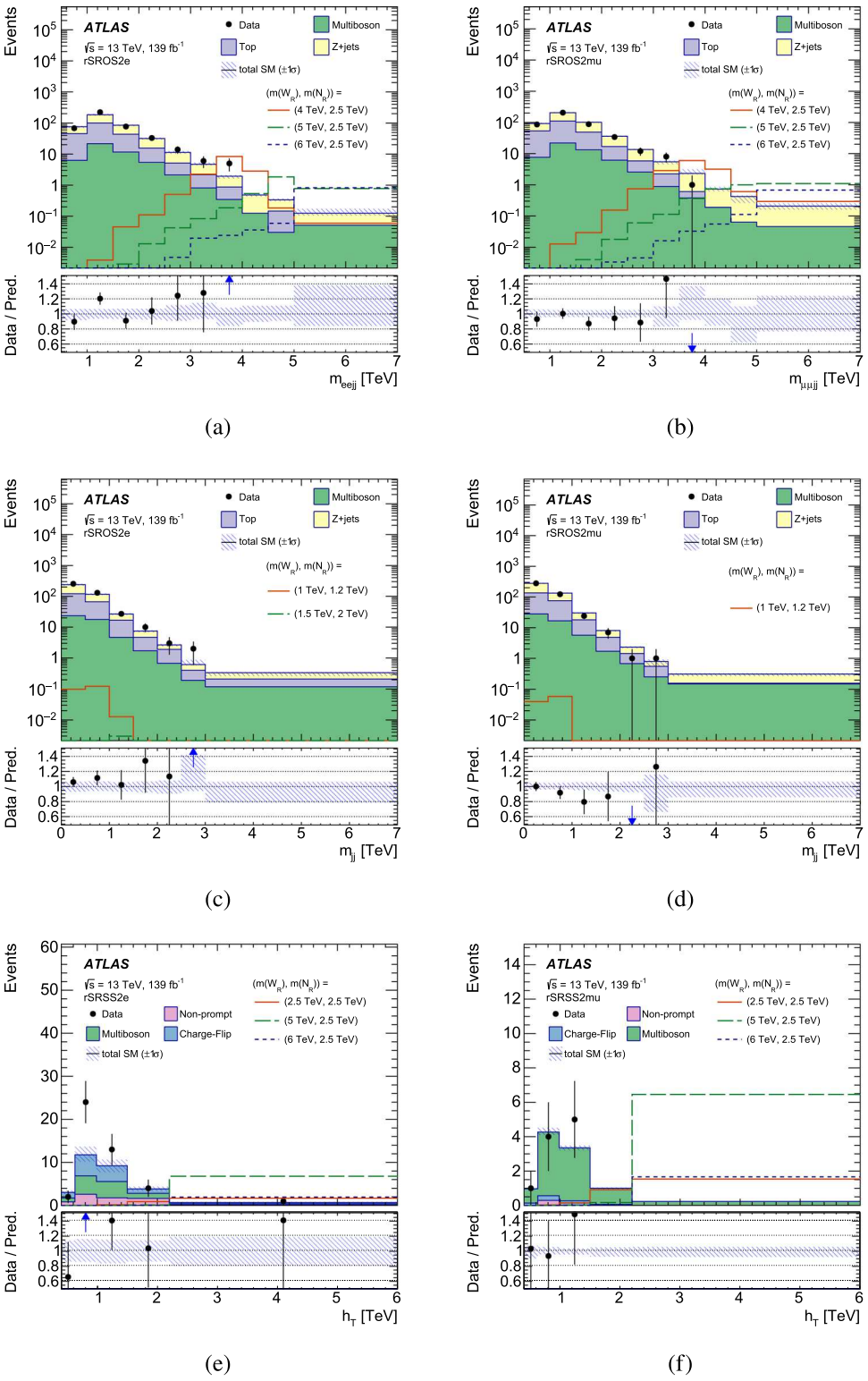

Fig. 7 SR fits in the resolved channel: The $m_{\ell\ell jj}$ distributions in **a** rSROS2e and **b** rSROS2mu, the m_{jj} distributions in **c** rSROS2e and **d** rSROS2mu, and the h_{T} distributions in **e** rSRSS2e and **f** rSRSS2mu. 'Top' refers to all processes containing at least one top quark. 'Multiboson' refers to VV and VVV processes, where $V = W$ or Z. 'Non-prompt' and 'Charge-Flip' refer to processes containing a mis-identified electron and Z + jets with charge mis-identification. The background expectation is the result of the fit to the CR data. The hatched bands ('total SM') include all systematic uncertainties post-fit with the correlation between various sources taken into account. A blue arrow indicates an out-of-range data point for a given bin

neutrinos, W_{R} masses of up to 5.7 TeV were excluded, and N_{R} masses of up to 3.6 TeV. For electron Dirac neutrinos, the excluded region extends to a W_{R} mass of 5.9 TeV and to a N_{R} mass of 3.6 TeV. For muon Dirac neutrinos, W_{R} masses of up to 5.8 TeV were excluded, and N_{R} masses of up to 3.8 TeV. Compared to the previous ATLAS analysis in the resolved channel [21], the exclusion limits on the W_{R} masses are extended by 0.8–1.2 TeV in the case of $m(W_{\mathrm{R}}) > m(N_{\mathrm{R}})$.

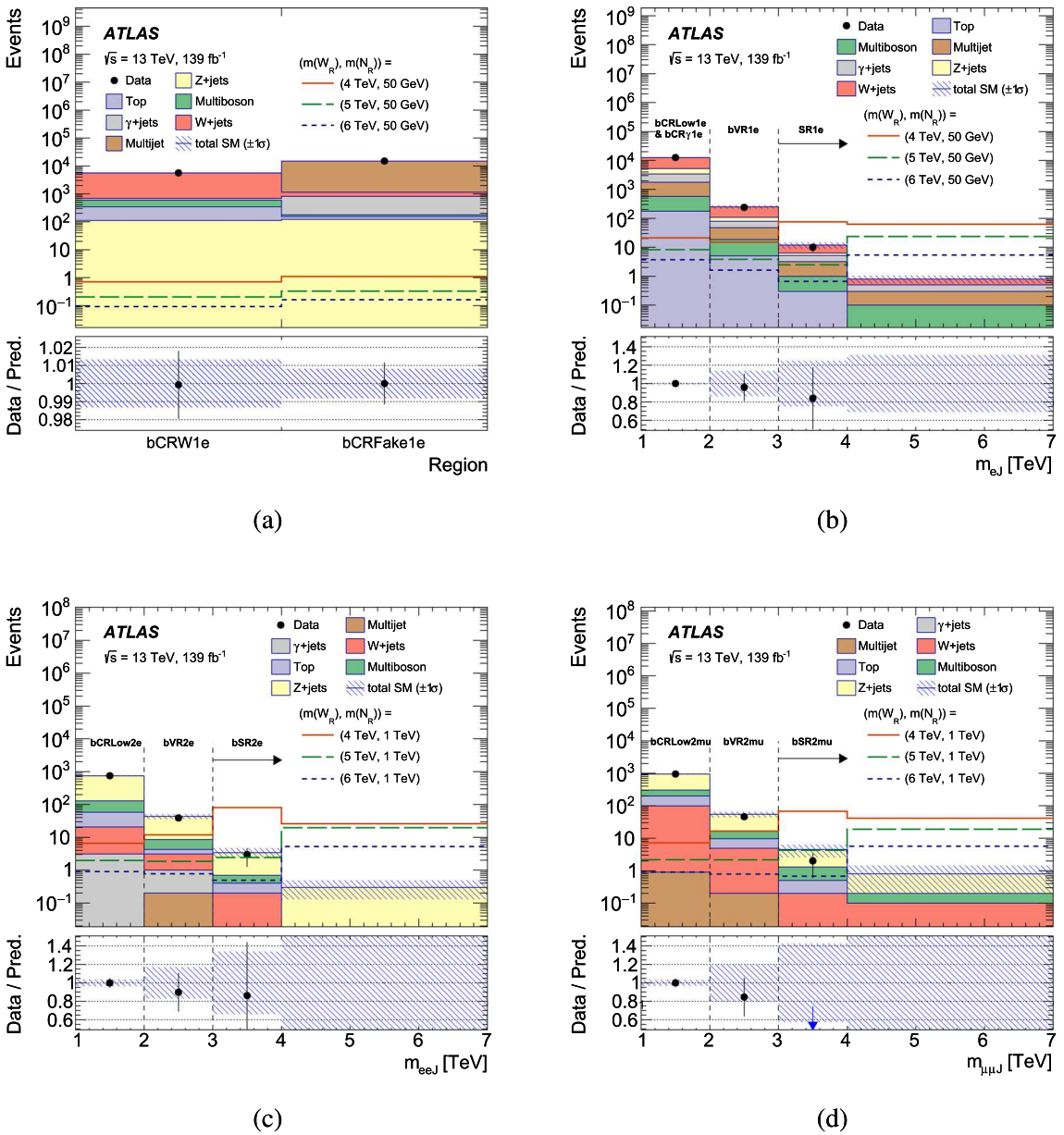

Fig. 8 CR/VR/SR fits in the boosted channel: Integrated number of events for observed data and expected background in bCRW1e and bCRFake1e (**a**), and observed $m(W_R)$ distributions in 1e (**b**), 2e (**c**) and 2mu (**d**) categories. For **b**–**d**, the first and second bins are used as CR and VR, and the third and fourth bins correspond to the SR. 'Top' refers to all processes containing at least one top quark. 'Multiboson' refers to VV and VVV processes, where $V = W$ or Z. The expected background is determined via a fit on the CR data. The hatched bands ('total SM') include all post-fit systematic uncertainties, having taken into account all correlations among various sources. A blue arrow indicates an out-of-range data point for a given bin

9.2 Boosted channel

In the boosted channel, the reconstructed $m(W_R)$ distribution (m_{eJ} or $m_{\ell\ell J}$) is used exclusively since $m(W_R) \gg m(N_R)$. In the electron channel, the normalisations of W + jets, Z + jets, γ + jets and multijet samples are simultaneously estimated by the fit in the CRs and SRs. In the muon channel, only the Z + jet contribution is estimated by the fit.

A combined "background-only" fit is performed separately in the electron and muon channels in the bCRW1e, bCRFake1e, bCRγ1e, bCRLow1e and bCRZ2e, and bCRZ2mu regions, respectively. The normalisation factors for W + jets, Z + jets, γ + jets and multijet are free to float in the electron channel, while only the Z + jets normalisation is treated as a free parameter in the muon channel. The validity of the method is confirmed by applying the normali-

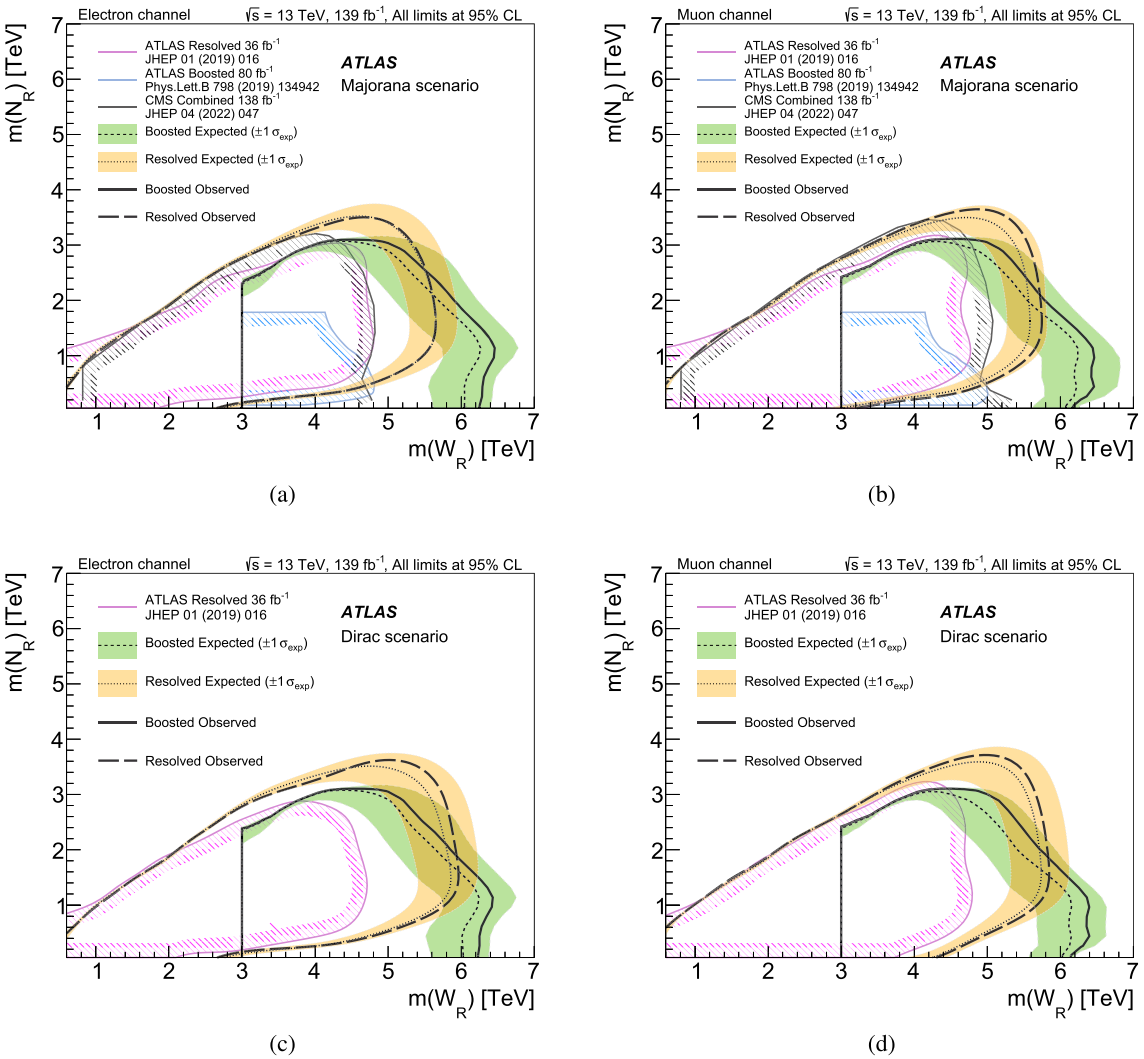

Fig. 9 Expected and observed 95% CL upper limits for the Majorana (top) and Dirac (bottom) neutrino interpretations in the electron (left) and muon (right) channels. Exclusion limits from previous ATLAS [21,22] and CMS [27] searches are overlaid for comparison

sation factors obtained with the fit in the bVR1e and bVR2e regions in the electron channel, and the bVR2mu region in the muon channel. As shown in Fig. 8, a good agreement between data and the estimated SM background is found in all CRs and VRs.

The post-fit $m(W_R)$ distributions for 1e, 2e and 2mu categories are found in Fig. 8. The first bin in the 1e category shows the sum of bCRLow1e and bCRγ1e. Again, no significant deviation above the expected background is observed in the data.

Exclusion limits at 95% CL on the signal strength of the KS process as a function of $m(W_R)$ and $m(N_R)$ are calculated again, with the results shown in Fig. 9. For Majorana neutrinos, the most stringent lower limit on the W_R mass is 6.4 TeV, observed in both electron and muon channels at $m(N_R) < 1$ TeV. This result is an improvement over previous ATLAS searches, and extends the exclusion limits on $m(W_R)$ by about 1.5 TeV. There is a particular improvement in the $m(N_R) < 100$ GeV region via the incorporation of the new bSR1e region and the optimisation of bSR2mu. The observed limit on $m(W_R)$ is 6.2 (6.1) TeV in the electron (muon) channel at $m(N_R) = 50$ GeV.

10 Conclusion

A search for right-handed W_R bosons and heavy right-handed Majorana or Dirac neutrinos N_R is presented. The analysis uses various final states depending on the mass difference between W_R and N_R: two jets and a pair of charged leptons ($\ell\ell jj$), one large-R jet and two charged leptons ($\ell\ell J$), or one large-R jet and one electron (eJ), with $\ell = e, \mu$. It is performed with a 139 fb^{-1} sample of pp collisions at $\sqrt{s}$ = 13 TeV recorded by the ATLAS detector at LHC. No

evidence of W_R bosons or Majorana or Dirac heavy neutrinos is found assuming the KS process, and lower limits are set on $m(W_R)$ and $m(N_R)$, assuming equality of left- and right-handed weak couplings ($g_L = g_R$). The excluded region for the Majorana neutrinos extends to about $m(W_R) = 6.4$ TeV for $m(N_R) = 1$ TeV in both electron and muon channels. The $m(N_R)$ limits reach about 3.5 TeV in the electron channel and 3.6 TeV in the muon channel (for $m(W_R) = 4.8$ TeV). For Dirac neutrinos, limits reach about $m(W_R) = 6.4$ TeV for $m(N_R) = 1$ TeV in both electron and muon channels. Limits of $m(N_R)$ up to 3.6 TeV in the electron channel and 3.8 TeV in the muon channel for $m(W_R) = 5.0$ TeV are set. The new results constitute the most stringent limits to date for the KS process.

Acknowledgements We thank CERN for the very successful operation of the LHC, as well as the support staff from our institutions without whom ATLAS could not be operated efficiently. We acknowledge the support of ANPCyT, Argentina; YerPhI, Armenia; ARC, Australia; BMWFW and FWF, Austria; ANAS, Azerbaijan; CNPq and FAPESP, Brazil; NSERC, NRC and CFI, Canada; CERN; ANID, Chile; CAS, MOST and NSFC, China; Minciencias, Colombia; MEYS CR, Czech Republic; DNRF and DNSRC, Denmark; IN2P3-CNRS and CEA-DRF/IRFU, France; SRNSFG, Georgia; BMBF, HGF and MPG, Germany; GSRI, Greece; RGC and Hong Kong SAR, China; ISF and Benoziyo Center, Israel; INFN, Italy; MEXT and JSPS, Japan; CNRST, Morocco; NWO, Netherlands; RCN, Norway; MEiN, Poland; FCT, Portugal; MNE/IFA, Romania; MESTD, Serbia; MSSR, Slovakia; ARRS and MIZŠ, Slovenia; DSI/NRF, South Africa; MICINN, Spain; SRC and Wallenberg Foundation, Sweden; SERI, SNSF and Cantons of Bern and Geneva, Switzerland; MOST, Taiwan; TENMAK, Türkiye; STFC, United Kingdom; DOE and NSF, United States of America. In addition, individual groups and members have received support from BCKDF, CANARIE, Compute Canada and CRC, Canada; PRIMUS 21/SCI/017 and UNCE SCI/013, Czech Republic; COST, ERC, ERDF, Horizon 2020 and Marie Skłodowska-Curie Actions, European Union; Investissements d'Avenir Labex, Investissements d'Avenir Idex and ANR, France; DFG and AvH Foundation, Germany; Herakleitos, Thales and Aristeia programmes co-financed by EU-ESF and the Greek NSRF, Greece; BSF-NSF and MINERVA, Israel; Norwegian Financial Mechanism 2014-2021, Norway; NCN and NAWA, Poland; La Caixa Banking Foundation, CERCA Programme Generalitat de Catalunya and PROMETEO and GenT Programmes Generalitat Valenciana, Spain; Göran Gustafssons Stiftelse, Sweden; The Royal Society and Leverhulme Trust, United Kingdom. The crucial computing support from all WLCG partners is acknowledged gratefully, in particular from CERN, the ATLAS Tier-1 facilities at TRIUMF (Canada), NDGF (Denmark, Norway, Sweden), CC-IN2P3 (France), KIT/GridKA (Germany), INFN-CNAF (Italy), NL-T1 (Netherlands), PIC (Spain), ASGC (Taiwan), RAL (UK) and BNL (USA), the Tier-2 facilities worldwide and large non-WLCG resource providers. Major contributors of computing resources are listed in Ref. [102].

Data Availability Statement This manuscript has associated data in a data repository. [Authors' comment: All ATLAS scientific output is published in journals, and preliminary results are made available in Conference Notes. All are openly available, without restriction on use by external parties beyond copyright law and the standard conditions agreed by CERN. Data associated with journal publications are also made available: tables and data from plots (e.g. cross section values, likelihood profiles, selection efficiencies, cross section limits, ...) are stored in appropriate repositories such as HEPDATA (http://hepdata.cedar.ac.uk/). ATLAS also strives to make additional material related to the paper available that allows a reinterpretation of the data in the context of new theoretical models. For example, an extended encapsulation of the analysis is often provided for measurements in the framework of RIVET (http://rivet.hepforge.org/). This information is taken from the ATLAS Data Access Policy, which is a public document that can be downloaded from http://opendata.cern.ch/record/413 [opendata.cern.ch.]

Funded by SCOAP[3]. SCOAP[3] supports the goals of the International Year of Basic Sciences for Sustainable Development.

References

1. P. Minkowski, $\mu \to e\gamma$ at a rate of one out of 10^9 muon decays? Phys. Lett. B **67**, 421 (1977). https://doi.org/10.1016/0370-2693(77)90435-X
2. T. Yanagida, Horizontal symmetry and masses of neutrinos. Conf. Proc. **C7902131**, 95 (1979)
3. M. Gell-Mann, P. Ramond, R. Slansky, Complex spinors and unified theories. Conf. Proc. **C790927**, 315 (1979). arXiv:1306.4669 [hep-th]
4. S. Weinberg, Baryon- and lepton-nonconserving processes. Phys. Rev. Lett. **43**, 1566 (1979). https://doi.org/10.1103/PhysRevLett.43.1566
5. M. Magg, C. Wetterich, Neutrino mass problem and gauge hierarchy. Phys. Lett. B **94**, 61 (1980). https://doi.org/10.1016/0370-2693(80)90825-4
6. T.P. Cheng, L.-F. Li, Neutrino masses, mixings, and oscillations in SU(2)×U(1) models of electroweak interactions. Phys. Rev. D **22**, 2860 (1980). https://doi.org/10.1103/PhysRevD.22.2860
7. R.N. Mohapatra, G. Senjanović, Neutrino masses and mixings in gauge models with spontaneous parity violation. Phys. Rev. D **23**, 165 (1981). https://doi.org/10.1103/PhysRevD.23.165
8. R. Foot, H. Lew, X.G. He, G.C. Joshi, See-saw neutrino masses induced by a triplet of leptons. Z. Phys. C **44**, 441 (1989). https://doi.org/10.1007/BF01415558
9. J.C. Pati, A. Salam, Lepton number as the fourth "color". Phys. Rev. D **10**, 275 (1974). https://doi.org/10.1103/PhysRevD.10.275. [Erratum: Phys. Rev. D **11**, 703 (1975)]
10. R.N. Mohapatra, J.C. Pati, "Natural" left-right symmetry. Phys. Rev. D **11**, 2558 (1975). https://doi.org/10.1103/PhysRevD.11.2558
11. G. Senjanović, R.N. Mohapatra, Exact left-right symmetry and spontaneous violation of parity. Phys. Rev. D **12**, 1502 (1975). https://doi.org/10.1103/PhysRevD.12.1502
12. M. Mitra, R. Ruiz, D.J. Scott, M. Spannowsky, Neutrino jets from high-mass W_R gauge bosons in TeV-scale left-right symmetric models. Phys. Rev. D (2016). https://doi.org/10.1103/physrevd.94.095016

13. A. Ferrari et al., Sensitivity study for new gauge bosons and right-handed Majorana neutrinos in pp collisions at $\sqrt{s} = 14$ TeV. Phys. Rev. D **62**(1), 013001 (2000). https://doi.org/10.1103/PhysRevD.62.013001
14. M. Lindner, F.S. Queiroz, W. Rodejohann, C.E. Yaguna, Left-right symmetry and lepton number violation at the large hadron electron collider. JHEP **06**, 140 (2016). https://doi.org/10.1007/JHEP06(2016)140. arXiv:1604.08596 [hep-ph]
15. S.S. Biswal, P.S.B. Dev, Probing left-right seesaw models using beam polarization at an e^+e^- collider. Phys. Rev. D **95**, 115031 (2017). https://doi.org/10.1103/PhysRevD.95.115031. arXiv:1701.08751 [hep-ph]
16. S. Bertolini, A. Maiezza, F. Nesti, Present and future K and B meson mixing constraints on TeV scale left-right symmetry. Phys. Rev. D **89**, 095028 (2014). https://doi.org/10.1103/PhysRevD.89.095028. arXiv:1403.7112 [hep-ph]
17. A. Maiezza, M. Nemevšek, Strong P invariance, neutron electric dipole moment, and minimal left-right parity at LHC. Phys. Rev. D **90**, 095002 (2014). https://doi.org/10.1103/PhysRevD.90.095002. arXiv:1407.3678 [hep-ph]
18. M. Agostini et al., Final results of GERDA on the search for neutrinoless double-*beta* decay. Phys. Rev. Lett. **125**, 252502 (2020). https://doi.org/10.1103/PhysRevLett.125.252502. arXiv:2009.06079 [nucl-ex]
19. S. Abe et al., Search for the Majorana nature of neutrinos in the inverted mass ordering region with KamLAND-Zen. Phys. Rev. Lett. **130**, 051801 (2023). https://doi.org/10.1103/PhysRevLett.130.051801. arXiv:2203.02139 [hep-ex]
20. ATLAS Collaboration, Search for heavy Majorana neutrinos with the ATLAS detector in pp collisions $\sqrt{s} = 8$ TeV. JHEP **07**, 162 (2015). https://doi.org/10.1007/JHEP07(2015)162. arXiv:1506.06020 [hep-ex]
21. ATLAS Collaboration, Search for heavy Majorana or Dirac neutrinos and right-handed W gauge bosons in final states with two charged leptons and two jets at $\sqrt{s} = 13$ TeV with the ATLAS detector. JHEP **01**, 016 (2019). https://doi.org/10.1007/JHEP01(2019)016. arXiv:1809.11105 [hep-ex]
22. ATLAS Collaboration, Search for a right-handed gauge boson decaying into a high-momentum heavy neutrino and a charged lepton in pp collisions with the ATLAS detector at $\sqrt{s} = 13$ TeV. Phys. Lett. B **798**, 134942 (2019). https://doi.org/10.1016/j.physletb.2019.134942. arXiv:1904.12679 [hep-ex]
23. CMS Collaboration, Search for heavy neutrinos and W_R bosons with right-handed couplings in a left-right symmetric model in pp collisions at $\sqrt{s} = 7$ TeV. Phys. Rev. Lett. **109**, 261802 (2012). https://doi.org/10.1103/PhysRevLett.109.261802. arXiv:1210.2402 [hep-ex]
24. CMS Collaboration, Search for a heavy right-handed W boson and a heavy neutrino in events with two same-flavor leptons and two jets at $\sqrt{s} = 13$ TeV. JHEP **05**, 148 (2018). https://doi.org/10.1007/JHEP05(2018)148. arXiv:1803.11116 [hep-ex]
25. CMS Collaboration, Search for heavy neutrinos and third-generation leptoquarks in hadronic states of two τ leptons and two jets in proton–proton collisions at $\sqrt{s} = 13$ TeV. JHEP **03**, 170 (2019). https://doi.org/10.1007/JHEP03(2019)170. arXiv:1811.00806 [hep-ex]
26. CMS Collaboration, Search for heavy Majorana neutrinos in same-sign dilepton channels in proton-proton collisions at $\sqrt{s} = 13$ TeV. JHEP **01**, 122 (2019). https://doi.org/10.1007/JHEP01(2019)122. arXiv:1806.10905 [hep-ex]
27. CMS Collaboration, Search for a right-handed W boson and a heavy neutrino in proton–proton collisions at $\sqrt{s} = 13$ TeV. JHEP **04**, 047 (2021). https://doi.org/10.1007/JHEP04(2022)047. arXiv:2112.03949 [hep-ex]
28. R.N. Mohapatra, Mechanism for understanding small neutrino mass in superstring theories. Phys. Rev. Lett. **56**, 561 (1986). https://doi.org/10.1103/PhysRevLett.56.561
29. R.N. Mohapatra, J.W.F. Valle, Neutrino mass and baryon-number nonconservation in superstring models. Phys. Rev. D **34**, 1642 (1986). https://doi.org/10.1103/PhysRevD.34.1642
30. C.-Y. Chen, P.S.B. Dev, Multilepton collider signatures of heavy Dirac and Majorana neutrinos. Phys. Rev. D **85**, 093018 (2012). https://doi.org/10.1103/PhysRevD.85.093018. arXiv:1112.6419 [hep-ph]
31. P.S. Bhupal Dev, R.N. Mohapatra, Unified explanation of the $eejj$, diboson and dijet resonances at the LHC. Phys. Rev. Lett. **115**, 181803 (2015). https://doi.org/10.1103/PhysRevLett.115.181803. arXiv:1508.02277 [hep-ph]
32. L. Wolfenstein, Different varieties of massive Dirac neutrinos. Nucl. Phys. B **186**, 147 (1981). https://doi.org/10.1016/0550-3213(81)90096-1
33. A. Das, P.S.B. Dev, R.N. Mohapatra, Same sign versus opposite sign dileptons as a probe of low scale seesaw mechanisms. Phys. Rev. D **97**, 015018 (2018). https://doi.org/10.1103/PhysRevD.97.015018. arXiv:1709.06553 [hep-ph]
34. ATLAS Collaboration, The ATLAS experiment at the CERN large hadron collider. JINST **3**, S08003 (2008). https://doi.org/10.1088/1748-0221/3/08/S08003
35. ATLAS Collaboration, The ATLAS Collaboration software and firmware. ATL-SOFT-PUB-2021-001 (2021). https://cds.cern.ch/record/2767187
36. ATLAS Collaboration, ATLAS data quality operations and performance for 2015–2018 data-taking. JINST **15**, P04003 (2020). https://doi.org/10.1088/1748-0221/15/04/P04003. arXiv:1911.04632 [physics.ins-det]
37. ATLAS Collaboration, Selection of jets produced in 13 TeV proton–proton collisions with the ATLAS detector. ATLAS-CONF-2015-029 (2015). https://cds.cern.ch/record/2037702
38. ATLAS Collaboration, Vertex reconstruction performance of the ATLAS detector at $\sqrt{s} = 13$ TeV. ATL-PHYS-PUB-2015-026 (2015) https://cds.cern.ch/record/2037717
39. ATLAS Collaboration, Reconstruction of primary vertices at the ATLAS experiment in Run 1 proton–proton collisions at the LHC. Eur. Phys. J. C **77**, 332 (2017). https://doi.org/10.1140/epjc/s10052-017-4887-5. arXiv:1611.10235 [hep-ex]
40. ATLAS Collaboration, Performance of the ATLAS muon triggers in Run 2. JINST **15**, P09015 (2020). https://doi.org/10.1088/1748-0221/15/09/p09015. arXiv:2004.13447 [hep-ex]
41. ATLAS Collaboration, Performance of electron and photon triggers in ATLAS during LHC Run 2. Eur. Phys. J. C **80**, 47 (2020). https://doi.org/10.1140/epjc/s10052-019-7500-2. arXiv:1909.00761 [hep-ex]
42. S. Agostinelli et al., Geant4—a simulation toolkit. Nucl. Instrum. Methods Phys. Res. Sect. A: Accel. Spectrom. Detect. Assoc. Equip. **506**, 250 (2003). ISSN:0168-9002
43. ATLAS Collaboration, The ATLAS simulation infrastructure. Eur. Phys. J. C **70**, 823 (2010). https://doi.org/10.1140/epjc/s10052-010-1429-9. arXiv:1005.4568 [physics.ins-det]
44. T. Sjöstrand et al., An introduction to PYTHIA 8.2. Comput. Phys. Commun **191**, 159 (2015). https://doi.org/10.1016/j.cpc.2015.01.024. arXiv:1410.3012 [hep-ph]
45. ATLAS Collaboration, The Pythia 8 A3 tune description of ATLAS minimum bias and inelastic measurements incorporating the Donnachie–Landshoff diffractive model. ATL-PHYS-PUB-2016-017 (2016). https://cds.cern.ch/record/2206965
46. NNPDF Collaboration, R.D. Ball et al., Parton distributions with LHC data. Nucl. Phys. B **867**, 244 (2013). https://doi.org/10.1016/j.nuclphysb.2012.10.003. arXiv:1207.1303 [hep-ph]
47. ATLAS Collaboration, Measurement of the production of a W boson in association with a charmed hadron in pp col-

lisions at $\sqrt{s} = 13$ TeV with the ATLAS detector Phys. Rev. D **108**, 032012, https://journals.aps.org/prd/abstract/10.1103/PhysRevD.108.032012 (2023). arXiv:2302.00336 [hep-ex]
48. Modelling and computational improvements to the simulation of single vector-boson plus jet processes for the ATLAS experiment. JHEP **2208**, 089 (2022). https://doi.org/10.1007/JHEP08(2022)089. arXiv:2112.09588. https://cds.cern.ch/record/2798348
49. ATLAS Collaboration, Studies on top-quark Monte Carlo modelling with Sherpa and MG5_aMC@NLO. ATL-PHYS-PUB-2017-007 (2017). https://cds.cern.ch/record/2261938
50. Prospects for the $\mathcal{B}(B^0_{(s)} \to \mu^+\mu^-)$ measurements with the ATLAS detector in the Run 2 and HL-LHC data campaigns. Technical report. All figures including auxiliary figures are available at https://atlas.web.cern.ch/Atlas/GROUPS/PHYSICS/PUBNOTES/ATL-PHYS-PUB-2018-005. CERN (2018). https://cds.cern.ch/record/2317211
51. A. Alloul, N.D. Christensen, C. Degrande, C. Duhr, B. Fuks, FeynRules 2.0—a complete toolbox for tree-level phenomenology. Comput. Phys. Commun. **185**, 2250 (2014). https://doi.org/10.1016/j.cpc.2014.04.012. arXiv:1310.1921 [hep-ph]
52. J. Alwall et al., The automated computation of tree-level and next-to-leading order differential cross sections, and their matching to parton shower simulations. JHEP **2014** (2014). https://doi.org/10.1007/jhep07(2014)079. arXiv:1405.0301 [hep-ph]
53. M. Nemevšek, F. Nesti, G. Popara, Keung–Senjanović process at the LHC: from lepton number violation to displaced vertices to invisible decays. Phys. Rev. D **97**, 115018 (2018). https://doi.org/10.1103/PhysRevD.97.115018. arXiv:1801.05813 [hep-ph]
54. ATLAS Collaboration, ATLAS Pythia 8 tunes to 7 TeV data. ATL-PHYS-PUB-2014-021 (2014). https://cds.cern.ch/record/1966419
55. The NNPDF Collaboration, R.D. Ball et al., Parton distributions for the LHC run II. JHEP **04**, 040 (2015). https://doi.org/10.1007/JHEP04(2015)040. arXiv:1410.8849 [hep-ph]
56. E. Bothmann et al., Event generation with Sherpa 2.2. SciPost Phys. **7**, 034 (2019). https://doi.org/10.21468/SciPostPhys.7.3.034. arXiv:1905.09127 [hep-ph]
57. S. Schumann, F. Krauss, A parton shower algorithm based on Catani–Seymour dipole factorisation. JHEP **03**, 038 (2008). https://doi.org/10.1088/1126-6708/2008/03/038. arXiv:0709.1027 [hep-ph]
58. C. Anastasiou, L. Dixon, K. Melnikov, F. Petriello, High-precision QCD at hadron colliders: electroweak gauge boson rapidity distributions at next-to-next-to leading order. Phys. Rev. D **69**, 094008 (2004). https://doi.org/10.1103/PhysRevD.69.094008. arXiv:hep-ph/0312266
59. S. Frixione, G. Ridolfi, P. Nason, A positive-weight next-to-leading-order Monte Carlo for heavy flavour hadroproduction. JHEP **09**, 126 (2007). https://doi.org/10.1088/1126-6708/2007/09/126. arXiv:0707.3088 [hep-ph]
60. P. Nason, A new method for combining NLO QCD with shower Monte Carlo algorithms. JHEP **11**, 040 (2004). https://doi.org/10.1088/1126-6708/2004/11/040. arXiv:hep-ph/0409146
61. S. Frixione, P. Nason, C. Oleari, Matching NLO QCD computations with parton shower simulations: the POWHEG method. JHEP **11**, 070 (2007). https://doi.org/10.1088/1126-6708/2007/11/070. arXiv:0709.2092 [hep-ph]
62. S. Alioli, P. Nason, C. Oleari, E. Re, A general framework for implementing NLO calculations in shower Monte Carlo programs: the POWHEG BOX. JHEP **06**, 043 (2010). https://doi.org/10.1007/JHEP06(2010)043. arXiv:1002.2581 [hep-ph]
63. M. Beneke, P. Falgari, S. Klein, C. Schwinn, Hadronic top-quark pair production with NNLL threshold resummation. Nucl. Phys. B **855**, 695 (2012). https://doi.org/10.1016/j.nuclphysb.2011.10.021. arXiv:1109.1536 [hep-ph]
64. M. Cacciari, M. Czakon, M. Mangano, A. Mitov, P. Nason, Top-pair production at hadron colliders with next-to-next-to-leading logarithmic soft-gluon resummation. Phys. Lett. B **710**, 612 (2012). https://doi.org/10.1016/j.physletb.2012.03.013. arXiv:1111.5869 [hep-ph]
65. P. Barnreuther, M. Czakon, A. Mitov, Percent-level-precision physics at the Tevatron: next-to-next-to-leading order QCD corrections to $q\bar{q} \to t\bar{t} + X$. Phys. Rev. Lett. **109**, 132001 (2012). https://doi.org/10.1103/PhysRevLett.109.132001. arXiv:1204.5201 [hep-ph]
66. M. Czakon, A. Mitov, NNLO corrections to top-pair production at hadron colliders: the all-fermionic scattering channels. JHEP **12**, 054 (2012). https://doi.org/10.1007/JHEP12(2012)054. arXiv:1207.0236 [hep-ph]
67. M. Czakon, A. Mitov, NNLO corrections to top pair production at hadron colliders: the quark-gluon reaction. JHEP **01**, 080 (2013). https://doi.org/10.1007/JHEP01(2013)080. arXiv:1210.6832 [hep-ph]
68. M. Czakon, P. Fiedler, A. Mitov, Total top-quark pair-production cross section at hadron colliders through $O(\alpha_S^4)$. Phys. Rev. Lett. **110**, 252004 (2013). https://doi.org/10.1103/PhysRevLett.110.252004. arXiv:1303.6254 [hep-ph]
69. M. Czakon, A. Mitov, Top++: a program for the calculation of the top-pair cross-section at hadron colliders. Comput. Phys. Commun. **185**, 2930 (2014). https://doi.org/10.1016/j.cpc.2014.06.021. arXiv:1112.5675 [hep-ph]
70. M. Chiesa, C. Oleari, E. Re, NLO QCD+NLO EW corrections to diboson production matched to parton shower. Eur. Phys. J. C (2020). https://doi.org/10.1140/epjc/s10052-020-8419-3
71. S. Kallweit, V. Sotnikov, M. Wiesemann, Triphoton production at hadron colliders in NNLO QCD. Phys. Lett. B **812**, 136013 (2021). ISSN:0370-2693. https://www.sciencedirect.com/science/article/pii/S0370269320308169
72. ATLAS Collaboration, Electron and photon performance measurements with the ATLAS detector using the 2015–2017 LHC proton–proton collision data. JINST **14**, P12006 (2019). https://doi.org/10.1088/1748-0221/14/12/P12006. arXiv:1908.00005 [hep-ex]
73. ATLAS Collaboration, Muon reconstruction performance of the ATLAS detector in proton–proton collision data at $\sqrt{s} = 13$ TeV. Eur. Phys. J. C **76**, 292 (2016). https://doi.org/10.1140/epjc/s10052-016-4120-y. arXiv:1603.05598 [hep-ex]
74. ATLAS Collaboration, Jet reconstruction and performance using particle flow with the ATLAS detector. Eur. Phys. J. C **77**, 466 (2017). https://doi.org/10.1140/epjc/s10052-017-5031-2. arXiv:1703.10485 [hep-ex]
75. M. Cacciari, G.P. Salam, G. Soyez, The anti-k_t jet clustering algorithm. JHEP **04**, 063 (2008). https://doi.org/10.1088/1126-6708/2008/04/063. arXiv:0802.1189 [hep-ph]
76. M. Cacciari, G.P. Salam, G. Soyez, FastJet user manual. Eur. Phys. J. C **72**, 1896 (2012). https://doi.org/10.1140/epjc/s10052-012-1896-2. arXiv:1111.6097 [hep-ph]
77. ATLAS Collaboration, Jet energy scale and resolution measured in proton–proton collisions at $\sqrt{s} = 13$ TeV with the ATLAS detector. Eur. Phys. J. C **81**, 689 (2020). https://doi.org/10.1140/epjc/s10052-021-09402-3. arXiv:2007.02645 [hep-ex]
78. ATLAS Collaboration, Performance of pile-up mitigation techniques for jets in pp collisions at $\sqrt{s} = 8$ TeV using the ATLAS detector. Eur. Phys. J. C **76**, 581 (2016). https://doi.org/10.1140/epjc/s10052-016-4395-z. arXiv:1510.03823 [hep-ex]
79. ATLAS Collaboration, ATLAS b-jet identification performance and efficiency measurement with $t\bar{t}$ events in pp collisions at $\sqrt{s} = 13$ TeV. Eur. Phys. J. C **79**, 970 (2019). https://doi.org/10.1140/epjc/s10052-019-7450-8. arXiv:1907.05120 [hep-ex]

80. ATLAS Collaboration, Optimisation and performance studies of the ATLAS b-tagging algorithms for the 2017-18 LHC run. ATL-PHYS-PUB-2017-013 (2017). https://cds.cern.ch/record/2273281
81. ATLAS Collaboration, Performance of missing transverse momentum reconstruction with the ATLAS detector using proton–proton collisions at $\sqrt{s} = 13$ TeV. Eur. Phys. J. C **78**, 903 (2018). https://doi.org/10.1140/epjc/s10052-018-6288-9. arXiv:1802.08168 [hep-ex]
82. ATLAS Collaboration, E_T^{miss} performance in the ATLAS detector using 2015–2016 LHC pp collisions. ATLAS-CONF-2018-023 (2018). https://cds.cern.ch/record/2625233
83. ATLAS Collaboration, Electron reconstruction and identification in the ATLAS experiment using the 2015 and 2016 LHC proton–proton collision data at $\sqrt{s} = 13$ TeV. Eur. Phys. J. C **79**, 639 (2019). https://doi.org/10.1140/epjc/s10052-019-7140-6. arXiv:1902.04655 [hep-ex]
84. ATLAS Collaboration, Search for type-III seesaw heavy leptons in dilepton final states in pp collisions at $\sqrt{s} = 13$ TeV with the ATLAS detector. Eur. Phys. J. C **81**, 218 (2021). https://doi.org/10.1140/epjc/s10052-021-08929-9. arXiv:2008.07949 [hep-ex]
85. ATLAS Collaboration, Luminosity determination in pp collisions at $\sqrt{s} = 13$ TeV using the ATLAS detector at the LHC. ATLAS-CONF-2019-021 (2019). https://cds.cern.ch/record/2677054
86. G. Avoni et al., The new LUCID-2 detector for luminosity measurement and monitoring in ATLAS. JINST **13**, P07017 (2018). https://doi.org/10.1088/1748-0221/13/07/P07017
87. ATLAS Collaboration, Measurement of the inelastic proton–proton cross section at $\sqrt{s} = 13$ TeV with the ATLAS detector at the LHC. Phys. Rev. Lett **117**, 182002 (2016). https://doi.org/10.1103/PhysRevLett.117.182002. arXiv:1606.02625 [hep-ex]
88. ATLAS Collaboration, Muon reconstruction and identification efficiency in ATLAS using the full Run 2 pp collision data set at $\sqrt{s} = 13$ TeV. Eur. Phys. J. C **81**, 578 (2021). https://doi.org/10.1140/epjc/s10052-021-09233-2. arXiv:2012.00578 [hep-ex]
89. ATLAS Collaboration, Measurement of the c-jet mistagging efficiency in $t\bar{t}$ events using pp collision data at $\sqrt{s} = 13$ TeV collected with the ATLAS detector. Eur. Phys. J. C **82**, 95 (2021). https://doi.org/10.1140/epjc/s10052-021-09843-w. arXiv:2109.10627 [hep-ex]
90. ATLAS Collaboration, Electron reconstruction and identification in the ATLAS experiment using the 2015 and 2016 LHC proton–proton collision data at $\sqrt{s} = 13$ TeV. Eur. Phys. J. C **79** (2019). https://doi.org/10.1140/epjc/s10052-019-7140-6
91. J. Butterworth et al., PDF4LHC recommendations for LHC Run II. J. Phys. G **43**, 023001 (2016). https://doi.org/10.1088/0954-3899/43/2/023001. arXiv:1510.03865 [hep-ph]
92. L.A. Harland-Lang, A.D. Martin, P. Motylinski, R.S. Thorne, Parton distributions in the LHC era: MMHT 2014 PDFs. Eur. Phys. J. C **75** (2015). https://doi.org/10.1140/epjc/s10052-015-3397-6. arXiv:1412.3989 [hep-ph]
93. S. Dulat et al., New parton distribution functions from a global analysis of quantum chromodynamics. Phys. Rev. D **93**, 033006 (2016). https://doi.org/10.1103/PhysRevD.93.033006. arXiv:1506.07443 [hep-ph]
94. T. Sjöstrand, S. Mrenna, P. Skands, A brief introduction to PYTHIA 8.1. Comput. Phys. Commun. **178**, 852 (2008). https://doi.org/10.1016/j.cpc.2008.01.036
95. M. Bähr et al., Herwig++ physics and manual. Eur. Phys. J. C **58**, 639 (2008). https://doi.org/10.1140/epjc/s10052-008-0798-9. arXiv:0803.0883 [hep-ph]
96. J. Pumplin et al., New generation of parton distributions with uncertainties from global QCD analysis. JHEP **2002**, 012 (2002). https://doi.org/10.1088/1126-6708/2002/07/012. arXiv:hep-ph/0201195
97. A.D. Martin, W.J. Stirling, R.S. Thorne, G. Watt, Parton distributions for the LHC. Eur. Phys. J. C **63**, 189 (2009). https://doi.org/10.1140/epjc/s10052-009-1072-5. arXiv:0901.0002 [hep-ph]
98. A. Kalogeropoulos, J. Alwall, The SysCalc code: a tool to derive theoretical systematic uncertainties (2018). arXiv:1801.08401 [hep-ph]
99. M. Baak et al., HistFitter software framework for statistical data analysis. Eur. Phys. J. C **75**, 153 (2015). https://doi.org/10.1140/epjc/s10052-015-3327-7. arXiv:1410.1280 [hep-ex]
100. A.L. Read, Presentation of search results: the CLs technique. J. Phys. G **28**, 2693 (2002). https://doi.org/10.1088/0954-3899/28/10/313
101. G. Cowan, K. Cranmer, E. Gross, O. Vitells, Asymptotic formulae for likelihood-based tests of new physics. Eur. Phys. J. C **71**, 1554 (2011). https://doi.org/10.1140/epjc/s10052-011-1554-0. arXiv:1007.1727 [physics.data-an]
102. ATLAS Collaboration, ATLAS computing acknowledgements. ATL-SOFT-PUB-2021-003 (2021). https://cds.cern.ch/record/2776662

ATLAS Collaboration*

G. Aad[102], B. Abbott[120], K. Abeling[55], N. J. Abicht[49], S. H. Abidi[29], A. Aboulhorma[35e], H. Abramowicz[151], H. Abreu[150], Y. Abulaiti[117], A. C. Abusleme Hoffman[137a], B. S. Acharya[69a,69b,p], C. Adam Bourdarios[4], L. Adamczyk[85a], L. Adamek[155], S. V. Addepalli[26], M. J. Addison[101], J. Adelman[115], A. Adiguzel[21c], T. Adye[134], A. A. Affolder[136], Y. Afik[36], M. N. Agaras[13], J. Agarwala[73a,73b], A. Aggarwal[100], C. Agheorghiesei[27c], A. Ahmad[36], F. Ahmadov[38,ac], W. S. Ahmed[104], S. Ahuja[95], X. Ai[62a], G. Aielli[76a,76b], M. Ait Tamlihat[35e], B. Aitbenchikh[35a], I. Aizenberg[169], M. Akbiyik[100], T. P. A. Åkesson[98], A. V. Akimov[37], D. Akiyama[168], N. N. Akolkar[24], K. Al Khoury[41], G. L. Alberghi[23b], J. Albert[165], P. Albicocco[53], G. L. Albouy[60], S. Alderweireldt[52], M. Aleksa[36], I. N. Aleksandrov[38], C. Alexa[27b], T. Alexopoulos[10], A. Alfonsi[114], F. Alfonsi[23b], M. Algren[56], M. Alhroob[120], B. Ali[132], H. M. J. Ali[91], S. Ali[148], S. W. Alibocus[92], M. Aliev[37], G. Alimonti[71a], W. Alkakhi[55], C. Allaire[66], B. M. M. Allbrooke[146], J. F. Allen[52], C. A. Allendes Flores[137f], P. P. Allport[20], A. Aloisio[72a,72b], F. Alonso[90], C. Alpigiani[138], M. Alvarez Estevez[99], A. Alvarez Fernandez[100], M. G. Alviggi[72a,72b], M. Aly[101], Y. Amaral Coutinho[82b], A. Ambler[104], C. Amelung[36], M. Amerl[101], C. G. Ames[109], D. Amidei[106], S. P. Amor Dos Santos[130a], K. R. Amos[163], V. Ananiev[125], C. Anastopoulos[139], T. Andeen[11], J. K. Anders[36], S. Y. Andrean[47a,47b], A. Andreazza[71a,71b], S. Angelidakis[9], A. Angerami[41,af], A. V. Anisenkov[37], A. Annovi[74a], C. Antel[56],

M. T. Anthony[139], E. Antipov[145], M. Antonelli[53], D. J. A. Antrim[17a], F. Anulli[75a], M. Aoki[83], T. Aoki[153], J. A. Aparisi Pozo[163], M. A. Aparo[146], L. Aperio Bella[48], C. Appelt[18], N. Aranzabal[36], C. Arcangeletti[53], A. T. H. Arce[51], E. Arena[92], J-F. Arguin[108], S. Argyropoulos[54], J. -H. Arling[48], A. J. Armbruster[36], O. Arnaez[4], H. Arnold[114], Z. P. Arrubarrena Tame[109], G. Artoni[75a,75b], H. Asada[111], K. Asai[118], S. Asai[153], N. A. Asbah[61], J. Assahsah[35d], K. Assamagan[29], R. Astalos[28a], S. Atashi[160], R. J. Atkin[33a], M. Atkinson[162], N. B. Atlay[18], H. Atmani[62b], P. A. Atmasiddha[106], K. Augsten[132], S. Auricchio[72a,72b], A. D. Auriol[20], V. A. Austrup[101], G. Avolio[36], K. Axiotis[56], G. Azuelos[108,aj], D. Babal[28b], H. Bachacou[135], K. Bachas[152,t], A. Bachiu[34], F. Backman[47a,47b], A. Badea[61], P. Bagnaia[75a,75b], M. Bahmani[18], A. J. Bailey[163], V. R. Bailey[162], J. T. Baines[134], L. Baines[94], C. Bakalis[10], O. K. Baker[172], E. Bakos[15], D. Bakshi Gupta[8], R. Balasubramanian[114], E. M. Baldin[37], P. Balek[85a], E. Ballabene[23b,23a], F. Balli[135], L. M. Baltes[63a], W. K. Balunas[32], J. Balz[100], E. Banas[86], M. Bandieramonte[129], A. Bandyopadhyay[24], S. Bansal[24], L. Barak[151], M. Barakat[48], E. L. Barberio[105], D. Barberis[57b,57a], M. Barbero[102], G. Barbour[96], K. N. Barends[33a], T. Barillari[110], M-S. Barisits[36], T. Barklow[143], P. Baron[122], D. A. Baron Moreno[101], A. Baroncelli[62a], G. Barone[29], A. J. Barr[126], J. D. Barr[96], L. Barranco Navarro[47a,47b], F. Barreiro[99], J. Barreiro Guimarães da Costa[14a], U. Barron[151], M. G. Barros Teixeira[130a], S. Barsov[37], F. Bartels[63a], R. Bartoldus[143], A. E. Barton[91], P. Bartos[28a], A. Basan[100], M. Baselga[49], A. Bassalat[66,b], M. J. Basso[156a], C. R. Basson[101], R. L. Bates[59], S. Batlamous[35e], J. R. Batley[32], B. Batool[141], M. Battaglia[136], D. Battulga[18], M. Bauce[75a,75b], M. Bauer[36], P. Bauer[24], L. T. Bazzano Hurrell[30], J. B. Beacham[51], T. Beau[127], P. H. Beauchemin[158], F. Becherer[54], P. Bechtle[24], H. P. Beck[19,s], K. Becker[167], A. J. Beddall[21d], V. A. Bednyakov[38], C. P. Bee[145], L. J. Beemster[15], T. A. Beermann[36], M. Begalli[82d], M. Begel[29], A. Behera[145], J. K. Behr[48], J. F. Beirer[55], F. Beisiegel[24], M. Belfkir[159], G. Bella[151], L. Bellagamba[23b], A. Bellerive[34], P. Bellos[20], K. Beloborodov[37], N. L. Belyaev[37], D. Benchekroun[35a], F. Bendebba[35a], Y. Benhammou[151], M. Benoit[29], J. R. Bensinger[26], S. Bentvelsen[114], L. Beresford[48], M. Beretta[53], E. Bergeaas Kuutmann[161], N. Berger[4], B. Bergmann[132], J. Beringer[17a], G. Bernardi[5], C. Bernius[143], F. U. Bernlochner[24], F. Bernon[36,102], T. Berry[95], P. Berta[133], A. Berthold[50], I. A. Bertram[91], S. Bethke[110], A. Betti[75a,75b], A. J. Bevan[94], M. Bhamjee[33c], S. Bhatta[145], D. S. Bhattacharya[166], P. Bhattarai[26], V. S. Bhopatkar[121], R. Bi[29,al], R. M. Bianchi[129], G. Bianco[23b,23a], O. Biebel[109], R. Bielski[123], M. Biglietti[77a], T. R. V. Billoud[132], M. Bindi[55], A. Bingul[21b], C. Bini[75a,75b], A. Biondini[92], C. J. Birch-sykes[101], G. A. Bird[20,134], M. Birman[169], M. Biros[133], T. Bisanz[49], E. Bisceglie[43b,43a], D. Biswas[141], A. Bitadze[101], K. Bjørke[125], I. Bloch[48], C. Blocker[26], A. Blue[59], U. Blumenschein[94], J. Blumenthal[100], G. J. Bobbink[114], V. S. Bobrovnikov[37], M. Boehler[54], B. Boehm[166], D. Bogavac[36], A. G. Bogdanchikov[37], C. Bohm[47a], V. Boisvert[95], P. Bokan[48], T. Bold[85a], M. Bomben[5], M. Bona[94], M. Boonekamp[135], C. D. Booth[95], A. G. Borbély[59], I. S. Bordulev[37], H. M. Borecka-Bielska[108], L. S. Borgna[96], G. Borissov[91], D. Bortoletto[126], D. Boscherini[23b], M. Bosman[13], J. D. Bossio Sola[36], K. Bouaouda[35a], N. Bouchhar[163], J. Boudreau[129], E. V. Bouhova-Thacker[91], D. Boumediene[40], R. Bouquet[5], A. Boveia[119], J. Boyd[36], D. Boye[29], I. R. Boyko[38], J. Bracinik[20], N. Brahimi[62d], G. Brandt[171], O. Brandt[32], F. Braren[48], B. Brau[103], J. E. Brau[123], R. Brener[169], L. Brenner[114], R. Brenner[161], S. Bressler[169], D. Britton[59], D. Britzger[110], I. Brock[24], G. Brooijmans[41], W. K. Brooks[137f], E. Brost[29], L. M. Brown[165,m], L. E. Bruce[61], T. L. Bruckler[126], P. A. Bruckman de Renstrom[86], B. Brüers[48], D. Bruncko[28b,*], A. Bruni[23b], G. Bruni[23b], M. Bruschi[23b], N. Bruscino[75a,75b], T. Buanes[16], Q. Buat[138], D. Buchin[110], A. G. Buckley[59], M. K. Bugge[125], O. Bulekov[37], B. A. Bullard[143], S. Burdin[92], C. D. Burgard[49], A. M. Burger[40], B. Burghgrave[8], O. Burlayenko[54], J. T. P. Burr[32], C. D. Burton[11], J. C. Burzynski[142], E. L. Busch[41], V. Büscher[100], P. J. Bussey[59], J. M. Butler[25], C. M. Buttar[59], J. M. Butterworth[96], W. Buttinger[134], C. J. Buxo Vazquez[107], A. R. Buzykaev[37], G. Cabras[23b], S. Cabrera Urbán[163], D. Caforio[58], H. Cai[129], Y. Cai[14a,14e], V. M. M. Cairo[36], O. Cakir[3a], N. Calace[36], P. Calafiura[17a], G. Calderini[127], P. Calfayan[68], G. Callea[59], L. P. Caloba[82b], D. Calvet[40], S. Calvet[40], T. P. Calvet[102], M. Calvetti[74a,74b], R. Camacho Toro[127], S. Camarda[36], D. Camarero Munoz[26], P. Camarri[76a,76b], M. T. Camerlingo[72a,72b], D. Cameron[125], C. Camincher[165], M. Campanelli[96], A. Camplani[42], V. Canale[72a,72b], A. Canesse[104], M. Cano Bret[80], J. Cantero[163], Y. Cao[162], F. Capocasa[26], M. Capua[43b,43a], A. Carbone[71a,71b], R. Cardarelli[76a], J. C. J. Cardenas[8], F. Cardillo[163], T. Carli[36], G. Carlino[72a], J. I. Carlotto[13], B. T. Carlson[129,u], E. M. Carlson[165,156a], L. Carminati[71a,71b], A. Carnelli[135], M. Carnesale[75a,75b], S. Caron[113], E. Carquin[137f], S. Carrá[71a,71b], G. Carratta[23b,23a], F. Carrio Argos[33g], J. W. S. Carter[155], T. M. Carter[52], M. P. Casado[13,j], M. Caspar[48], E. G. Castiglia[172], F. L. Castillo[4], L. Castillo Garcia[13], V. Castillo Gimenez[163],

N. F. Castro[130a,130e], A. Catinaccio[36], J. R. Catmore[125], V. Cavaliere[29], N. Cavalli[23b,23a], V. Cavasinni[74a,74b], Y. C. Cekmecelioglu[48], E. Celebi[21a], F. Celli[126], M. S. Centonze[70a,70b], K. Cerny[122], A. S. Cerqueira[82a], A. Cerri[146], L. Cerrito[76a,76b], F. Cerutti[17a], B. Cervato[141], A. Cervelli[23b], G. Cesarini[53], S. A. Cetin[21d], Z. Chadi[35a], D. Chakraborty[115], M. Chala[130f], J. Chan[170], W. Y. Chan[153], J. D. Chapman[32], E. Chapon[135], B. Chargeishvili[149b], D. G. Charlton[20], T. P. Charman[94], M. Chatterjee[19], C. Chauhan[133], S. Chekanov[6], S. V. Chekulaev[156a], G. A. Chelkov[38,a], A. Chen[106], B. Chen[151], B. Chen[165], H. Chen[14c], H. Chen[29], J. Chen[62c], J. Chen[142], M. Chen[126], S. Chen[153], S. J. Chen[14c], X. Chen[62c], X. Chen[14b,ai], Y. Chen[62a], C. L. Cheng[170], H. C. Cheng[64a], S. Cheong[143], A. Cheplakov[38], E. Cheremushkina[48], E. Cherepanova[114], R. Cherkaoui El Moursli[35e], E. Cheu[7], K. Cheung[65], L. Chevalier[135], V. Chiarella[53], G. Chiarelli[74a], N. Chiedde[102], G. Chiodini[70a], A. S. Chisholm[20], A. Chitan[27b], M. Chitishvili[163], M. V. Chizhov[38], K. Choi[11], A. R. Chomont[75a,75b], Y. Chou[103], E. Y. S. Chow[114], T. Chowdhury[33g], K. L. Chu[169], M. C. Chu[64a], X. Chu[14a,14e], J. Chudoba[131], J. J. Chwastowski[86], D. Cieri[110], K. M. Ciesla[85a], V. Cindro[93], A. Ciocio[17a], F. Cirotto[72a,72b], Z. H. Citron[169,n], M. Citterio[71a], D. A. Ciubotaru[27b], B. M. Ciungu[155], A. Clark[56], P. J. Clark[52], J. M. Clavijo Columbie[48], S. E. Clawson[48], C. Clement[47a,47b], J. Clercx[48], L. Clissa[23b,23a], Y. Coadou[102], M. Cobal[69a,69c], A. Coccaro[57b], R. F. Coelho Barrue[130a], R. Coelho Lopes De Sa[103], S. Coelli[71a], H. Cohen[151], A. E. C. Coimbra[71a,71b], B. Cole[41], J. Collot[60], P. Conde Muiño[130a,130g], M. P. Connell[33c], S. H. Connell[33c], I. A. Connelly[59], E. I. Conroy[126], F. Conventi[72a,ak], H. G. Cooke[20], A. M. Cooper-Sarkar[126], A. Cordeiro Oudot Choi[127], F. Cormier[164], L. D. Corpe[40], M. Corradi[75a,75b], F. Corriveau[104,aa], A. Cortes-Gonzalez[18], M. J. Costa[163], F. Costanza[4], D. Costanzo[139], B. M. Cote[119], G. Cowan[95], K. Cranmer[170], D. Cremonini[23b,23a], S. Crépé-Renaudin[60], F. Crescioli[127], M. Cristinziani[141], M. Cristoforetti[78a,78b], V. Croft[114], J. E. Crosby[121], G. Crosetti[43b,43a], A. Cueto[99], T. Cuhadar Donszelmann[160], H. Cui[14a,14e], Z. Cui[7], W. R. Cunningham[59], F. Curcio[43b,43a], P. Czodrowski[36], M. M. Czurylo[63b], M. J. Da Cunha Sargedas De Sousa[62a], J. V. Da Fonseca Pinto[82b], C. Da Via[101], W. Dabrowski[85a], T. Dado[49], S. Dahbi[33g], T. Dai[106], C. Dallapiccola[103], M. Dam[42], G. D'amen[29], V. D'Amico[109], J. Damp[100], J. R. Dandoy[128], M. F. Daneri[30], M. Danninger[142], V. Dao[36], G. Darbo[57b], S. Darmora[6], S. J. Das[29,al], S. D'Auria[71a,71b], C. David[156b], T. Davidek[133], B. Davis-Purcell[34], I. Dawson[94], H. A. Day-hall[132], K. De[8], R. De Asmundis[72a], N. De Biase[48], S. De Castro[23b,23a], N. De Groot[113], P. de Jong[114], H. De la Torre[107], A. De Maria[14c], A. De Salvo[75a], U. De Sanctis[76a,76b], A. De Santo[146], J. B. De Vivie De Regie[60], D. V. Dedovich[38], J. Degens[114], A. M. Deiana[44], F. Del Corso[23b,23a], J. Del Peso[99], F. Del Rio[63a], F. Deliot[135], C. M. Delitzsch[49], M. Della Pietra[72a,72b], D. Della Volpe[56], A. Dell'Acqua[36], L. Dell'Asta[71a,71b], M. Delmastro[4], P. A. Delsart[60], S. Demers[172], M. Demichev[38], S. P. Denisov[37], L. D'Eramo[40], D. Derendarz[86], F. Derue[127], P. Dervan[92], K. Desch[24], C. Deutsch[24], F. A. Di Bello[57b,57a], A. Di Ciaccio[76a,76b], L. Di Ciaccio[4], A. Di Domenico[75a,75b], C. Di Donato[72a,72b], A. Di Girolamo[36], G. Di Gregorio[5], A. Di Luca[78a,78b], B. Di Micco[77a,77b], R. Di Nardo[77a,77b], C. Diaconu[102], F. A. Dias[114], T. Dias Do Vale[142], M. A. Diaz[137a,137b], F. G. Diaz Capriles[24], M. Didenko[163], E. B. Diehl[106], L. Diehl[54], S. Díez Cornell[48], C. Diez Pardos[141], C. Dimitriadi[24,161], A. Dimitrievska[17a], J. Dingfelder[24], I-M. Dinu[27b], S. J. Dittmeier[63b], F. Dittus[36], F. Djama[102], T. Djobava[149b], J. I. Djuvsland[16], C. Doglioni[101,98], J. Dolejsi[133], Z. Dolezal[133], M. Donadelli[82c], B. Dong[107], J. Donini[40], A. D'Onofrio[77a,77b], M. D'Onofrio[92], J. Dopke[134], A. Doria[72a], N. Dos Santos Fernandes[130a], M. T. Dova[90], A. T. Doyle[59], M. A. Draguet[126], E. Dreyer[169], I. Drivas-koulouris[10], A. S. Drobac[158], M. Drozdova[56], D. Du[62a], T. A. du Pree[114], F. Dubinin[37], M. Dubovsky[28a], E. Duchovni[169], G. Duckeck[109], O. A. Ducu[27b], D. Duda[52], A. Dudarev[36], E. R. Duden[26], M. D'uffizi[101], L. Duflot[66], M. Dührssen[36], C. Dülsen[171], A. E. Dumitriu[27b], M. Dunford[63a], S. Dungs[49], K. Dunne[47a,47b], A. Duperrin[102], H. Duran Yildiz[3a], M. Düren[58], A. Durglishvili[149b], B. L. Dwyer[115], G. I. Dyckes[17a], M. Dyndal[85a], S. Dysch[101], B. S. Dziedzic[86], Z. O. Earnshaw[146], G. H. Eberwein[126], B. Eckerova[28a], S. Eggebrecht[55], M. G. Eggleston[51], E. Egidio Purcino De Souza[127], L. F. Ehrke[56], G. Eigen[16], K. Einsweiler[17a], T. Ekelof[161], P. A. Ekman[98], S. El Farkh[35b], Y. El Ghazali[35b], H. El Jarrari[35e,148], A. El Moussaouy[35a], V. Ellajosyula[161], M. Ellert[161], F. Ellinghaus[171], A. A. Elliot[94], N. Ellis[36], J. Elmsheuser[29], M. Elsing[36], D. Emeliyanov[134], Y. Enari[153], I. Ene[17a], S. Epari[13], J. Erdmann[49], P. A. Erland[86], M. Errenst[171], M. Escalier[66], C. Escobar[163], E. Etzion[151], G. Evans[130a], H. Evans[68], L. S. Evans[95], M. O. Evans[146], A. Ezhilov[37], S. Ezzarqtouni[35a], F. Fabbri[59], L. Fabbri[23b,23a], G. Facini[96], V. Fadeyev[136], R. M. Fakhrutdinov[37], S. Falciano[75a], L. F. Falda Ulhoa Coelho[36], P. J. Falke[24], J. Faltova[133], C. Fan[162], Y. Fan[14a], Y. Fang[14a,14e], M. Fanti[71a,71b], M. Faraj[69a,69b], Z. Farazpay[97], A. Farbin[8], A. Farilla[77a], T. Farooque[107],

S. M. Farrington[52], F. Fassi[35e], D. Fassouliotis[9], M. Faucci Giannelli[76a,76b], W. J. Fawcett[32], L. Fayard[66], P. Federic[133], P. Federicova[131], O. L. Fedin[37,a], G. Fedotov[37], M. Feickert[170], L. Feligioni[102], A. Fell[139], D. E. Fellers[123], C. Feng[62b], M. Feng[14b], Z. Feng[114], M. J. Fenton[160], A. B. Fenyuk[37], L. Ferencz[48], R. A. M. Ferguson[91], S. I. Fernandez Luengo[137f], M. J. V. Fernoux[102], J. Ferrando[48], A. Ferrari[161], P. Ferrari[114,113], R. Ferrari[73a], D. Ferrere[56], C. Ferretti[106], F. Fiedler[100], A. Filipčič[93], E. K. Filmer[1], F. Filthaut[113], M. C. N. Fiolhais[130a,130c,d], L. Fiorini[163], W. C. Fisher[107], T. Fitschen[101], P. M. Fitzhugh[135], I. Fleck[141], P. Fleischmann[106], T. Flick[171], L. Flores[128], M. Flores[33d,ag], L. R. Flores Castillo[64a], L. Flores Sanz De Acedo[36], F. M. Follega[78a,78b], N. Fomin[16], J. H. Foo[155], B. C. Forland[68], A. Formica[135], A. C. Forti[101], E. Fortin[36], A. W. Fortman[61], M. G. Foti[17a], L. Fountas[9,k], D. Fournier[66], H. Fox[91], P. Francavilla[74a,74b], S. Francescato[61], S. Franchellucci[56], M. Franchini[23b,23a], S. Franchino[63a], D. Francis[36], L. Franco[113], L. Franconi[48], M. Franklin[61], G. Frattari[26], A. C. Freegard[94], W. S. Freund[82b], Y. Y. Frid[151], N. Fritzsche[50], A. Froch[54], D. Froidevaux[36], J. A. Frost[126], Y. Fu[62a], M. Fujimoto[118], E. Fullana Torregrosa[163,*], K. Y. Fung[64a], E. Furtado De Simas Filho[82b], M. Furukawa[153], J. Fuster[163], A. Gabrielli[23b,23a], A. Gabrielli[155], P. Gadow[48], G. Gagliardi[57b,57a], L. G. Gagnon[17a], E. J. Gallas[126], B. J. Gallop[134], K. K. Gan[119], S. Ganguly[153], J. Gao[62a], Y. Gao[52], F. M. Garay Walls[137a,137b], B. Garcia[29,al], C. García[163], A. Garcia Alonso[114], A. G. Garcia Caffaro[172], J. E. García Navarro[163], M. Garcia-Sciveres[17a], G. L. Gardner[128], R. W. Gardner[39], N. Garelli[158], D. Garg[80], R. B. Garg[143,r], J. M. Gargan[52], C. A. Garner[155], S. J. Gasiorowski[138], P. Gaspar[82b], G. Gaudio[73a], V. Gautam[13], P. Gauzzi[75a,75b], I. L. Gavrilenko[37], A. Gavrilyuk[37], C. Gay[164], G. Gaycken[48], E. N. Gazis[10], A. A. Geanta[27b], C. M. Gee[136], C. Gemme[57b], M. H. Genest[60], S. Gentile[75a,75b], S. George[95], W. F. George[20], T. Geralis[46], P. Gessinger-Befurt[36], M. E. Geyik[171], M. Ghneimat[141], K. Ghorbanian[94], A. Ghosal[141], A. Ghosh[160], A. Ghosh[7], B. Giacobbe[23b], S. Giagu[75a,75b], P. Giannetti[74a], A. Giannini[62a], S. M. Gibson[95], M. Gignac[136], D. T. Gil[85b], A. K. Gilbert[85a], B. J. Gilbert[41], D. Gillberg[34], G. Gilles[114], N. E. K. Gillwald[48], L. Ginabat[127], D. M. Gingrich[2,aj], M. P. Giordani[69a,69c], P. F. Giraud[135], G. Giugliarelli[69a,69c], D. Giugni[71a], F. Giuli[36], I. Gkialas[9,k], L. K. Gladilin[37], C. Glasman[99], G. R. Gledhill[123], M. Glisic[123], I. Gnesi[43b,g], Y. Go[29,al], M. Goblirsch-Kolb[36], B. Gocke[49], D. Godin[108], B. Gokturk[21a], S. Goldfarb[105], T. Golling[56], M. G. D. Gololo[33g], D. Golubkov[37], J. P. Gombas[107], A. Gomes[130a,130b], G. Gomes Da Silva[141], A. J. Gomez Delegido[163], R. Gonçalo[130a,130c], G. Gonella[123], L. Gonella[20], A. Gongadze[38], F. Gonnella[20], J. L. Gonski[41], R. Y. González Andana[52], S. González de la Hoz[163], S. Gonzalez Fernandez[13], R. Gonzalez Lopez[92], C. Gonzalez Renteria[17a], R. Gonzalez Suarez[161], S. Gonzalez-Sevilla[56], G. R. Gonzalvo Rodriguez[163], L. Goossens[36], P. A. Gorbounov[37], B. Gorini[36], E. Gorini[70a,70b], A. Gorišek[93], T. C. Gosart[128], A. T. Goshaw[51], M. I. Gostkin[38], S. Goswami[121], C. A. Gottardo[36], M. Gouighri[35b], V. Goumarre[48], A. G. Goussiou[138], N. Govender[33c], I. Grabowska-Bold[85a], K. Graham[34], E. Gramstad[125], S. Grancagnolo[70a,70b], M. Grandi[146], V. Gratchev[37,*], P. M. Gravila[27f], F. G. Gravili[70a,70b], H. M. Gray[17a], M. Greco[70a,70b], C. Grefe[24], I. M. Gregor[48], P. Grenier[143], C. Grieco[13], A. A. Grillo[136], K. Grimm[31], S. Grinstein[13,w], J. -F. Grivaz[66], E. Gross[169], J. Grosse-Knetter[55], C. Grud[106], J. C. Grundy[126], L. Guan[106], W. Guan[29], C. Gubbels[164], J. G. R. Guerrero Rojas[163], G. Guerrieri[69a,69b], F. Guescini[110], R. Gugel[100], J. A. M. Guhit[106], A. Guida[18], T. Guillemin[4], E. Guilloton[167,134], S. Guindon[36], F. Guo[14a,14e], J. Guo[62c], L. Guo[48], Y. Guo[106], R. Gupta[48], S. Gurbuz[24], S. S. Gurdasani[54], G. Gustavino[36], M. Guth[56], P. Gutierrez[120], L. F. Gutierrez Zagazeta[128], C. Gutschow[96], C. Gwenlan[126], C. B. Gwilliam[92], E. S. Haaland[125], A. Haas[117], M. Habedank[48], C. Haber[17a], H. K. Hadavand[8], A. Hadef[100], S. Hadzic[110], J. J. Hahn[141], E. H. Haines[96], M. Haleem[166], J. Haley[121], J. J. Hall[139], G. D. Hallewell[102], L. Halser[19], K. Hamano[165], H. Hamdaoui[35e], M. Hamer[24], G. N. Hamity[52], E. J. Hampshire[95], J. Han[62b], K. Han[62a], L. Han[14c], L. Han[62a], S. Han[17a], Y. F. Han[155], K. Hanagaki[83], M. Hance[136], D. A. Hangal[41,af], H. Hanif[142], M. D. Hank[128], R. Hankache[101], J. B. Hansen[42], J. D. Hansen[42], P. H. Hansen[42], K. Hara[157], D. Harada[56], T. Harenberg[171], S. Harkusha[37], M. L. Harris[103], Y. T. Harris[126], J. Harrison[13], N. M. Harrison[119], P. F. Harrison[167], N. M. Hartman[110], N. M. Hartmann[109], Y. Hasegawa[140], A. Hasib[52], S. Haug[19], R. Hauser[107], C. M. Hawkes[20], R. J. Hawkings[36], Y. Hayashi[153], S. Hayashida[111], D. Hayden[107], C. Hayes[106], R. L. Hayes[114], C. P. Hays[126], J. M. Hays[94], H. S. Hayward[92], F. He[62a], M. He[14a,14e], Y. He[154], Y. He[127], N. B. Heatley[94], V. Hedberg[98], A. L. Heggelund[125], N. D. Hehir[94], C. Heidegger[54], K. K. Heidegger[54], W. D. Heidorn[81], J. Heilman[34], S. Heim[48], T. Heim[17a], J. G. Heinlein[128], J. J. Heinrich[123], L. Heinrich[110,ah], J. Hejbal[131], L. Helary[48], A. Held[170], S. Hellesund[16], C. M. Helling[164], S. Hellman[47a,47b], C. Helsens[36], R. C. W. Henderson[91], L. Henkelmann[32], A. M. Henriques Correia[36], H. Herde[98],

Y. Hernández Jiménez[145], L. M. Herrmann[24], T. Herrmann[50], G. Herten[54], R. Hertenberger[109], L. Hervas[36], M. E. Hesping[100], N. P. Hessey[156a], H. Hibi[84], S. J. Hillier[20], J. R. Hinds[107], F. Hinterkeuser[24], M. Hirose[124], S. Hirose[157], D. Hirschbuehl[171], T. G. Hitchings[101], B. Hiti[93], J. Hobbs[145], R. Hobincu[27e], N. Hod[169], M. C. Hodgkinson[139], B. H. Hodkinson[32], A. Hoecker[36], J. Hofer[48], T. Holm[24], M. Holzbock[110], L. B. A. H. Hommels[32], B. P. Honan[101], J. Hong[62c], T. M. Hong[129], B. H. Hooberman[162], W. H. Hopkins[6], Y. Horii[111], S. Hou[148], A. S. Howard[93], J. Howarth[59], J. Hoya[6], M. Hrabovsky[122], A. Hrynevich[48], T. Hryn'ova[4], P. J. Hsu[65], S. -C. Hsu[138], Q. Hu[41], Y. F. Hu[14a,14e], S. Huang[64b], X. Huang[14c], Y. Huang[62a], Y. Huang[14a], Z. Huang[101], Z. Hubacek[132], M. Huebner[24], F. Huegging[24], T. B. Huffman[126], C. A. Hugli[48], M. Huhtinen[36], S. K. Huiberts[16], R. Hulsken[104], N. Huseynov[12,a], J. Huston[107], J. Huth[61], R. Hyneman[143], G. Iacobucci[56], G. Iakovidis[29], I. Ibragimov[141], L. Iconomidou-Fayard[66], P. Iengo[72a,72b], R. Iguchi[153], T. Iizawa[83], Y. Ikegami[83], N. Ilic[155], H. Imam[35a], M. Ince Lezki[56], T. Ingebretsen Carlson[47a,47b], G. Introzzi[73a,73b], M. Iodice[77a], V. Ippolito[75a,75b], R. K. Irwin[92], M. Ishino[153], W. Islam[170], C. Issever[18,48], S. Istin[21a,an], H. Ito[168], J. M. Iturbe Ponce[64a], R. Iuppa[78a,78b], A. Ivina[169], J. M. Izen[45], V. Izzo[72a], P. Jacka[131,132], P. Jackson[1], R. M. Jacobs[48], B. P. Jaeger[142], C. S. Jagfeld[109], P. Jain[54], G. Jäkel[171], K. Jakobs[54], T. Jakoubek[169], J. Jamieson[59], K. W. Janas[85a], A. E. Jaspan[92], M. Javurkova[103], F. Jeanneau[135], L. Jeanty[123], J. Jejelava[149a,ad], P. Jenni[54,h], C. E. Jessiman[34], S. Jézéquel[4], C. Jia[62b], J. Jia[145], X. Jia[61], X. Jia[14a,14e], Z. Jia[14c], Y. Jiang[62a], S. Jiggins[48], J. Jimenez Pena[13], S. Jin[14c], A. Jinaru[27b], O. Jinnouchi[154], P. Johansson[139], K. A. Johns[7], J. W. Johnson[136], D. M. Jones[32], E. Jones[48], P. Jones[32], R. W. L. Jones[91], T. J. Jones[92], R. Joshi[119], J. Jovicevic[15], X. Ju[17a], J. J. Junggeburth[36], T. Junkermann[63a], A. Juste Rozas[13,w], M. K. Juzek[86], S. Kabana[137e], A. Kaczmarska[86], M. Kado[110], H. Kagan[119], M. Kagan[143], A. Kahn[41], A. Kahn[128], C. Kahra[100], T. Kaji[168], E. Kajomovitz[150], N. Kakati[169], I. Kalaitzidou[54], C. W. Kalderon[29], A. Kamenshchikov[155], S. Kanayama[154], N. J. Kang[136], D. Kar[33g], K. Karava[126], M. J. Kareem[156b], E. Karentzos[54], I. Karkanias[152], O. Karkout[114], S. N. Karpov[38], Z. M. Karpova[38], V. Kartvelishvili[91], A. N. Karyukhin[37], E. Kasimi[152], J. Katzy[48], S. Kaur[34], K. Kawade[140], T. Kawamoto[135], E. F. Kay[36], F. I. Kaya[158], S. Kazakos[107], V. F. Kazanin[37], Y. Ke[145], J. M. Keaveney[33a], R. Keeler[165], G. V. Kehris[61], J. S. Keller[34], A. S. Kelly[96], J. J. Kempster[146], K. E. Kennedy[41], P. D. Kennedy[100], O. Kepka[131], B. P. Kerridge[167], S. Kersten[171], B. P. Kerševan[93], S. Keshri[66], L. Keszeghova[28a], S. Ketabchi Haghighat[155], M. Khandoga[127], A. Khanov[121], A. G. Kharlamov[37], T. Kharlamova[37], E. E. Khoda[138], T. J. Khoo[18], G. Khoriauli[166], J. Khubua[149b], Y. A. R. Khwaira[66], M. Kiehn[36], A. Kilgallon[123], D. W. Kim[47a,47b], Y. K. Kim[39], N. Kimura[96], A. Kirchhoff[55], C. Kirfel[24], F. Kirfel[24], J. Kirk[134], A. E. Kiryunin[110], C. Kitsaki[10], O. Kivernyk[24], M. Klassen[63a], C. Klein[34], L. Klein[166], M. H. Klein[106], M. Klein[92], S. B. Klein[56], U. Klein[92], P. Klimek[36], A. Klimentov[29], T. Klioutchnikova[36], P. Kluit[114], S. Kluth[110], E. Kneringer[79], T. M. Knight[155], A. Knue[54], R. Kobayashi[87], S. F. Koch[126], M. Kocian[143], P. Kodyš[133], D. M. Koeck[123], P. T. Koenig[24], T. Koffas[34], M. Kolb[135], I. Koletsou[4], T. Komarek[122], K. Köneke[54], A. X. Y. Kong[1], T. Kono[118], N. Konstantinidis[96], B. Konya[98], R. Kopeliansky[68], S. Koperny[85a], K. Korcyl[86], K. Kordas[152,f], G. Koren[151], A. Korn[96], S. Korn[55], I. Korolkov[13], N. Korotkova[37], B. Kortman[114], O. Kortner[110], S. Kortner[110], W. H. Kostecka[115], V. V. Kostyukhin[141], A. Kotsokechagia[135], A. Kotwal[51], A. Koulouris[36], A. Kourkoumeli-Charalampidi[73a,73b], C. Kourkoumelis[9], E. Kourlitis[6], O. Kovanda[146], R. Kowalewski[165], W. Kozanecki[135], A. S. Kozhin[37], V. A. Kramarenko[37], G. Kramberger[93], P. Kramer[100], M. W. Krasny[127], A. Krasznahorkay[36], J. W. Kraus[171], J. A. Kremer[100], T. Kresse[50], J. Kretzschmar[92], K. Kreul[18], P. Krieger[155], S. Krishnamurthy[103], M. Krivos[133], K. Krizka[20], K. Kroeninger[49], H. Kroha[110], J. Kroll[131], J. Kroll[128], K. S. Krowpman[107], U. Kruchonak[38], H. Krüger[24], N. Krumnack[81], M. C. Kruse[51], J. A. Krzysiak[86], O. Kuchinskaia[37], S. Kuday[3a], S. Kuehn[36], R. Kuesters[54], T. Kuhl[48], V. Kukhtin[38], Y. Kulchitsky[37,a], S. Kuleshov[137d,137b], M. Kumar[33g], N. Kumari[102], A. Kupco[131], T. Kupfer[49], A. Kupich[37], O. Kuprash[54], H. Kurashige[84], L. L. Kurchaninov[156a], O. Kurdysh[66], Y. A. Kurochkin[37], A. Kurova[37], M. Kuze[154], A. K. Kvam[103], J. Kvita[122], T. Kwan[104], N. G. Kyriacou[106], L. A. O. Laatu[102], C. Lacasta[163], F. Lacava[75a,75b], H. Lacker[18], D. Lacour[127], N. N. Lad[96], E. Ladygin[38], B. Laforge[127], T. Lagouri[137e], S. Lai[55], I. K. Lakomiec[85a], N. Lalloue[60], J. E. Lambert[165,m], S. Lammers[68], W. Lampl[7], C. Lampoudis[152,f], A. N. Lancaster[115], E. Lançon[29], U. Landgraf[54], M. P. J. Landon[94], V. S. Lang[54], R. J. Langenberg[103], O. K. B. Langrekken[125], A. J. Lankford[160], F. Lanni[36], K. Lantzsch[24], A. Lanza[73a], A. Lapertosa[57b,57a], J. F. Laporte[135], T. Lari[71a], F. Lasagni Manghi[23b], M. Lassnig[36], V. Latonova[131], A. Laudrain[100], A. Laurier[150], S. D. Lawlor[95], Z. Lawrence[101], M. Lazzaroni[71a,71b], B. Le[101], E. M. Le Boulicaut[51], B. Leban[93], A. Lebedev[81], M. LeBlanc[36], F. Ledroit-Guillon[60], A. C. A. Lee[96], S. C. Lee[148], S. Lee[47a,47b],

T. F. Lee[92], L. L. Leeuw[33c], H. P. Lefebvre[95], M. Lefebvre[165], C. Leggett[17a], G. Lehmann Miotto[36], M. Leigh[56], W. A. Leight[103], W. Leinonen[113], A. Leisos[152,v], M. A. L. Leite[82c], C. E. Leitgeb[48], R. Leitner[133], K. J. C. Leney[44], T. Lenz[24], S. Leone[74a], C. Leonidopoulos[52], A. Leopold[144], C. Leroy[108], R. Les[107], C. G. Lester[32], M. Levchenko[37], J. Levêque[4], D. Levin[106], L. J. Levinson[169], M. P. Lewicki[86], D. J. Lewis[4], A. Li[5], B. Li[62b], C. Li[62a], C-Q. Li[62c], H. Li[62a], H. Li[62b], H. Li[14c], H. Li[62b], K. Li[138], L. Li[62c], M. Li[14a,14e], Q. Y. Li[62a], S. Li[14a,14e], S. Li[62d,62c,e], T. Li[5,c], X. Li[104], Z. Li[126], Z. Li[104], Z. Li[92], Z. Li[14a,14e], Z. Liang[14a], M. Liberatore[48], B. Liberti[76a], K. Lie[64c], J. Lieber Marin[82b], H. Lien[68], K. Lin[107], R. E. Lindley[7], J. H. Lindon[2], A. Linss[48], E. Lipeles[128], A. Lipniacka[16], A. Lister[164], J. D. Little[4], B. Liu[14a], B. X. Liu[142], D. Liu[62d,62c], J. B. Liu[62a], J. K. K. Liu[32], K. Liu[62d,62c], M. Liu[62a], M. Y. Liu[62a], P. Liu[14a], Q. Liu[62d,138,62c], X. Liu[62a], Y. Liu[14d,14e], Y. L. Liu[106], Y. W. Liu[62a], J. Llorente Merino[142], S. L. Lloyd[94], E. M. Lobodzinska[48], P. Loch[7], S. Loffredo[76a,76b], T. Lohse[18], K. Lohwasser[139], E. Loiacono[48], M. Lokajicek[131,*], J. D. Lomas[20], J. D. Long[162], I. Longarini[160], L. Longo[70a,70b], R. Longo[162], I. Lopez Paz[67], A. Lopez Solis[48], J. Lorenz[109], N. Lorenzo Martinez[4], A. M. Lory[109], G. Löschcke Centeno[146], O. Loseva[37], X. Lou[47a,47b], X. Lou[14a,14e], A. Lounis[66], J. Love[6], P. A. Love[91], G. Lu[14a,14e], M. Lu[80], S. Lu[128], Y. J. Lu[65], H. J. Lubatti[138], C. Luci[75a,75b], F. L. Lucio Alves[14c], A. Lucotte[60], F. Luehring[68], I. Luise[145], O. Lukianchuk[66], O. Lundberg[144], B. Lund-Jensen[144], N. A. Luongo[123], M. S. Lutz[151], D. Lynn[29], H. Lyons[92], R. Lysak[131], E. Lytken[98], V. Lyubushkin[38], T. Lyubushkina[38], M. M. Lyukova[145], H. Ma[29], L. L. Ma[62b], Y. Ma[121], D. M. Mac Donell[165], G. Maccarrone[53], J. C. MacDonald[100], R. Madar[40], W. F. Mader[50], J. Maeda[84], T. Maeno[29], M. Maerker[50], H. Maguire[139], V. Maiboroda[135], A. Maio[130a,130b,130d], K. Maj[85a], O. Majersky[48], S. Majewski[123], N. Makovec[66], V. Maksimovic[15], B. Malaescu[127], Pa. Malecki[86], V. P. Maleev[37], F. Malek[60], M. Mali[93], D. Malito[95,q], U. Mallik[80], S. Maltezos[10], S. Malyukov[38], J. Mamuzic[13], G. Mancini[53], G. Manco[73a,73b], J. P. Mandalia[94], I. Mandić[93], L. Manhaes de Andrade Filho[82a], I. M. Maniatis[169], J. Manjarres Ramos[102,ae], D. C. Mankad[169], A. Mann[109], B. Mansoulie[135], S. Manzoni[36], A. Marantis[152,v], G. Marchiori[5], M. Marcisovsky[131], C. Marcon[71a,71b], M. Marinescu[20], M. Marjanovic[120], E. J. Marshall[91], Z. Marshall[17a], S. Marti-Garcia[163], T. A. Martin[167], V. J. Martin[52], B. Martin dit Latour[16], L. Martinelli[75a,75b], M. Martinez[13,w], P. Martinez Agullo[163], V. I. Martinez Outschoorn[103], P. Martinez Suarez[13], S. Martin-Haugh[134], V. S. Martoiu[27b], A. C. Martyniuk[96], A. Marzin[36], D. Mascione[78a,78b], L. Masetti[100], T. Mashimo[153], J. Masik[101], A. L. Maslennikov[37], L. Massa[23b], P. Massarotti[72a,72b], P. Mastrandrea[74a,74b], A. Mastroberardino[43b,43a], T. Masubuchi[153], T. Mathisen[161], J. Matousek[133], N. Matsuzawa[153], J. Maurer[27b], B. Maček[93], D. A. Maximov[37], R. Mazini[148], I. Maznas[152], M. Mazza[107], S. M. Mazza[136], E. Mazzeo[71a,71b], C. Mc Ginn[29], J. P. Mc Gowan[104], S. P. Mc Kee[106], E. F. McDonald[105], A. E. McDougall[114], J. A. Mcfayden[146], R. P. McGovern[128], G. Mchedlidze[149b], R. P. Mckenzie[33g], T. C. Mclachlan[48], D. J. Mclaughlin[96], K. D. McLean[165], S. J. McMahon[134], P. C. McNamara[105], C. M. Mcpartland[92], R. A. McPherson[165,aa], S. Mehlhase[109], A. Mehta[92], D. Melini[150], B. R. Mellado Garcia[33g], A. H. Melo[55], F. Meloni[48], A. M. Mendes Jacques Da Costa[101], H. Y. Meng[155], L. Meng[91], S. Menke[110], M. Mentink[36], E. Meoni[43b,43a], C. Merlassino[126], L. Merola[72a,72b], C. Meroni[71a,71b], G. Merz[106], O. Meshkov[37], J. Metcalfe[6], A. S. Mete[6], C. Meyer[68], J-P. Meyer[135], R. P. Middleton[134], L. Mijović[52], G. Mikenberg[169], M. Mikestikova[131], M. Mikuž[93], H. Mildner[100], A. Milic[36], C. D. Milke[44], D. W. Miller[39], L. S. Miller[34], A. Milov[169], D. A. Milstead[47a,47b], T. Min[14c], A. A. Minaenko[37], I. A. Minashvili[149b], L. Mince[59], A. I. Mincer[117], B. Mindur[85a], M. Mineev[38], Y. Mino[87], L. M. Mir[13], M. Miralles Lopez[163], M. Mironova[17a], A. Mishima[153], M. C. Missio[113], T. Mitani[168], A. Mitra[167], V. A. Mitsou[163], O. Miu[155], P. S. Miyagawa[94], Y. Miyazaki[89], A. Mizukami[83], T. Mkrtchyan[63a], M. Mlinarevic[96], T. Mlinarevic[96], M. Mlynarikova[36], S. Mobius[19], K. Mochizuki[108], P. Moder[48], P. Mogg[109], A. F. Mohammed[14a,14e], S. Mohapatra[41], G. Mokgatitswane[33g], L. Moleri[169], B. Mondal[141], S. Mondal[132], K. Mönig[48], E. Monnier[102], L. Monsonis Romero[163], J. Montejo Berlingen[13,83], M. Montella[119], F. Montereali[77a,77b], F. Monticelli[90], S. Monzani[69a,69c], N. Morange[66], A. L. Moreira De Carvalho[130a], M. Moreno Llácer[163], C. Moreno Martinez[56], P. Morettini[57b], S. Morgenstern[36], M. Morii[61], M. Morinaga[153], A. K. Morley[36], F. Morodei[75a,75b], L. Morvaj[36], P. Moschovakos[36], B. Moser[36], M. Mosidze[149b], T. Moskalets[54], P. Moskvitina[113], J. Moss[31,o], E. J. W. Moyse[103], O. Mtintsilana[33g], S. Muanza[102], J. Mueller[129], D. Muenstermann[91], R. Müller[19], G. A. Mullier[161], A. J. Mullin[32], J. J. Mullin[128], D. P. Mungo[155], D. Munoz Perez[163], F. J. Munoz Sanchez[101], M. Murin[101], W. J. Murray[167,134], A. Murrone[71a,71b], J. M. Muse[120], M. Muškinja[17a], C. Mwewa[29], A. G. Myagkov[37,a], A. J. Myers[8], A. A. Myers[129],

G. Myers[68], M. Myska[132], B. P. Nachman[17a], O. Nackenhorst[49], A. Nag[50], K. Nagai[126], K. Nagano[83], J. L. Nagle[29,al], E. Nagy[102], A. M. Nairz[36], Y. Nakahama[83], K. Nakamura[83], K. Nakkalil[5], H. Nanjo[124], R. Narayan[44], E. A. Narayanan[112], I. Naryshkin[37], M. Naseri[34], S. Nasri[159], C. Nass[24], G. Navarro[22a], J. Navarro-Gonzalez[163], R. Nayak[151], A. Nayaz[18], P. Y. Nechaeva[37], F. Nechansky[48], L. Nedic[126], T. J. Neep[20], A. Negri[73a,73b], M. Negrini[23b], C. Nellist[114], C. Nelson[104], K. Nelson[106], S. Nemecek[131], M. Nessi[36,i], M. S. Neubauer[162], F. Neuhaus[100], J. Neundorf[48], R. Newhouse[164], P. R. Newman[20], C. W. Ng[129], Y. W. Y. Ng[48], B. Ngair[35e], H. D. N. Nguyen[108], R. B. Nickerson[126], R. Nicolaidou[135], J. Nielsen[136], M. Niemeyer[55], J. Niermann[55,36], N. Nikiforou[36], V. Nikolaenko[37,a], I. Nikolic-Audit[127], K. Nikolopoulos[20], P. Nilsson[29], I. Ninca[48], H. R. Nindhito[56], G. Ninio[151], A. Nisati[75a], N. Nishu[2], R. Nisius[110], J-E. Nitschke[50], E. K. Nkadimeng[33g], S. J. Noacco Rosende[90], T. Nobe[153], D. L. Noel[32], T. Nommensen[147], M. B. Norfolk[139], R. R. B. Norisam[96], B. J. Norman[34], J. Novak[93], T. Novak[48], L. Novotny[132], R. Novotny[112], L. Nozka[122], K. Ntekas[160], N. M. J. Nunes De Moura Junior[82b], E. Nurse[96], J. Ocariz[127], A. Ochi[84], I. Ochoa[130a], S. Oerdek[161], J. T. Offermann[39], A. Ogrodnik[133], A. Oh[101], C. C. Ohm[144], H. Oide[83], R. Oishi[153], M. L. Ojeda[48], Y. Okazaki[87], M. W. O'Keefe[92], Y. Okumura[153], L. F. Oleiro Seabra[130a], S. A. Olivares Pino[137d], D. Oliveira Damazio[29], D. Oliveira Goncalves[82a], J. L. Oliver[160], M. J. R. Olsson[160], A. Olszewski[86], Ö. O. Öncel[54], D. C. O'Neil[142], A. P. O'Neill[19], A. Onofre[130a,130e], P. U. E. Onyisi[11], M. J. Oreglia[39], G. E. Orellana[90], D. Orestano[77a,77b], N. Orlando[13], R. S. Orr[155], V. O'Shea[59], L. M. Osojnak[128], R. Ospanov[62a], G. Otero y Garzon[30], H. Otono[89], P. S. Ott[63a], G. J. Ottino[17a], M. Ouchrif[35d], J. Ouellette[29], F. Ould-Saada[125], M. Owen[59], R. E. Owen[134], K. Y. Oyulmaz[21a], V. E. Ozcan[21a], N. Ozturk[8], S. Ozturk[21d], H. A. Pacey[32], A. Pacheco Pages[13], C. Padilla Aranda[13], G. Padovano[75a,75b], S. Pagan Griso[17a], G. Palacino[68], A. Palazzo[70a,70b], S. Palestini[36], J. Pan[172], T. Pan[64a], D. K. Panchal[11], C. E. Pandini[114], J. G. Panduro Vazquez[95], H. Pang[14b], P. Pani[48], G. Panizzo[69a,69c], L. Paolozzi[56], C. Papadatos[108], S. Parajuli[44], A. Paramonov[6], C. Paraskevopoulos[10], D. Paredes Hernandez[64b], T. H. Park[155], M. A. Parker[32], F. Parodi[57b,57a], E. W. Parrish[115], V. A. Parrish[52], J. A. Parsons[41], U. Parzefall[54], B. Pascual Dias[108], L. Pascual Dominguez[151], F. Pasquali[114], E. Pasqualucci[75a], S. Passaggio[57b], F. Pastore[95], P. Pasuwan[47a,47b], P. Patel[86], U. M. Patel[51], J. R. Pater[101], T. Pauly[36], J. Pearkes[143], M. Pedersen[125], R. Pedro[130a], S. V. Peleganchuk[37], O. Penc[36], E. A. Pender[52], H. Peng[62a], K. E. Penski[109], M. Penzin[37], B. S. Peralva[82d], A. P. Pereira Peixoto[60], L. Pereira Sanchez[47a,47b], D. V. Perepelitsa[29,al], E. Perez Codina[156a], M. Perganti[10], L. Perini[71a,71b,*], H. Pernegger[36], A. Perrevoort[113], O. Perrin[40], K. Peters[48], R. F. Y. Peters[101], B. A. Petersen[36], T. C. Petersen[42], E. Petit[102], V. Petousis[132], C. Petridou[152,f], A. Petrukhin[141], M. Pettee[17a], N. E. Pettersson[36], A. Petukhov[37], K. Petukhova[133], A. Peyaud[135], R. Pezoa[137f], L. Pezzotti[36], G. Pezzullo[172], T. M. Pham[170], T. Pham[105], P. W. Phillips[134], G. Piacquadio[145], E. Pianori[17a], F. Piazza[71a,71b], R. Piegaia[30], D. Pietreanu[27b], A. D. Pilkington[101], M. Pinamonti[69a,69c], J. L. Pinfold[2], B. C. Pinheiro Pereira[130a], A. E. Pinto Pinoargote[135], K. M. Piper[146], A. Pirttikoski[56], C. Pitman Donaldson[96], D. A. Pizzi[34], L. Pizzimento[76a,76b], A. Pizzini[114], M. -A. Pleier[29], V. Plesanovs[54], V. Pleskot[133], E. Plotnikova[38], G. Poddar[4], R. Poettgen[98], L. Poggioli[127], I. Pokharel[55], S. Polacek[133], G. Polesello[73a], A. Poley[142,156a], R. Polifka[132], A. Polini[23b], C. S. Pollard[167], Z. B. Pollock[119], V. Polychronakos[29], E. Pompa Pacchi[75a,75b], D. Ponomarenko[113], L. Pontecorvo[36], S. Popa[27a], G. A. Popeneciu[27d], A. Poreba[36], D. M. Portillo Quintero[156a], S. Pospisil[132], M. A. Postill[139], P. Postolache[27c], K. Potamianos[167], P. A. Potepa[85a], I. N. Potrap[38], C. J. Potter[32], H. Potti[1], T. Poulsen[48], J. Poveda[163], M. E. Pozo Astigarraga[36], A. Prades Ibanez[163], J. Pretel[54], D. Price[101], M. Primavera[70a], M. A. Principe Martin[99], R. Privara[122], T. Procter[59], M. L. Proffitt[138], N. Proklova[128], K. Prokofiev[64c], G. Proto[110], S. Protopopescu[29], J. Proudfoot[6], M. Przybycien[85a], W. W. Przygoda[85b], J. E. Puddefoot[139], D. Pudzha[37], D. Pyatiizbyantseva[37], J. Qian[106], D. Qichen[101], Y. Qin[101], T. Qiu[52], A. Quadt[55], M. Queitsch-Maitland[101], G. Quetant[56], G. Rabanal Bolanos[61], D. Rafanoharana[54], F. Ragusa[71a,71b], J. L. Rainbolt[39], J. A. Raine[56], S. Rajagopalan[29], E. Ramakoti[37], K. Ran[48,14e], N. P. Rapheeha[33g], H. Rasheed[27b], V. Raskina[127], D. F. Rassloff[63a], S. Rave[100], B. Ravina[55], I. Ravinovich[169], M. Raymond[36], A. L. Read[125], N. P. Readioff[139], D. M. Rebuzzi[73a,73b], G. Redlinger[29], A. S. Reed[110], K. Reeves[26], J. A. Reidelsturz[171], D. Reikher[151], A. Rej[141], C. Rembser[36], A. Renardi[48], M. Renda[27b], M. B. Rendel[110], F. Renner[48], A. G. Rennie[59], S. Resconi[71a], M. Ressegotti[57b,57a], S. Rettie[36], J. G. Reyes Rivera[107], B. Reynolds[119], E. Reynolds[17a], O. L. Rezanova[37], P. Reznicek[133], N. Ribaric[91], E. Ricci[78a,78b], R. Richter[110], S. Richter[47a,47b], E. Richter-Was[85b], M. Ridel[127], S. Ridouani[35d], P. Rieck[117], P. Riedler[36], M. Rijssenbeek[145], A. Rimoldi[73a,73b], M. Rimoldi[48], L. Rinaldi[23b,23a], T. T. Rinn[29], M. P. Rinnagel[109],

G. Ripellino[161], I. Riu[13], P. Rivadeneira[48], J. C. Rivera Vergara[165], F. Rizatdinova[121], E. Rizvi[94], B. A. Roberts[167], B. R. Roberts[17a], S. H. Robertson[104,aa], M. Robin[48], D. Robinson[32], C. M. Robles Gajardo[137f], M. Robles Manzano[100], A. Robson[59], A. Rocchi[76a,76b], C. Roda[74a,74b], S. Rodriguez Bosca[63a], Y. Rodriguez Garcia[22a], A. Rodriguez Rodriguez[54], A. M. Rodríguez Vera[156b], S. Roe[36], J. T. Roemer[160], A. R. Roepe-Gier[136], J. Roggel[171], O. Røhne[125], R. A. Rojas[103], C. P. A. Roland[68], J. Roloff[29], A. Romaniouk[37], E. Romano[73a,73b], M. Romano[23b], A. C. Romero Hernandez[162], N. Rompotis[92], L. Roos[127], S. Rosati[75a], B. J. Rosser[39], E. Rossi[126], E. Rossi[72a,72b], L. P. Rossi[57b], L. Rossini[48], R. Rosten[119], M. Rotaru[27b], B. Rottler[54], C. Rougier[102,ae], D. Rousseau[66], D. Rousso[32], A. Roy[162], S. Roy-Garand[155], A. Rozanov[102], Y. Rozen[150], X. Ruan[33g], A. Rubio Jimenez[163], A. J. Ruby[92], V. H. Ruelas Rivera[18], T. A. Ruggeri[1], A. Ruggiero[126], A. Ruiz-Martinez[163], A. Rummler[36], Z. Rurikova[54], N. A. Rusakovich[38], H. L. Russell[165], G. Russo[75a,75b], J. P. Rutherfoord[7], S. Rutherford Colmenares[32], K. Rybacki[91], M. Rybar[133], E. B. Rye[125], A. Ryzhov[44], J. A. Sabater Iglesias[56], P. Sabatini[163], L. Sabetta[75a,75b], H. F-W. Sadrozinski[136], F. Safai Tehrani[75a], B. Safarzadeh Samani[146], M. Safdari[143], S. Saha[165], M. Sahinsoy[110], M. Saimpert[135], M. Saito[153], T. Saito[153], D. Salamani[36], A. Salnikov[143], J. Salt[163], A. Salvador Salas[13], D. Salvatore[43b,43a], F. Salvatore[146], A. Salzburger[36], D. Sammel[54], D. Sampsonidis[152,f], D. Sampsonidou[123], J. Sánchez[163], A. Sanchez Pineda[4], V. Sanchez Sebastian[163], H. Sandaker[125], C. O. Sander[48], J. A. Sandesara[103], M. Sandhoff[171], C. Sandoval[22b], D. P. C. Sankey[134], T. Sano[87], A. Sansoni[53], L. Santi[75a,75b], C. Santoni[40], H. Santos[130a,130b], S. N. Santpur[17a], A. Santra[169], K. A. Saoucha[139], J. G. Saraiva[130a,130d], J. Sardain[7], O. Sasaki[83], K. Sato[157], C. Sauer[63b], F. Sauerburger[54], E. Sauvan[4], P. Savard[155,aj], R. Sawada[153], C. Sawyer[134], L. Sawyer[97], I. Sayago Galvan[163], C. Sbarra[23b], A. Sbrizzi[23b,23a], T. Scanlon[96], J. Schaarschmidt[138], P. Schacht[110], D. Schaefer[39], U. Schäfer[100], A. C. Schaffer[66,44], D. Schaile[109], R. D. Schamberger[145], C. Scharf[18], M. M. Schefer[19], V. A. Schegelsky[37], D. Scheirich[133], F. Schenck[18], M. Schernau[160], C. Scheulen[55], C. Schiavi[57b,57a], E. J. Schioppa[70a,70b], M. Schioppa[43b,43a], B. Schlag[143,r], K. E. Schleicher[54], S. Schlenker[36], J. Schmeing[171], M. A. Schmidt[171], K. Schmieden[100], C. Schmitt[100], S. Schmitt[48], L. Schoeffel[135], A. Schoening[63b], P. G. Scholer[54], E. Schopf[126], M. Schott[100], J. Schovancova[36], S. Schramm[56], F. Schroeder[171], T. Schroer[56], H-C. Schultz-Coulon[63a], M. Schumacher[54], B. A. Schumm[136], Ph. Schune[135], A. J. Schuy[138], H. R. Schwartz[136], A. Schwartzman[143], T. A. Schwarz[106], Ph. Schwemling[135], R. Schwienhorst[107], A. Sciandra[136], G. Sciolla[26], F. Scuri[74a], C. D. Sebastiani[92], K. Sedlaczek[115], P. Seema[18], S. C. Seidel[112], A. Seiden[136], B. D. Seidlitz[41], C. Seitz[48], J. M. Seixas[82b], G. Sekhniaidze[72a], S. J. Sekula[44], L. Selem[60], N. Semprini-Cesari[23b,23a], D. Sengupta[56], V. Senthilkumar[163], L. Serin[66], L. Serkin[69a,69b], M. Sessa[76a,76b], H. Severini[120], F. Sforza[57b,57a], A. Sfyrla[56], E. Shabalina[55], R. Shaheen[144], J. D. Shahinian[128], D. Shaked Renous[169], L. Y. Shan[14a], M. Shapiro[17a], A. Sharma[36], A. S. Sharma[164], P. Sharma[80], S. Sharma[48], P. B. Shatalov[37], K. Shaw[146], S. M. Shaw[101], A. Shcherbakova[37], Q. Shen[62c,5], P. Sherwood[96], L. Shi[96], X. Shi[14a], C. O. Shimmin[172], Y. Shimogama[168], J. D. Shinner[95], I. P. J. Shipsey[126], S. Shirabe[56,i], M. Shiyakova[38,y], J. Shlomi[169], M. J. Shochet[39], J. Shojaii[105], D. R. Shope[125], S. Shrestha[119,am], E. M. Shrif[33g], M. J. Shroff[165], P. Sicho[131], A. M. Sickles[162], E. Sideras Haddad[33g], A. Sidoti[23b], F. Siegert[50], Dj. Sijacki[15], R. Sikora[85a], F. Sili[90], J. M. Silva[20], M. V. Silva Oliveira[29], S. B. Silverstein[47a], S. Simion[66], R. Simoniello[36], E. L. Simpson[59], H. Simpson[146], L. R. Simpson[106], N. D. Simpson[98], S. Simsek[21d], S. Sindhu[55], P. Sinervo[155], S. Singh[155], S. Sinha[48], S. Sinha[101], M. Sioli[23b,23a], I. Siral[36], E. Sitnikova[48], S. Yu. Sivoklokov[37,*], J. Sjölin[47a,47b], A. Skaf[55], E. Skorda[98], P. Skubic[120], M. Slawinska[86], V. Smakhtin[169], B. H. Smart[134], J. Smiesko[36], S. Yu. Smirnov[37], Y. Smirnov[37], L. N. Smirnova[37,a], O. Smirnova[98], A. C. Smith[41], E. A. Smith[39], H. A. Smith[126], J. L. Smith[92], R. Smith[143], M. Smizanska[91], K. Smolek[132], A. A. Snesarev[37], S. R. Snider[155], H. L. Snoek[114], S. Snyder[29], R. Sobie[165,aa], A. Soffer[151], C. A. Solans Sanchez[36], E. Yu. Soldatov[37], U. Soldevila[163], A. A. Solodkov[37], S. Solomon[26], A. Soloshenko[38], K. Solovieva[54], O. V. Solovyanov[40], V. Solovyev[37], P. Sommer[36], A. Sonay[13], W. Y. Song[156b], J. M. Sonneveld[114], A. Sopczak[132], A. L. Sopio[96], F. Sopkova[28b], V. Sothilingam[63a], S. Sottocornola[68], R. Soualah[116b], Z. Soumaimi[35e], D. South[48], S. Spagnolo[70a,70b], M. Spalla[110], D. Sperlich[54], G. Spigo[36], M. Spina[146], S. Spinali[91], D. P. Spiteri[59], M. Spousta[133], E. J. Staats[34], A. Stabile[71a,71b], R. Stamen[63a], M. Stamenkovic[114], A. Stampekis[20], M. Standke[24], E. Stanecka[86], M. V. Stange[50], B. Stanislaus[17a], M. M. Stanitzki[48], B. Stapf[48], E. A. Starchenko[37], G. H. Stark[136], J. Stark[102,ae], D. M. Starko[156b], P. Staroba[131], P. Starovoitov[63a], S. Stärz[104], R. Staszewski[86], G. Stavropoulos[46], J. Steentoft[161], P. Steinberg[29], B. Stelzer[142,156a], H. J. Stelzer[129], O. Stelzer-Chilton[156a],

H. Stenzel[58], T. J. Stevenson[146], G. A. Stewart[36], J. R. Stewart[121], M. C. Stockton[36], G. Stoicea[27b], M. Stolarski[130a], S. Stonjek[110], A. Straessner[50], J. Strandberg[144], S. Strandberg[47a,47b], M. Strauss[120], T. Strebler[102], P. Strizenec[28b], R. Ströhmer[166], D. M. Strom[123], L. R. Strom[48], R. Stroynowski[44], A. Strubig[47a,47b], S. A. Stucci[29], B. Stugu[16], J. Stupak[120], N. A. Styles[48], D. Su[143], S. Su[62a], W. Su[62d], X. Su[62a,66], K. Sugizaki[153], V. V. Sulin[37], M. J. Sullivan[92], D. M. S. Sultan[78a,78b], L. Sultanaliyeva[37], S. Sultansoy[3b], T. Sumida[87], S. Sun[106], S. Sun[170], O. Sunneborn Gudnadottir[161], M. R. Sutton[146], H. Suzuki[157], M. Svatos[131], M. Swiatlowski[156a], T. Swirski[166], I. Sykora[28a], M. Sykora[133], T. Sykora[133], D. Ta[100], K. Tackmann[48,x], A. Taffard[160], R. Tafirout[156a], J. S. Tafoya Vargas[66], R. Takashima[88], E. P. Takeva[52], Y. Takubo[83], M. Talby[102], A. A. Talyshev[37], K. C. Tam[64b], N. M. Tamir[151], A. Tanaka[153], J. Tanaka[153], R. Tanaka[66], M. Tanasini[57b,57a], Z. Tao[164], S. Tapia Araya[137f], S. Tapprogge[100], A. Tarek Abouelfadl Mohamed[107], S. Tarem[150], K. Tariq[62b], G. Tarna[102,27b], G. F. Tartarelli[71a], P. Tas[133], M. Tasevsky[131], E. Tassi[43b,43a], A. C. Tate[162], G. Tateno[153], Y. Tayalati[35e,z], G. N. Taylor[105], W. Taylor[156b], H. Teagle[92], A. S. Tee[170], R. Teixeira De Lima[143], P. Teixeira-Dias[95], J. J. Teoh[155], K. Terashi[153], J. Terron[99], S. Terzo[13], M. Testa[53], R. J. Teuscher[155,aa], A. Thaler[79], O. Theiner[56], N. Themistokleous[52], T. Theveneaux-Pelzer[102], O. Thielmann[171], D. W. Thomas[95], J. P. Thomas[20], E. A. Thompson[17a], P. D. Thompson[20], E. Thomson[128], Y. Tian[55], V. Tikhomirov[37,a], Yu. A. Tikhonov[37], S. Timoshenko[37], D. Timoshyn[133], E. X. L. Ting[1], P. Tipton[172], S. H. Tlou[33g], A. Tnourji[40], K. Todome[23b,23a], S. Todorova-Nova[133], S. Todt[50], M. Togawa[83], J. Tojo[89], S. Tokár[28a], K. Tokushuku[83], O. Toldaiev[68], R. Tombs[32], M. Tomoto[83,111], L. Tompkins[143,r], K. W. Topolnicki[85b], E. Torrence[123], H. Torres[102,ae], E. Torró Pastor[163], M. Toscani[30], C. Tosciri[39], M. Tost[11], D. R. Tovey[139], A. Traeet[16], I. S. Trandafir[27b], T. Trefzger[166], A. Tricoli[29], I. M. Trigger[156a], S. Trincaz-Duvoid[127], D. A. Trischuk[26], B. Trocmé[60], C. Troncon[71a], L. Truong[33c], M. Trzebinski[86], A. Trzupek[86], F. Tsai[145], M. Tsai[106], A. Tsiamis[152,f], P. V. Tsiareshka[37], S. Tsigaridas[156a], A. Tsirigotis[152,v], V. Tsiskaridze[155], E. G. Tskhadadze[149a], M. Tsopoulou[152,f], Y. Tsujikawa[87], I. I. Tsukerman[37], V. Tsulaia[17a], S. Tsuno[83], O. Tsur[150], K. Tsuri[118], D. Tsybychev[145], Y. Tu[64b], A. Tudorache[27b], V. Tudorache[27b], A. N. Tuna[36], S. Turchikhin[38], I. Turk Cakir[3a], R. Turra[71a], T. Turtuvshin[38,ab], P. M. Tuts[41], S. Tzamarias[152,f], P. Tzanis[10], E. Tzovara[100], K. Uchida[153], F. Ukegawa[157], P. A. Ulloa Poblete[137c,137b], E. N. Umaka[29], G. Unal[36], M. Unal[11], A. Undrus[29], G. Unel[160], J. Urban[28b], P. Urquijo[105], G. Usai[8], R. Ushioda[154], M. Usman[108], Z. Uysal[21b], L. Vacavant[102], V. Vacek[132], B. Vachon[104], K. O. H. Vadla[125], T. Vafeiadis[36], A. Vaitkus[96], C. Valderanis[109], E. Valdes Santurio[47a,47b], M. Valente[156a], S. Valentinetti[23b,23a], A. Valero[163], E. Valiente Moreno[163], A. Vallier[102,ae], J. A. Valls Ferrer[163], D. R. Van Arneman[114], T. R. Van Daalen[138], A. Van Der Graaf[49], P. Van Gemmeren[6], M. Van Rijnbach[125,36], S. Van Stroud[96], I. Van Vulpen[114], M. Vanadia[76a,76b], W. Vandelli[36], M. Vandenbroucke[135], E. R. Vandewall[121], D. Vannicola[151], L. Vannoli[57b,57a], R. Vari[75a], E. W. Varnes[7], C. Varni[17a], T. Varol[148], D. Varouchas[66], L. Varriale[163], K. E. Varvell[147], M. E. Vasile[27b], L. Vaslin[40], G. A. Vasquez[165], F. Vazeille[40], T. Vazquez Schroeder[36], J. Veatch[31], V. Vecchio[101], M. J. Veen[103], I. Veliscek[126], L. M. Veloce[155], F. Veloso[130a,130c], S. Veneziano[75a], A. Ventura[70a,70b], A. Verbytskyi[110], M. Verducci[74a,74b], C. Vergis[24], M. Verissimo De Araujo[82b], W. Verkerke[114], J. C. Vermeulen[114], C. Vernieri[143], P. J. Verschuuren[95], M. Vessella[103], M. C. Vetterli[142,aj], A. Vgenopoulos[152,f], N. Viaux Maira[137f], T. Vickey[139], O. E. Vickey Boeriu[139], G. H. A. Viehhauser[126], L. Vigani[63b], M. Villa[23b,23a], M. Villaplana Perez[163], E. M. Villhauer[52], E. Vilucchi[53], M. G. Vincter[34], G. S. Virdee[20], A. Vishwakarma[52], A. Visibile[114], C. Vittori[36], I. Vivarelli[146], V. Vladimirov[167], E. Voevodina[110], F. Vogel[109], P. Vokac[132], J. Von Ahnen[48], E. Von Toerne[24], B. Vormwald[36], V. Vorobel[133], K. Vorobev[37], M. Vos[163], K. Voss[141], J. H. Vossebeld[92], M. Vozak[114], L. Vozdecky[94], N. Vranjes[15], M. Vranjes Milosavljevic[15], M. Vreeswijk[114], N. K. Vu[62d,62c], R. Vuillermet[36], O. Vujinovic[100], I. Vukotic[39], S. Wada[157], C. Wagner[103], J. M. Wagner[17a], W. Wagner[171], S. Wahdan[171], H. Wahlberg[90], R. Wakasa[157], M. Wakida[111], J. Walder[134], R. Walker[109], W. Walkowiak[141], A. Wall[128], T. Wamorkar[6], A. Z. Wang[170], C. Wang[100], C. Wang[62c], H. Wang[17a], J. Wang[64a], R. -J. Wang[100], R. Wang[61], R. Wang[6], S. M. Wang[148], S. Wang[62b], T. Wang[62a], W. T. Wang[80], W. Wang[14a], X. Wang[14c], X. Wang[162], X. Wang[62c], Y. Wang[62d], Y. Wang[14c], Z. Wang[106], Z. Wang[62d,51,62c], Z. Wang[106], A. Warburton[104], R. J. Ward[20], N. Warrack[59], A. T. Watson[20], H. Watson[59], M. F. Watson[20], E. Watton[59,134], G. Watts[138], B. M. Waugh[96], C. Weber[29], H. A. Weber[18], M. S. Weber[19], S. M. Weber[63a], C. Wei[62a], Y. Wei[126], A. R. Weidberg[126], E. J. Weik[117], J. Weingarten[49], M. Weirich[100], C. Weiser[54], C. J. Wells[48], T. Wenaus[29], B. Wendland[49], T. Wengler[36], N. S. Wenke[110], N. Wermes[24], M. Wessels[63a], K. Whalen[123], A. M. Wharton[91], A. S. White[61], A. White[8], M. J. White[1], D. Whiteson[160],

L. Wickremasinghe[124], W. Wiedenmann[170], C. Wiel[50], M. Wielers[134], C. Wiglesworth[42], D. J. Wilbern[120], H. G. Wilkens[36], D. M. Williams[41], H. H. Williams[128], S. Williams[32], S. Willocq[103], B. J. Wilson[101], P. J. Windischhofer[39], F. I. Winkel[30], F. Winklmeier[123], B. T. Winter[54], J. K. Winter[101], M. Wittgen[143], M. Wobisch[97], Z. Wolffs[114], R. Wölker[126], J. Wollrath[160], M. W. Wolter[86], H. Wolters[130a,130c], A. F. Wongel[48], S. D. Worm[48], B. K. Wosiek[86], K. W. Woźniak[86], S. Wozniewski[55], K. Wraight[59], C. Wu[20], J. Wu[14a,14e], M. Wu[64a], M. Wu[113], S. L. Wu[170], X. Wu[56], Y. Wu[62a], Z. Wu[135], J. Wuerzinger[110], T. R. Wyatt[101], B. M. Wynne[52], S. Xella[42], L. Xia[14c], M. Xia[14b], J. Xiang[64c], X. Xiao[106], M. Xie[62a], X. Xie[62a], S. Xin[14a,14e], J. Xiong[17a], D. Xu[14a], H. Xu[62a], L. Xu[62a], R. Xu[128], T. Xu[106], Y. Xu[14b], Z. Xu[52], Z. Xu[14a], B. Yabsley[147], S. Yacoob[33a], N. Yamaguchi[89], Y. Yamaguchi[154], E. Yamashita[153], H. Yamauchi[157], T. Yamazaki[17a], Y. Yamazaki[84], J. Yan[62c], S. Yan[126], Z. Yan[25], H. J. Yang[62c,62d], H. T. Yang[62a], S. Yang[62a], T. Yang[64c], X. Yang[62a], X. Yang[14a], Y. Yang[44], Y. Yang[62a], Z. Yang[62a], W-M. Yao[17a], Y. C. Yap[48], H. Ye[14c], H. Ye[55], J. Ye[44], S. Ye[29], X. Ye[62a], Y. Yeh[96], I. Yeletskikh[38], B. K. Yeo[17a], M. R. Yexley[96], P. Yin[41], K. Yorita[168], S. Younas[27b], C. J. S. Young[54], C. Young[143], Y. Yu[62a], M. Yuan[106], R. Yuan[62b,l], L. Yue[96], M. Zaazoua[62a], B. Zabinski[86], E. Zaid[52], T. Zakareishvili[149b], N. Zakharchuk[34], S. Zambito[56], J. A. Zamora Saa[137d,137b], J. Zang[153], D. Zanzi[54], O. Zaplatilek[132], C. Zeitnitz[171], H. Zeng[14a], J. C. Zeng[162], D. T. Zenger Jr[26], O. Zenin[37], T. Ženiš[28a], S. Zenz[94], S. Zerradi[35a], D. Zerwas[66], M. Zhai[14a,14e], B. Zhang[14c], D. F. Zhang[139], J. Zhang[62b], J. Zhang[6], K. Zhang[14a,14e], L. Zhang[14c], P. Zhang[14a,14e], R. Zhang[170], S. Zhang[106], T. Zhang[153], X. Zhang[62c], X. Zhang[62b], Y. Zhang[62c,5], Y. Zhang[96], Z. Zhang[17a], Z. Zhang[66], H. Zhao[138], P. Zhao[51], T. Zhao[62b], Y. Zhao[136], Z. Zhao[62a], A. Zhemchugov[38], K. Zheng[162], X. Zheng[62a], Z. Zheng[143], D. Zhong[162], B. Zhou[106], H. Zhou[7], N. Zhou[62c], Y. Zhou[7], C. G. Zhu[62b], J. Zhu[106], Y. Zhu[62c], Y. Zhu[62a], X. Zhuang[14a], K. Zhukov[37], V. Zhulanov[37], N. I. Zimine[38], J. Zinsser[63b], M. Ziolkowski[141], L. Živković[15], A. Zoccoli[23b,23a], K. Zoch[56], T. G. Zorbas[139], O. Zormpa[46], W. Zou[41], L. Zwalinski[36]

[1] Department of Physics, University of Adelaide, Adelaide, Australia
[2] Department of Physics, University of Alberta, Edmonton, AB, Canada
[3] [(a)]Department of Physics, Ankara University, Ankara, Türkiye; [(b)]Division of Physics, TOBB University of Economics and Technology, Ankara, Türkiye
[4] LAPP, Université Savoie Mont Blanc, CNRS/IN2P3, Annecy, France
[5] APC, Université Paris Cité, CNRS/IN2P3, Paris, France
[6] High Energy Physics Division, Argonne National Laboratory, Argonne, IL, USA
[7] Department of Physics, University of Arizona, Tucson, AZ, USA
[8] Department of Physics, University of Texas at Arlington, Arlington, TX, USA
[9] Physics Department, National and Kapodistrian University of Athens, Athens, Greece
[10] Physics Department, National Technical University of Athens, Zografou, Greece
[11] Department of Physics, University of Texas at Austin, Austin, TX, USA
[12] Institute of Physics, Azerbaijan Academy of Sciences, Baku, Azerbaijan
[13] Institut de Física d'Altes Energies (IFAE), Barcelona Institute of Science and Technology, Barcelona, Spain
[14] [(a)]Institute of High Energy Physics, Chinese Academy of Sciences, Beijing, China; [(b)]Physics Department, Tsinghua University, Beijing, China; [(c)]Department of Physics, Nanjing University, Nanjing, China; [(d)]School of Science, Shenzhen Campus of Sun Yat-sen University, Shenzhen, China; [(e)]University of Chinese Academy of Science (UCAS), Beijing, China
[15] Institute of Physics, University of Belgrade, Belgrade, Serbia
[16] Department for Physics and Technology, University of Bergen, Bergen, Norway
[17] [(a)]Physics Division, Lawrence Berkeley National Laboratory, Berkeley, CA, USA; [(b)]University of California, Berkeley, CA, USA
[18] Institut für Physik, Humboldt Universität zu Berlin, Berlin, Germany
[19] Albert Einstein Center for Fundamental Physics and Laboratory for High Energy Physics, University of Bern, Bern, Switzerland
[20] School of Physics and Astronomy, University of Birmingham, Birmingham, UK
[21] [(a)]Department of Physics, Bogazici University, Istanbul, Türkiye; [(b)]Department of Physics Engineering, Gaziantep University, Gaziantep, Türkiye; [(c)]Department of Physics, Istanbul University, Istanbul, Türkiye; [(d)]Istinye University, Sariyer, Istanbul, Türkiye

[22] [(a)]Facultad de Ciencias y Centro de Investigaciónes, Universidad Antonio Nariño, Bogotá, Colombia; [(b)]Departamento de Física, Universidad Nacional de Colombia, Bogotá, Colombia
[23] [(a)]Dipartimento di Fisica e Astronomia A. Righi, Università di Bologna, Bologna, Italy; [(b)]INFN Sezione di Bologna, Bologna, Italy
[24] Physikalisches Institut, Universität Bonn, Bonn, Germany
[25] Department of Physics, Boston University, Boston, MA, USA
[26] Department of Physics, Brandeis University, Waltham, MA, USA
[27] [(a)]Transilvania University of Brasov, Brasov, Romania; [(b)]Horia Hulubei National Institute of Physics and Nuclear Engineering, Bucharest, Romania; [(c)]Department of Physics, Alexandru Ioan Cuza University of Iasi, Iasi, Romania; [(d)]Physics Department, National Institute for Research and Development of Isotopic and Molecular Technologies, Cluj-Napoca, Romania; [(e)]University Politehnica Bucharest, Bucharest, Romania; [(f)]West University in Timisoara, Timisoara, Romania; [(g)]Faculty of Physics, University of Bucharest, Bucharest, Romania
[28] [(a)]Faculty of Mathematics, Physics and Informatics, Comenius University, Bratislava, Slovak Republic; [(b)]Department of Subnuclear Physics, Institute of Experimental Physics of the Slovak Academy of Sciences, Kosice, Slovak Republic
[29] Physics Department, Brookhaven National Laboratory, Upton, NY, USA
[30] Departamento de Física, y CONICET, Facultad de Ciencias Exactas y Naturales, Instituto de Física de Buenos Aires (IFIBA), Universidad de Buenos Aires, Buenos Aires, Argentina
[31] California State University, Long Beach, CA, USA
[32] Cavendish Laboratory, University of Cambridge, Cambridge, UK
[33] [(a)]Department of Physics, University of Cape Town, Cape Town, South Africa; [(b)]iThemba Labs, Cape Town, Western Cape, South Africa; [(c)]Department of Mechanical Engineering Science, University of Johannesburg, Johannesburg, South Africa; [(d)]National Institute of Physics, University of the Philippines Diliman, Quezon City, Philippines; [(e)]Department of Physics, University of South Africa, Pretoria, South Africa; [(f)]University of Zululand, KwaDlangezwa, Richards Bay, South Africa; [(g)]School of Physics, University of the Witwatersrand, Johannesburg, South Africa
[34] Department of Physics, Carleton University, Ottawa, ON, Canada
[35] [(a)]Faculté des Sciences Ain Chock, Réseau Universitaire de Physique des Hautes Energies-Université Hassan II, Casablanca, Morocco; [(b)]Faculté des Sciences, Université Ibn-Tofail, Kénitra, Morocco; [(c)]Faculté des Sciences Semlalia, Université Cadi Ayyad, LPHEA-Marrakech, Marrakech, Morocco; [(d)]LPMR, Faculté des Sciences, Université Mohamed Premier, Oujda, Morocco; [(e)]Faculté des sciences, Université Mohammed V, Rabat, Morocco; [(f)]Institute of Applied Physics, Mohammed VI Polytechnic University, Ben Guerir, Morocco
[36] CERN, Geneva, Switzerland
[37] Affiliated with an Institute Covered by a Cooperation Agreement with CERN, Geneva, Switzerland
[38] Affiliated with an International Laboratory Covered by a Cooperation Agreement with CERN, Geneva, Switzerland
[39] Enrico Fermi Institute, University of Chicago, Chicago, IL, USA
[40] LPC, Université Clermont Auvergne, CNRS/IN2P3, Clermont-Ferrand, France
[41] Nevis Laboratory, Columbia University, Irvington, NY, USA
[42] Niels Bohr Institute, University of Copenhagen, Copenhagen, Denmark
[43] [(a)]Dipartimento di Fisica, Università della Calabria, Rende, Italy; [(b)]INFN Gruppo Collegato di Cosenza, Laboratori Nazionali di Frascati, Frascati, Italy
[44] Physics Department, Southern Methodist University, Dallas, TX, USA
[45] Physics Department, University of Texas at Dallas, Richardson, TX, USA
[46] National Centre for Scientific Research "Demokritos", Agia Paraskevi, Greece
[47] [(a)]Department of Physics, Stockholm University, Stockholm, Sweden; [(b)]Oskar Klein Centre, Stockholm, Sweden
[48] Deutsches Elektronen-Synchrotron DESY, Hamburg and Zeuthen, Germany
[49] Fakultät Physik, Technische Universität Dortmund, Dortmund, Germany
[50] Institut für Kern- und Teilchenphysik, Technische Universität Dresden, Dresden, Germany
[51] Department of Physics, Duke University, Durham, NC, USA
[52] SUPA-School of Physics and Astronomy, University of Edinburgh, Edinburgh, UK
[53] INFN e Laboratori Nazionali di Frascati, Frascati, Italy
[54] Physikalisches Institut, Albert-Ludwigs-Universität Freiburg, Freiburg, Germany
[55] II. Physikalisches Institut, Georg-August-Universität Göttingen, Göttingen, Germany
[56] Département de Physique Nucléaire et Corpusculaire, Université de Genève, Geneva, Switzerland

[57] [(a)]Dipartimento di Fisica, Università di Genova, Genoa, Italy; [(b)]INFN Sezione di Genova, Genoa, Italy
[58] II. Physikalisches Institut, Justus-Liebig-Universität Giessen, Giessen, Germany
[59] SUPA-School of Physics and Astronomy, University of Glasgow, Glasgow, UK
[60] LPSC, Université Grenoble Alpes, CNRS/IN2P3, Grenoble INP, Grenoble, France
[61] Laboratory for Particle Physics and Cosmology, Harvard University, Cambridge, MA, USA
[62] [(a)]Department of Modern Physics and State Key Laboratory of Particle Detection and Electronics, University of Science and Technology of China, Hefei, China; [(b)]Institute of Frontier and Interdisciplinary Science and Key Laboratory of Particle Physics and Particle Irradiation (MOE), Shandong University, Qingdao, China; [(c)]Key Laboratory for Particle Astrophysics and Cosmology (MOE), SKLPPC, School of Physics and Astronomy, Shanghai Jiao Tong University, Shanghai, China; [(d)]Tsung-Dao Lee Institute, Shanghai, China
[63] [(a)]Kirchhoff-Institut für Physik, Ruprecht-Karls-Universität Heidelberg, Heidelberg, Germany; [(b)]Physikalisches Institut, Ruprecht-Karls-Universität Heidelberg, Heidelberg, Germany
[64] [(a)]Department of Physics, Chinese University of Hong Kong, Shatin, N.T., Hong Kong, China; [(b)]Department of Physics, University of Hong Kong, Hong Kong, China; [(c)]Department of Physics and Institute for Advanced Study, Hong Kong University of Science and Technology, Clear Water Bay, Kowloon, Hong Kong, China
[65] Department of Physics, National Tsing Hua University, Hsinchu, Taiwan
[66] IJCLab, Université Paris-Saclay, CNRS/IN2P3, 91405 Orsay, France
[67] Centro Nacional de Microelectrónica (IMB-CNM-CSIC), Barcelona, Spain
[68] Department of Physics, Indiana University, Bloomington, IN, USA
[69] [(a)]INFN Gruppo Collegato di Udine, Sezione di Trieste, Udine, Italy; [(b)]ICTP, Trieste, Italy; [(c)]Dipartimento Politecnico di Ingegneria e Architettura, Università di Udine, Udine, Italy
[70] [(a)]INFN Sezione di Lecce, Lecce, Italy; [(b)]Dipartimento di Matematica e Fisica, Università del Salento, Lecce, Italy
[71] [(a)]INFN Sezione di Milano, Milan, Italy; [(b)]Dipartimento di Fisica, Università di Milano, Milano, Italy
[72] [(a)]INFN Sezione di Napoli, Naples, Italy; [(b)]Dipartimento di Fisica, Università di Napoli, Naples, Italy
[73] [(a)]INFN Sezione di Pavia, Pavia, Italy; [(b)]Dipartimento di Fisica, Università di Pavia, Pavia, Italy
[74] [(a)]INFN Sezione di Pisa, Pisa, Italy; [(b)]Dipartimento di Fisica E. Fermi, Università di Pisa, Pisa, Italy
[75] [(a)]INFN Sezione di Roma, Rome, Italy; [(b)]Dipartimento di Fisica, Sapienza Università di Roma, Rome, Italy
[76] [(a)]INFN Sezione di Roma Tor Vergata, Rome, Italy; [(b)]Dipartimento di Fisica, Università di Roma Tor Vergata, Rome, Italy
[77] [(a)]INFN Sezione di Roma Tre, Rome, Italy; [(b)]Dipartimento di Matematica e Fisica, Università Roma Tre, Rome, Italy
[78] [(a)]INFN-TIFPA, Povo, Italy; [(b)]Università degli Studi di Trento, Trento, Italy
[79] Department of Astro and Particle Physics, Universität Innsbruck, Innsbruck, Austria
[80] University of Iowa, Iowa City, IA, USA
[81] Department of Physics and Astronomy, Iowa State University, Ames, IA, USA
[82] [(a)]Departamento de Engenharia Elétrica, Universidade Federal de Juiz de Fora (UFJF), Juiz de Fora, Brazil; [(b)]Universidade Federal do Rio De Janeiro COPPE/EE/IF, Rio de Janeiro, Brazil; [(c)]Instituto de Física, Universidade de São Paulo, São Paulo, Brazil; [(d)]Rio de Janeiro State University, Rio de Janeiro, Brazil
[83] KEK, High Energy Accelerator Research Organization, Tsukuba, Japan
[84] Graduate School of Science, Kobe University, Kobe, Japan
[85] [(a)]Faculty of Physics and Applied Computer Science, AGH University of Science and Technology, Kraków, Poland; [(b)]Marian Smoluchowski Institute of Physics, Jagiellonian University, Kraków, Poland
[86] Institute of Nuclear Physics Polish Academy of Sciences, Kraków, Poland
[87] Faculty of Science, Kyoto University, Kyoto, Japan
[88] Kyoto University of Education, Kyoto, Japan
[89] Research Center for Advanced Particle Physics and Department of Physics, Kyushu University, Fukuoka, Japan
[90] Instituto de Física La Plata, Universidad Nacional de La Plata and CONICET, La Plata, Argentina
[91] Physics Department, Lancaster University, Lancaster, UK
[92] Oliver Lodge Laboratory, University of Liverpool, Liverpool, UK
[93] Department of Experimental Particle Physics, Jožef Stefan Institute and Department of Physics, University of Ljubljana, Ljubljana, Slovenia
[94] School of Physics and Astronomy, Queen Mary University of London, London, UK
[95] Department of Physics, Royal Holloway University of London, Egham, UK
[96] Department of Physics and Astronomy, University College London, London, UK

[97] Louisiana Tech University, Ruston, LA, USA
[98] Fysiska institutionen, Lunds universitet, Lund, Sweden
[99] Departamento de Física Teorica C-15 and CIAFF, Universidad Autónoma de Madrid, Madrid, Spain
[100] Institut für Physik, Universität Mainz, Mainz, Germany
[101] School of Physics and Astronomy, University of Manchester, Manchester, UK
[102] CPPM, Aix-Marseille Université, CNRS/IN2P3, Marseille, France
[103] Department of Physics, University of Massachusetts, Amherst, MA, USA
[104] Department of Physics, McGill University, Montreal, QC, Canada
[105] School of Physics, University of Melbourne, Melbourne, VIC, Australia
[106] Department of Physics, University of Michigan, Ann Arbor, MI, USA
[107] Department of Physics and Astronomy, Michigan State University, East Lansing, MI, USA
[108] Group of Particle Physics, University of Montreal, Montreal, QC, Canada
[109] Fakultät für Physik, Ludwig-Maximilians-Universität München, Munich, Germany
[110] Max-Planck-Institut für Physik (Werner-Heisenberg-Institut), München, Germany
[111] Graduate School of Science and Kobayashi-Maskawa Institute, Nagoya University, Nagoya, Japan
[112] Department of Physics and Astronomy, University of New Mexico, Albuquerque, NM, USA
[113] Institute for Mathematics, Astrophysics and Particle Physics, Radboud University/Nikhef, Nijmegen, The Netherlands
[114] Nikhef National Institute for Subatomic Physics and University of Amsterdam, Amsterdam, The Netherlands
[115] Department of Physics, Northern Illinois University, DeKalb, IL, USA
[116] [(a)]New York University Abu Dhabi, Abu Dhabi, United Arab Emirates; [(b)]University of Sharjah, Sharjah, United Arab Emirates
[117] Department of Physics, New York University, New York, NY, USA
[118] Ochanomizu University, Otsuka, Bunkyo-ku, Tokyo, Japan
[119] Ohio State University, Columbus, OH, USA
[120] Homer L. Dodge Department of Physics and Astronomy, University of Oklahoma, Norman, OK, USA
[121] Department of Physics, Oklahoma State University, Stillwater, OK, USA
[122] Joint Laboratory of Optics, Palacký University, Olomouc, Czech Republic
[123] Institute for Fundamental Science, University of Oregon, Eugene, OR, USA
[124] Graduate School of Science, Osaka University, Osaka, Japan
[125] Department of Physics, University of Oslo, Oslo, Norway
[126] Department of Physics, Oxford University, Oxford, UK
[127] LPNHE, Sorbonne Université, Université Paris Cité, CNRS/IN2P3, Paris, France
[128] Department of Physics, University of Pennsylvania, Philadelphia, PA, USA
[129] Department of Physics and Astronomy, University of Pittsburgh, Pittsburgh, PA, USA
[130] [(a)]Laboratório de Instrumentação e Física Experimental de Partículas-LIP, Lisbon, Portugal; [(b)]Departamento de Física, Faculdade de Ciências, Universidade de Lisboa, Lisbon, Portugal; [(c)]Departamento de Física, Universidade de Coimbra, Coimbra, Portugal; [(d)]Centro de Física Nuclear da Universidade de Lisboa, Lisbon, Portugal; [(e)]Departamento de Física, Universidade do Minho, Braga, Portugal; [(f)]Departamento de Física Teórica y del Cosmos, Universidad de Granada, Granada, Spain; [(g)]Departamento de Física, Instituto Superior Técnico, Universidade de Lisboa, Lisbon, Portugal
[131] Institute of Physics of the Czech Academy of Sciences, Prague, Czech Republic
[132] Czech Technical University in Prague, Prague, Czech Republic
[133] Faculty of Mathematics and Physics, Charles University, Prague, Czech Republic
[134] Particle Physics Department, Rutherford Appleton Laboratory, Didcot, UK
[135] IRFU, CEA, Université Paris-Saclay, Gif-sur-Yvette, France
[136] Santa Cruz Institute for Particle Physics, University of California Santa Cruz, Santa Cruz, CA, USA
[137] [(a)]Departamento de Física, Pontificia Universidad Católica de Chile, Santiago, Chile; [(b)]Millennium Institute for Subatomic physics at high energy frontier (SAPHIR), Santiago, Chile; [(c)]Instituto de Investigación Multidisciplinario en Ciencia y Tecnología, y Departamento de Física, Universidad de La Serena, La Serena, Chile; [(d)]Department of Physics, Universidad Andres Bello, Santiago, Chile; [(e)]Instituto de Alta Investigación, Universidad de Tarapacá, Arica, Chile; [(f)]Departamento de Física, Universidad Técnica Federico Santa María, Valparaíso, Chile
[138] Department of Physics, University of Washington, Seattle, WA, USA
[139] Department of Physics and Astronomy, University of Sheffield, Sheffield, UK
[140] Department of Physics, Shinshu University, Nagano, Japan

[141] Department Physik, Universität Siegen, Siegen, Germany
[142] Department of Physics, Simon Fraser University, Burnaby, BC, Canada
[143] SLAC National Accelerator Laboratory, Stanford, CA, USA
[144] Department of Physics, Royal Institute of Technology, Stockholm, Sweden
[145] Departments of Physics and Astronomy, Stony Brook University, Stony Brook, NY, USA
[146] Department of Physics and Astronomy, University of Sussex, Brighton, UK
[147] School of Physics, University of Sydney, Sydney, Australia
[148] Institute of Physics, Academia Sinica, Taipei, Taiwan
[149] [(a)]E. Andronikashvili Institute of Physics, Iv. Javakhishvili Tbilisi State University, Tbilisi, Georgia; [(b)]High Energy Physics Institute, Tbilisi State University, Tbilisi, Georgia; [(c)]University of Georgia, Tbilisi, Georgia
[150] Department of Physics, Technion, Israel Institute of Technology, Haifa, Israel
[151] Raymond and Beverly Sackler School of Physics and Astronomy, Tel Aviv University, Tel Aviv, Israel
[152] Department of Physics, Aristotle University of Thessaloniki, Thessaloniki, Greece
[153] International Center for Elementary Particle Physics and Department of Physics, University of Tokyo, Tokyo, Japan
[154] Department of Physics, Tokyo Institute of Technology, Tokyo, Japan
[155] Department of Physics, University of Toronto, Toronto, ON, Canada
[156] [(a)]TRIUMF, Vancouver, BC, Canada; [(b)]Department of Physics and Astronomy, York University, Toronto, ON, Canada
[157] Division of Physics and Tomonaga Center for the History of the Universe, Faculty of Pure and Applied Sciences, University of Tsukuba, Tsukuba, Japan
[158] Department of Physics and Astronomy, Tufts University, Medford, MA, USA
[159] United Arab Emirates University, Al Ain, United Arab Emirates
[160] Department of Physics and Astronomy, University of California Irvine, Irvine, CA, USA
[161] Department of Physics and Astronomy, University of Uppsala, Uppsala, Sweden
[162] Department of Physics, University of Illinois, Urbana, IL, USA
[163] Instituto de Física Corpuscular (IFIC), Centro Mixto Universidad de Valencia-CSIC, Valencia, Spain
[164] Department of Physics, University of British Columbia, Vancouver, BC, Canada
[165] Department of Physics and Astronomy, University of Victoria, Victoria, BC, Canada
[166] Fakultät für Physik und Astronomie, Julius-Maximilians-Universität Würzburg, Würzburg, Germany
[167] Department of Physics, University of Warwick, Coventry, UK
[168] Waseda University, Tokyo, Japan
[169] Department of Particle Physics and Astrophysics, Weizmann Institute of Science, Rehovot, Israel
[170] Department of Physics, University of Wisconsin, Madison, WI, USA
[171] Fakultät für Mathematik und Naturwissenschaften, Fachgruppe Physik, Bergische Universität Wuppertal, Wuppertal, Germany
[172] Department of Physics, Yale University, New Haven, CT, USA

[a] Also Affiliated with an Institute Covered by a Cooperation Agreement with CERN, Geneva, Switzerland
[b] Also at An-Najah National University, Nablus, Palestine
[c] Also at APC, Université Paris Cité, CNRS/IN2P3, Paris, France
[d] Also at Borough of Manhattan Community College, City University of New York, New York, NY, USA
[e] Also at Center for High Energy Physics, Peking University, Beijing, China
[f] Also at Center for Interdisciplinary Research and Innovation (CIRI-AUTH), Thessaloniki, Greece
[g] Also at Centro Studi e Ricerche Enrico Fermi, Rome, Italy
[h] Also at CERN, Geneva, Switzerland
[i] Also at Département de Physique Nucléaire et Corpusculaire, Université de Genève, Geneva, Switzerland
[j] Also at Departament de Fisica de la Universitat Autonoma de Barcelona, Barcelona, Spain
[k] Also at Department of Financial and Management Engineering, University of the Aegean, Chios, Greece
[l] Also at Department of Physics and Astronomy, Michigan State University, East Lansing, MI, USA
[m] Also at Department of Physics and Astronomy, University of Victoria, Victoria, BC, Canada
[n] Also at Department of Physics, Ben Gurion University of the Negev, Beersheba, Israel
[o] Also at Department of Physics, California State University, Sacramento, USA
[p] Also at Department of Physics, King's College London, London, UK
[q] Also at Department of Physics, Royal Holloway University of London, Egham, UK

[r] Also at Department of Physics, Stanford University, Stanford, CA, USA
[s] Also at Department of Physics, University of Fribourg, Fribourg, Switzerland
[t] Also at Department of Physics, University of Thessaly, Vólos, Greece
[u] Also at Department of Physics, Westmont College, Santa Barbara, USA
[v] Also at Hellenic Open University, Patras, Greece
[w] Also at Institucio Catalana de Recerca i Estudis Avancats, ICREA, Barcelona, Spain
[x] Also at Institut für Experimentalphysik, Universität Hamburg, Hamburg, Germany
[y] Also at Institute for Nuclear Research and Nuclear Energy (INRNE) of the Bulgarian Academy of Sciences, Sofia, Bulgaria
[z] Also at Institute of Applied Physics, Mohammed VI Polytechnic University, Ben Guerir, Morocco
[aa] Also at Institute of Particle Physics (IPP), Victoria, Canada
[ab] Also at Institute of Physics and Technology, Ulaanbaatar, Mongolia
[ac] Also at Institute of Physics, Azerbaijan Academy of Sciences, Baku, Azerbaijan
[ad] Also at Institute of Theoretical Physics, Ilia State University, Tbilisi, Georgia
[ae] Also at L2IT, Université de Toulouse, CNRS/IN2P3, UPS, Toulouse, France
[af] Also at Lawrence Livermore National Laboratory, Livermore, USA
[ag] Also at National Institute of Physics, University of the Philippines Diliman, Quezon City, Philippines
[ah] Also at Technical University of Munich, Munich, Germany
[ai] Also at The Collaborative Innovation Center of Quantum Matter (CICQM), Beijing, China
[aj] Also at TRIUMF, Vancouver, BC, Canada
[ak] Also at Università di Napoli Parthenope, Naples, Italy
[al] Also at Department of Physics, University of Colorado Boulder, Colorado, USA
[am] Also at Washington College, Chestertown, MD, USA
[an] Also at Physics Department, Yeditepe University, Istanbul, Türkiye
* Deceased